2013

Planning And Control Of Swarm Motion As Continua

Hossein Rastgoftar
University of Central Florida

PLANNING AND CONTROL OF SWARM MOTION AS CONTINUA

by

HOSSEIN RASTGOFTAR

B.S. Shiraz University, 2006
M.S. Shiraz University, 2010

A thesis submitted in partial fulfillment of the requirements
for the degree of Master of Science
in the Department of Mechanical, and Aerospace Engineering
in the College of Engineering and Computer Sciences
at the University of Central Florida
Orlando, Florida

Summer Term
2013

Major Professor: Suhada Jayasuriya

ABSTRACT

In this thesis, new algorithms for formation control of multi agent systems (MAS) based on continuum mechanics principles will be investigated. For this purpose agents of the MAS are treated as particles in a continuum, evolving in an *n-D* space, whose desired configuration is required to satisfy an admissible deformation function. Considered is a specific class of mappings that is called *homogenous* where the Jacobian of the mapping is only a function of time and is not spatially varying. The primary objectives of this thesis are to develop the necessary theory and its validation via simulation on a mobile-agent based swarm test bed that includes two primary tasks: 1) homogenous transformation of MAS and 2) deployment of a random distribution of agents on to a desired configuration. Developed will be a framework based on homogenous transformations for the evolution of a MAS in an *n-D* space (n=*1, 2,* and *3*), under two scenarios: 1) no inter-agent communication (predefined motion plan); and 2) local inter-agent communication. Additionally, homogenous transformations based on communication protocols will be used to deploy an arbitrary distribution of a MAS on to a desired curve.

Homogenous transformation with no communication: A homogenous transformation of a MAS, evolving in an R^n space, under zero inter agent communication is first considered. Here the homogenous mapping, is characterized by an *n* x *n* Jacobian matrix $Q(t)$ and an *n* x *1* rigid body displacement vector $D(t)$, that are based on positions of *n+1* agents of the MAS, called leader agents. The designed Jacobian $Q(t)$ and rigid body displacement vector $D(t)$ are passed onto rest of the agents of the MAS, called *followers*, who will then use that information to update their positions under a pre-

defined motion plan. Consequently, the motion of MAS will evolve as a homogenous transformation of the initial configuration without explicit communication among agents.

Homogenous Transformation under Local Communication: We develop a framework for homogenous transformation of MAS, evolving in R^n, under a local inter agent communication topology. Here we assume that some agents are the leaders, that are transformed homogenously in an *n-D* space. In addition, every follower agent of the MAS communicates with some local agents to update its position, in order to grasp the homogenous mapping that is prescribed by the leader agents. We show that some distance ratios that are assigned based on initial formation, if preserved, lead to asymptotic convergence of the initial formation to a final formation under a homogenous mapping.

Deployment of a Random Distribution on a Desired Manifold: Deployment of agents of a MAS, moving in a plane, on to a desired curve, is a task that is considered as an application of the proposed approach. In particular, a 2-D MAS evolution problem is considered as two 1-D MAS evolution problems, where *x* or *y* coordinates of the position of all agents are modeled as points confined to move on a straight line. Then, for every coordinate of MAS evolution, bulk motion is controlled by two agents considered leaders that move independently, with rest of the follower agents motions evolving through each follower agent communicating with two adjacent agents.

DEDICATION

I dedicate this work to my mother and father who have been my greatest support through my efforts to complete my schooling and receive my degrees. Their unfailing love for me and dedication to my higher education has made my success possible.

ACKNOWLEDGMENT

I would like to express my deepest appreciation to my adviser, Professor Suhada Jayasuriya, for his patience and great guidance during past two years. It is a great honor for me that I am graduated under his grand supervision.

I am also very grateful to members of the advisory committee, Dr. Tuhin Das and Dr. Marcel Ilie, for valuable guidance and encouragements extended to me.

TABLE OF CONTENT

LIST OF FIGURES

LIST OF TABLES

CHAPTER 1: LITERATURE SURVEY

A MAS usually consists of a finite number of agents (e.g., small robots), collaborating together to do a specific job. Formation control of a MAS has been an active area of research during the past two decades. Moving in a formation can be observed in some natural biological group behavior, like birds, fish, ants, and bees, where each individual species adjusts its location and orientation in the group intrinsically [1]. Some advantages of collaboration among agents and preserving a formation are [2,3]: reducing cost of the system, increasing robustness and efficiency of the system and having better fault tolerance, structural flexibility and capability of reconfiguration. Formation control has applications in terrain mapping, doing challenging tasks in a hazardous environment, surveillance, monitoring of oil spills in the oceans [4], security patrol, small satellite clustering [4-6], automated highway systems, [4,7], finding and neutralizing mines, containing spills [8] and many other applications.

Dynamics of a MAS, consisting of agents, in general, can be modeled by the dynamics of a n dimensional vector field which consists of state vectors, representing the positions of the agents of the MAS. In mechanical systems, position vectors of a finite number of robots collaborating together, are usually considered the state vectors of the MAS. Therefore, the kinematics of the MAS is modeled by one, two, or three dimensional vector fields consisting of vectors, where each vector represents the position of every agent (robot) of the MAS. Control strategies for the motion of a MAS can be categorized as centralized or decentralized approaches [1]. For the case of centralized control, dynamics of the MAS is defined and so, any agent's dynamics is organized such

that conform other group mates' dynamics, and tend the whole group toward the assigned goal [5, 9-14]. However, centralized methods are more costly, less scalable and less robust [1]. On the other hand, most of decentralized control methods, necessitate inter agent communications and collaboration among the agents for understanding the dynamics of the whole multi agent system. Decentralized control approaches are more versatile as they provide flexibility of changing the motion map. Some common approaches for control of formation of MAS are leader-follower [14-50], potential function [53-76], virtual structure [77-91] behavior based method [91-96], consensus algorithm [97-100] and partial differential equations (PDE) based techniques [103-106].

In the leader follower approach, the leader prescribes the trajectory of the motion and the followers figure out their trajectory by adjusting their distances and orientations with respect to leader's position, so, this method can be viewed as a trajectory-tracking problem [15]. Feedback linearization is a common approach for control of kinematics of a MAS using leader follower approach for collaboration [16-26]. A feedback linearization based technique for formation control of large number of robots has been presented in [16] where desired distances between robots are achieved exponentially. Reference [17], proposes a flexible leader follower model for formation control, where robots are not rigid with respect to the leader. In reference [18], a full state feedback and input-output feedback linearized strategies are suggested for followers and leaders, respectively, to achieve a given trajectory. In [19], an extended Kalman filter is applied to estimate states of the system (multi robots) and a new observabilty condition for nonlinear systems was proposed. A different kinematics model for formation control based on leader follower approach was presented in [20], where centroid acceleration and

angular acceleration of any follower are considered as 4 control inputs, and each control input consists of feedback linearization and sliding mode parts. In [21-23], a leader-leader- follower first order and second order model for formation control of mobile robots, using state feedback linearization was presented, where each follower updates its position by adjusting its distance from two leaders. An observer based input output feedback linearization method for formation control of mobile robots was presented in [24]. Some experimental results of formation and noise control of mobile robots based on leader follower method were developed in [25]. Furthermore, some other strategies like backstepping [26-32], Lyapunov direct[33-37], fuzzy logic [38-44], neural network [45-51] center manifold [52], have been proposed for formation control based on the leader follower model.

Formation control of a MAS can also be achieved by defining artificial potential functions. Potential function based methods, for kinematics control, consider a positive function, as the potential function of the whole MAS, where it is sum of two positive definite functions. The first term of the potential function, which corresponds to aggregation [53] or formation of the MAS, is the sum of two positive repulsion and attractions components. This term can be seen as the structural or strain potential energy of the MAS [54]. The second term of the potential function is usually a positive definite potential function with respect to a target. Advantage of the potential function based technique is in self organization of arrangement of agents which avoid inter-agent collision among them. This is because of repulsive and attractive forces existing among agents which adjusts inter agent distances in a reasonable range, not to be too close or too far. In addition a similar potential function can be defined for a MAS with respect to an

obstacle to avoid collision of MAS with an external obstacle. References [52-65] present, formation control and obstacle avoidance of MAS using the artificial potential function model, which is applicable in navigation and transportation control [55-59] and path planning [60-61]. In [67-69] a potential function is defined to preserve the connectivity of the communication graph of a multi agent system. Also, robust-adaptive [70-72], adaptive-H^{∞} [73, 74], robust-H^{∞} [75], and adaptive [76] for formation control strategies of MAS with uncertain parameters, based on potential function, have been proposed.

Keeping formation of a MAS using virtual structure is another strategy for formation control [77-91]. Using this model, a whole MAS is considered as a single body, so, desired trajectories of the agents are designed such that inter-agent distances don't change during MAS motion. One advantage of the virtual structure is that it is not a leader based approach; therefore it is robust enough in case of desired trajectory perturbation of agents of a MAS [77]. Furthermore, prescription of the desired kinematics to the MAS is easy in comparison with leader follower approach. However, Rigidity of the virtual structure influences the turning performance of the multi agent system [78]. Another disadvantage of rigid virtual structure is that the multi agent system has problem of passing through the narrow channel and collision avoidance [79]. To resolve the rigidity problem of the virtual structures, flexible virtual structure formation control has been proposed in [78, 80] which is curve compliant and has better turning performance [78, 80].

Behavioral based approach has also been suggested for formation control of MAS [92-96]. This method uses one of these three strategies: 1- Unit-center-referenced (each robot updates its own position based on average of the position of its neighbors), 2-

Leader-referenced (each robot communicates with a leader to set its position), and 3-Neighbor-referenced (each robot keeps its relative distance and orientation with respect to its neighbors) [92, 93].

Basics of consensus algorithm for cooperative control of teams of agents are described in references [97-99]. In this regard, Perron-Ferobenius theorem [99 and 101] for non-negative matrices is used to show that cooperative (consensus) stability of the system can be achieved if communication matrix of a network is irreducible or completely triangular reducible matrix [99]. As the result, all states of the cooperatively stable network eventually converge to a constant vector $C\mathbf{1}$, where scalar C depends on right and left eigenvectors of the network and initial states of the system [99]. Also, when a MAS evolves under single integrator kinematics model and based on consensus algorithm, time derivative of states of the agents is equal to minus of the Laplacian of the network [97, 98 and 100]. Based on principles of graph theory [101 and 102], all eigenvalues of the Laplacian of a graph is non-negative, when the first eigenvalue of a connected graph is zero and the corresponding eigenvector is **1.** Therefore, final states of all agents of the MAS are the same. This results in cooperative stability of the MAS evolution. In addition, formation control of output vector field of a MAS using consensus algorithm has been presented in [100].

By utilizing consensus algorithms, formation control of a multi robot system can be achieved, where all agents compromise to settle on a unique state, as the desired state, during MAS evolution. In the case of kinematics control, this leads to rigid body translation of desired formation of the MAS in an *n-D* space. Therefore, similar to virtual

structures and leader follower methods, consensus algorithms face a rigidity problem in cases where the size of the MAS is required to shrink.

PDE based models for formation control of MAS is an elegant approach that has been presented in [103-106]. PDE based techniques are indeed boundary control based. Boundary control method is a common technique to control distributed parameter systems governed by hyperbolic and parabolic PDEs [107-112]. An effective method for boundary control of an unstable first order one dimensional parabolic PDE has been proposed in [107, 108 and 110]. Furthermore, modeling of the single integrator based dynamics of a multi agent system by a one dimensional first order parabolic PDE has been presented in [103-105]. Moreover, double integrator based dynamics of a multi agent system has been modeled using a stable one dimensional second order PDE in [106].

PDE approach treats evolution of MAS in an n-D space as *n* one-dimensional MAS evolution problems, where every coordinate of motion of the MAS is modeled as a first order PDE (for single integrator kinematics model) and second order PDE (for double integrator kinematic model). The bulk motion and size of every coordinate of the MAS motion is controlled by imposing desired boundary conditions on the motion of the leader agents placed at the boundaries. In addition, the inter-agent distances are adjusted by spatially varying parameters of the PDEs. In this regard, two leader agents are required to guide the MAS while every follower agent communicates with two adjacent agents, in order to achieve evolution of every coordinate of the MAS. Consequently, MAS evolution in an n-D space is achieved when *2n* agents lead the MAS and every follower agent communicates with *2n* local agents in nearby. However, there are still

some issues which have not been addressed by PDE based techniques. First, desired formation of the MAS is the solution of a set of PDEs with spatially varying parameters; therefore, it may be difficult to obtain exact desired formation of the MAS. On the other hand, discretization of PDE may lead to obtaining an inaccurate distribution for the desired formation of the MAS. Second, although PDE based techniques guarantee asymptotic convergence of initial formation of the MAS to a desired final formation, the follower agents may leave the region bounded by leaders during transition, and there is no mechanism to check under what conditions followers will remain surrounded by the leader agents. Third, alteration of formation using PDE based approaches is achieved when leader agents move such that size of the MAS shrinks or expands.

CHAPTER 2: KINEMATICS OF CONTINUA

2.1 Kinematics of General Continuum Deformations

2.1.1 Position Field

Mapping $\boldsymbol{r}$: $(R^n, t) \rightarrow (R^n, t)$ is called continuum based if

- It is homeomorphic. A mapping $\boldsymbol{r} = \boldsymbol{r}(\boldsymbol{R}, t)$ is called homeomorphic if the Jacobian of the mapping is non-singular,

$$F(\boldsymbol{R}, t) = \frac{\partial \boldsymbol{r}}{\partial \boldsymbol{R}} \neq 0 \tag{2.1}$$

- $\boldsymbol{r}(\boldsymbol{R}, 0) = \boldsymbol{R}$, where I is the identity matrix.

Let the position of particles of a continuum in the initial domain called *material coordinates* be denoted by $\boldsymbol{R}$. Schematic of a continuum based mapping is shown in Fig. 2.1. As illustrated initial domain Ω_0 at time $t = t_0$ is mapped to the domain Ω_t at time $t \geq t_0$ under a continuum based mapping $\boldsymbol{r} = \boldsymbol{r}(\boldsymbol{R}, t)$.

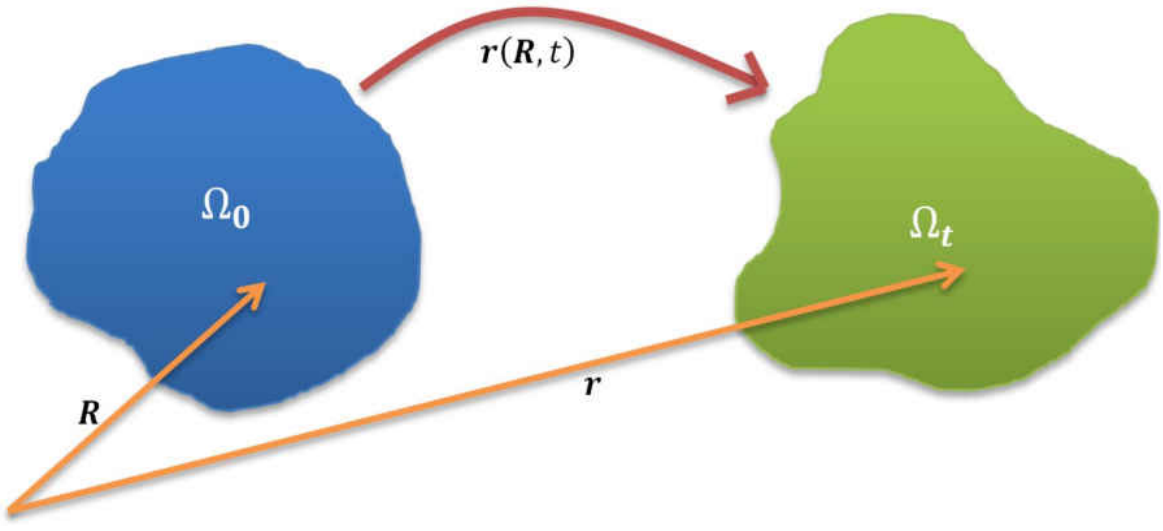

Figure 2.1 Schematic of a continuum based mappings

One interesting feature of transformation of a continuum under a continuum based mapping is that no of two material points can occupy the same location during the transformation. This is because the Jacobian of continuum based mappings remain non-singular during the transformation.

Material coordinate $\boldsymbol{R}$, and current position $\boldsymbol{r}(t)$ can be expressed with respect to the Cartesian coordinate system that is constructed with orthogonal unit vectors $\boldsymbol{e}_1$, $\boldsymbol{e}_2$, and $\boldsymbol{e}_3$. Let $\boldsymbol{r} = x_1\boldsymbol{e}_1 + x_2\boldsymbol{e}_2 + x_3\boldsymbol{e}_3$ be current position of a material particle which was initially located at $\boldsymbol{R} = X_1\boldsymbol{e}_1 + X_2\boldsymbol{e}_2 + X_3\boldsymbol{e}_3$, position vector $\boldsymbol{r}(t)$ can be written in the following component form:

$$x_1 = x_1(X_1, X_2, X_3, t) \tag{2.2}$$

$$x_2 = x_2(X_1, X_2, X_3, t) \tag{2.3}$$

$$x_3 = x_3(X_1, X_2, X_3, t) \tag{2.4}$$

It is noted that characteristics of continuum based mapping $\boldsymbol{r}$ that was listed above can be restated as

- $F(X_1, X_2, X_3, t) = \frac{\partial(x_1, x_2, x_3)}{\partial(X_1, X_2, X_3)} \neq 0$ (2.5)
- and $x_1(X_1, X_2, X_3, 0) = X_1$, $x_2(X_1, X_2, X_3, 0) = X_2$, and $x_3(X_1, X_2, X_3, 0) = X_3$.

2.1.2 Material and Spatial Descriptions

Let φ be a distributed state function that is defined over position field of a continuum, then, φ can be expressed in terms of either initial position field or current position field of a continuum. In other words, φ can be formulated based on material coordinate of a continuum, $\varphi = \varphi(X_1, X_2, X_3, t)$, or based current position field of a

continuum, $\varphi = \varphi(x_1, x_2, x_3, t)$. The first expression is called *material description* and the second one is called *spatial description*.

The time derivative of φ is called the *material derivative* and denoted by $\frac{D}{Dt}$ [113]. For material derivative of the material description of φ, $\varphi(X_1, X_2, X_3, t)$, we can write

$$\frac{D\varphi}{Dt} = \frac{\partial \varphi(X_1, X_2, X_3, t)}{\partial t} \tag{2.6}$$

Also, material derivative of spatial description of φ, $\varphi(x_1, x_2, x_3, t)$ is formulated by:

$$\frac{D\varphi}{Dt} = \frac{\partial \varphi(x_1, x_2, x_3, t)}{\partial t} + v_i(x_1, x_2, x_3, t)\frac{\partial \varphi(x_1, x_2, x_3, t)}{\partial x_i} \tag{2.7}$$

where

$$v_i(X_1, X_2, X_3, t) = \frac{Dx_i(X_1, X_2, X_3, t)}{Dt} \tag{2.8}$$

is the i-th component of velocity of material point initially located at (X_1, X_2, X_3), and $v_i \frac{\partial \varphi}{\partial x_i}$ is known as Einstein's summation convention. By using this convention, expression of summation terms in mathematical equations is shortened and simplified.

2.1.3 Velocity and Acceleration Fields

Material description of velocity field is already formulated by eqn. (2.8). Since $\boldsymbol{r} = \boldsymbol{r}(\boldsymbol{R}, t)$ is invertible, current position vector of a material point $\boldsymbol{r} = x_i \boldsymbol{e}_i$ can be related to the material coordinate $\boldsymbol{R} = X_i \boldsymbol{e}_i$, and velocity can be expressed by spatial description ($\boldsymbol{v} = v_i(x_1, x_2, x_3, t)\boldsymbol{e}_i$).

Acceleration of a continuum is the material derivative of the velocity field that can be expressed by material description,

$$\boldsymbol{a}(X_1, X_2, X_3, t) = a_i(X_1, X_2, X_3, t)\boldsymbol{e}_i = \frac{\partial v_i(X_1, X_2, X_3, t)}{\partial t}\boldsymbol{e}_i, \tag{2.9}$$

or by spatial description,

$$\boldsymbol{a}(x_1, x_2, x_3, t) = a_i(x_1, x_2, x_3, t)\boldsymbol{e}_i$$

$$= \left(\frac{\partial v_i(x_1, x_2, x_3, t)}{\partial t} + v_i(x_1, x_2, x_3, t)\frac{\partial \varphi(x_1, x_2, x_3, t)}{\partial x_i}\right)\boldsymbol{e}_i \tag{2.10}$$

2.1.4 Deformation Gradient Tensor

Deformation gradient of a continuum based mapping,

$$F = \nabla_{\boldsymbol{X}}\boldsymbol{x} = \begin{bmatrix} \frac{\partial x_1}{\partial X_1} & \frac{\partial x_1}{\partial X_2} & \frac{\partial x_1}{\partial X_3} \\ \frac{\partial x_2}{\partial X_1} & \frac{\partial x_2}{\partial X_2} & \frac{\partial x_2}{\partial X_3} \\ \frac{\partial x_3}{\partial X_1} & \frac{\partial x_3}{\partial X_2} & \frac{\partial x_3}{\partial X_3} \end{bmatrix}, \tag{2.11}$$

relates $d\boldsymbol{X}$ to $d\boldsymbol{x}$ by

$$d\boldsymbol{x} = Fd\boldsymbol{X} \tag{2.12}$$

It is noted that deformation gradient tensor F can be viewed as the Jacobian of a continuum based mapping. By using *polar decomposition theorem* [113], deformation gradient tensor F can be decomposed to a product of an orthogonal tensor and a symmetric tensor. One can write

$$F = RU = VR \tag{2.13}$$

where R is an orthogonal tensor, $U$and V are symmetric positive definite tensors. It is noted that eigenvalues of U and V are the same. Also, U and V can be related by

$$V = RUR^T \tag{2.14}$$

Pre-multiplying a material element $d\boldsymbol{X}$ by U leads to pure stretch of $Ud\boldsymbol{X}$. If stretched element $Ud\boldsymbol{X}$ is pre-multiplied by an orthogonal (rotation) tensor, the deformed element $d\boldsymbol{x}$ is achieved. In Fig. 2.2, it is shown that a 2-D material elements is stretched under U and then it is rotated under R.

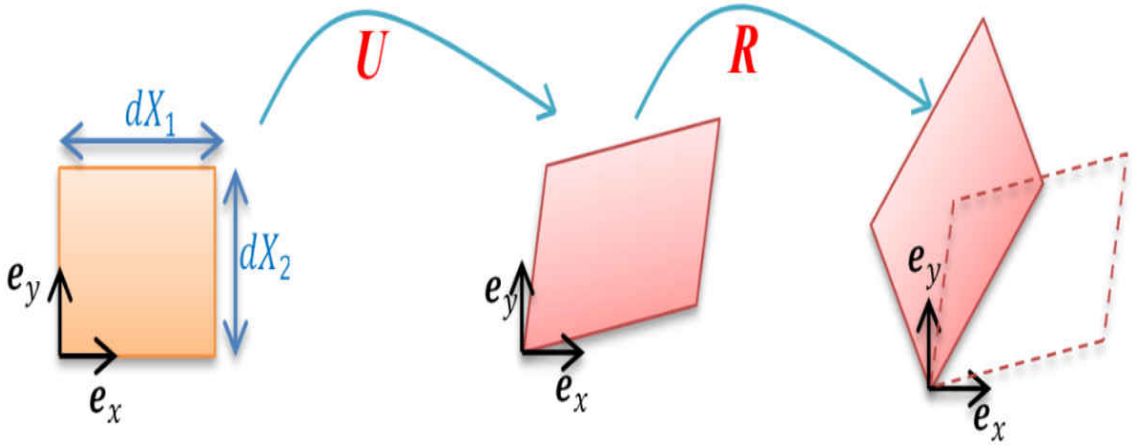

Figure 2.2 Stretch and subsequent rotation of a material element

2.2 Homogenous Transformations

Let deformation gradient (Jacobian) tensor of a continuum be only time varying (not spatially varying) at any time $t \geq t_0$ ($F = F(t)$) and

$$F|_{t=t_0} = \begin{bmatrix} 1 & 0 & 0 \\ 0 & 1 & 0 \\ 0 & 0 & 1 \end{bmatrix}, \tag{2.15}$$

then, the corresponding continuum based mapping is called *homogenous transformation*. By considering eqn. (2.12), homogenous transformation can be formulated by

$$\boldsymbol{r} = F(t)\boldsymbol{R} + \boldsymbol{D}(t) \tag{2.16}$$

where $\boldsymbol{D}(t)$ is called *rigid body displacement vector*.

2.2.1 Position Field

Under homogenous transformation of a continuum, the position field of the current domain of the continuum, Ω_t, is related to the initial domain Ω_0 by eqn. (2.16). Let Position field of a continuum be formulated by using Einstein's convention as follows:

$$x_i(t) = F_{ij}(t)X_j + D_i(t), \tag{2.17}$$

where free index *i* can take either *1* or *2* or 3.

As it is obvious, homogenous transformation is a linear mapping that transforms a line in the initial domain Ω_0 to another line in the current domain Ω_t. In addition, under homogenous transformation an ellipsoidal domain inside Ω_0 is mapped to another ellipsoidal domain inside Ω_t.

2.2.2 Velocity and Acceleration Field

Material description of the velocity field of a continuum can be obtained by taking time derivative from eqn. (2.16), that is

$$\boldsymbol{v} = \dot{F}(t)\boldsymbol{R} + \dot{\boldsymbol{D}}(t) \tag{2.18}$$

where $\dot{F}(t)$ and $\dot{\boldsymbol{D}}(t)$ denote time derivative of $F(t)$ and $\boldsymbol{D}(t)$, respectively. Equation (2.18) can also be written by using Einstein's convention as

$$v_i = \dot{F}_{ij}X_j + \dot{D}_i \tag{2.19}$$

Moreover, velocity field can be stated in the spatial form if $\boldsymbol{R}$ in eqn. (2.18) is replaced by $F^{-1}(\boldsymbol{r} - \boldsymbol{D})$. Thus,

$$\boldsymbol{v} = \dot{F}F^{-1}\boldsymbol{r} + \left(\dot{\boldsymbol{D}} - \dot{F}F^{-1}\boldsymbol{D}\right) \tag{2.20}$$

Equation (2.20) can also be formulated by using Einstein's convention as follows:

$$v_i = \dot{F}_{ij}F^{-1}{}_{jm}x_m + \dot{D}_i - \dot{F}_{ij}F^{-1}{}_{jm}D_m \tag{2.21}$$

Furthermore, acceleration field of homogenous transformation can be similarly obtained by taking time derivative from the velocity field and expressed in material or spatial forms. Material description of the velocity field is obtained to be

$$\boldsymbol{a} = \ddot{F}(t)\boldsymbol{R} + \ddot{\boldsymbol{D}}(t) \tag{2.22}$$

Also, spatial description of acceleration field is expressed by relation (2.23).

$$\boldsymbol{v} = \ddot{F}F^{-1}\boldsymbol{r} + \left(\ddot{\boldsymbol{D}} - \ddot{F}F^{-1}\boldsymbol{D}\right) \tag{2.23}$$

In addition, material and spatial description of the acceleration field are restated by using Einstein's convention in eqns. (2.24) and (2.25).

$$a_i = \ddot{F}_{ij}X_j + \ddot{D}_i \tag{2.24}$$

$$a_i = \ddot{F}_{ij}F^{-1}{}_{jm}x_m + \ddot{D}_i - \ddot{F}_{ij}F^{-1}{}_{jm}D_m \tag{2.25}$$

2.3 Prescription of Homogenous Maps

2.3.1 Homogenous Mapping in an $n-D$ Space

In this section, homogenous transformation of an *n-D* (*n>1)* domain is formulated based on positions of *n+1* material points of an *n-D* manifold. Let $\boldsymbol{R}_1$, $\boldsymbol{R}_2$, …, $\boldsymbol{R}_{n+1}$ denote positions of *n+1* material points *1, 2, ..., n+1,* of an initial *n-D* manifold Ω_0 such that

$$Rank\{\boldsymbol{R}_1, \boldsymbol{R}_2, \dots, \boldsymbol{R}_{n+1}\} = n, \tag{2.26}$$

then, these material points are mapped to $\boldsymbol{r}_1$, $\boldsymbol{r}_2$, …, $\boldsymbol{r}_{n+1}$ in the current manifold Ω_t at time $t \geq t_0$ under a homogenous transformation, where

$$Rank\{\boldsymbol{r}_1(t), \boldsymbol{r}_2(t), \dots, \boldsymbol{r}_{n+1}(t)\} = n. \tag{2.27}$$

as well.

Suppose that $\boldsymbol{R}_i$ is mapped to $\boldsymbol{r}_i$ (*i* spans *1, 2, ..., n+1*) under a homogenous mapping and it is desired that elements of the Jacobian matrix *F* and rigid body displacement vector $\boldsymbol{D}$ are assigned based on components of $\boldsymbol{R}_i$ and $\boldsymbol{r}_i$. Replacing $\boldsymbol{R}$ and $\boldsymbol{r}$ in eqn. (2.16) by $\boldsymbol{R}_i$ and $\boldsymbol{r}_i$ (*i =1, 2, ..., n+1*) leads to following set of *n+1* linear algebraic equations with *n+1* unknowns:

$$J = [I_n \otimes L_0 \quad \vdots \quad I_n \otimes \mathbf{1}_{(n+1)\times 1}]^{-1} P_t \tag{2.28}$$

where

$$L_0 = \begin{bmatrix} X_{1_1} & \cdots & X_{n_1} \\ \vdots & \ddots & \vdots \\ X_{1_{n+1}} & \cdots & X_{n_{n+1}} \end{bmatrix}_{(n+1)\times n}, \tag{2.29}$$

$$J_{n(n+1)\times 1} = [Q_{11} \quad \dots \quad Q_{1n} \quad \dots \quad Q_{n1} \quad \dots \quad Q_{nn} D_1 \quad \dots \quad D_n]^T, \tag{2.30}$$

and

$$P_{t_{(n+1)\times 1}} = [x_{1_1}(t) \quad \dots \quad x_{1_{n+1}}(t) \dots \quad x_{n_1}(t) \quad \dots \quad x_{n_{n+1}}(t)]^T \tag{2.31}$$

It is noted that if the rank condition (2.26) is met, then, rank of the augmented matrix

$$L_1 = [L_0 \quad \vdots \quad \mathbf{1}_{(n+1)\times 1}]_{(n+1)\times(n+1)} \tag{2.32}$$

is *n+1* and consequently *J* is invertible.

2.3.2 Homogenous Mapping in a $2-D$ Space

Suppose that material points *1*, *2,* and *3* are initially non-aligned and placed at $\boldsymbol{R}_1$, $\boldsymbol{R}_2$, and $\boldsymbol{R}_3$. Since they are non-aligned, therefore

$$Rank\{\boldsymbol{R}_1, \boldsymbol{R}_2, \boldsymbol{R}_3\} = 2, \tag{2.33}$$

and rank of the augmented matrix

$$L_1 = \begin{bmatrix} X_1 & Y_1 & 1 \\ X_2 & Y_2 & 1 \\ X_3 & Y_3 & 1 \end{bmatrix} \tag{2.34}$$

is 3.

This leads elements of the Jacobian matrix *F* and rigid body displacement vector *D* to be uniquely related to the current position vectors of material points *1, 2,* and *3* by simplification of eqn. (2.28) to the following form:

$$\begin{bmatrix} F_{11}(t) \\ F_{12}(t) \\ F_{21}(t) \\ F_{22}(t) \\ D_{11}(t) \\ D_{21}(t) \end{bmatrix} = \begin{bmatrix} X_1 & Y_1 & 0 & 0 & 1 & 0 \\ X_2 & Y_2 & 0 & 0 & 1 & 0 \\ X_3 & Y_3 & 0 & 0 & 1 & 0 \\ 0 & 0 & X_1 & Y_1 & 0 & 1 \\ 0 & 0 & X_2 & Y_2 & 0 & 1 \\ 0 & 0 & X_3 & Y_3 & 0 & 1 \end{bmatrix}^{-1} \begin{bmatrix} x_1(t) \\ x_2(t) \\ x_3(t) \\ y_1(t) \\ y_2(t) \\ y_3(t) \end{bmatrix} \tag{2.35}$$

Shown in Fig. 2.3 is the schematic of homogenous transformation of a 2-D continuum in a plane. As illustrated, material points *1, 2,* and *3* remain non-aligned during transformation at any time $t \geq t_0$. Thus, they can be considered as the vertices of a triangle called *leading triangle*.

It is noted that determinant of the Jacobian matrix *F* is equal to ratio of the area of the leading triangle in the current domain Ω_t to the area of the leading triangle in the initial domain Ω_0.

Although, material points *1, 2,* and *3* can be any three non-aligned material points of the continuum, nevertheless, we desire choose vertices of a triangle embedding the continuum as fictitious or material points *1*, *2*, and *3*. It is also noted that if points *1*, *2*, and *3* belong to the continuum then they are material points; otherwise they are fictitious. Without loss of generality, in the following we assume that initial domain of a continuum

is a leading triangle that is constructed with material points *1*, *2*, *3*. These material points are called *leading points*.

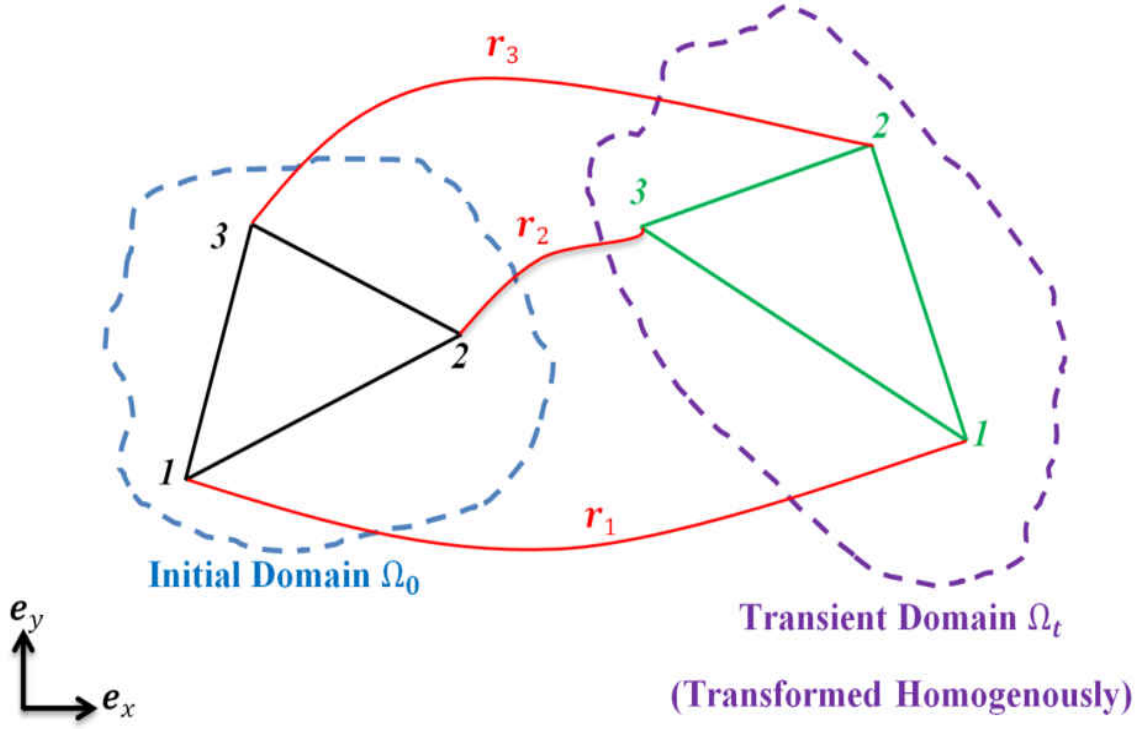

Figure 2.3 Schematic of homogenous transformation of a 2-D domain

It is advantageous to surround a continuum in a leading triangle since one can assure that the continuum does not leave the leading triangle while it transforms under a homogenous mapping. Therefore, collision of the continuum as a moving deformable body with obstacles in the 2-D plane can be avoided if paths of leading points *1*, *2*, and *3* are designed properly. Shown in Fig. 2.4 is a homogenous transformation of a moving deformable body in a 2-D plane that contains some obstacles. As seen paths of the leading points *1*, *2*, and *3* are chosen appropriately such that they don't collide with the obstacles, and consequently, collision avoidance of material points of the continuum is assured as well.

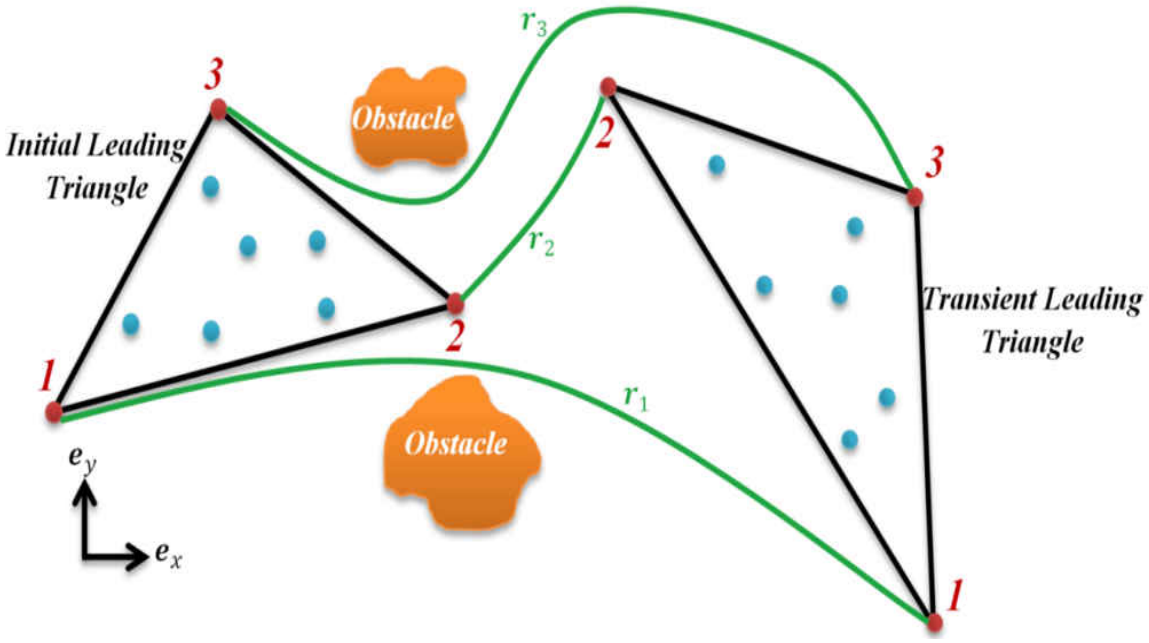

Figure 2.4 Homogenous transformation of a triangular continuum in a motion field with obstacles

2.3.3 Formulation of 2-D Homogenous Mappings Using Einstein's Convention

Since homogenous transformation is linear, displacement field of a continuum can be considered as a linear combination of position vectors of three non-aligned points of the continuum, $\boldsymbol{r}_1(t)$, $\boldsymbol{r}_2(t)$, and $\boldsymbol{r}_3(t)$, as follows [4, 114, and 115]:

$$\forall t \geq 0, \boldsymbol{r}(t) = \sum_{k=1}^{3} \alpha_k \boldsymbol{r}_k(t) \tag{2.36}$$

where $\alpha_i$are constant parameters assigned based on initial position of continuum [4], and

$$\sum_{k=1}^{3} \alpha_k = 1. \tag{2.37}$$

Let $\boldsymbol{R} = X\boldsymbol{e}_x + Y\boldsymbol{e}_y$ be the initial position of an arbitrary point of the continuum, and $\boldsymbol{R_1} = X_1\boldsymbol{e}_x + Y_1\boldsymbol{e}_y$, $\boldsymbol{R_2} = X_2\boldsymbol{e}_x + Y_2\boldsymbol{e}_y$, and $\boldsymbol{R_3} = X_3\boldsymbol{e}_x + Y_3\boldsymbol{e}_y$ denote initial positions of the leading points of the continuum, then considering eqns. (2.36) and (2.37) for the time $t = 0$, leads to obtaining α_1, α_2, and α_3 by solving following set of three linear algebraic equations:

$$\begin{bmatrix} X_1 & X_2 & X_3 \\ Y_1 & Y_2 & Y_3 \\ 1 & 1 & 1 \end{bmatrix} \begin{Bmatrix} \alpha_1 \\ \alpha_2 \\ \alpha_3 \end{Bmatrix} = \begin{Bmatrix} X \\ Y \\ 1 \end{Bmatrix}. \tag{2.38}$$

Thus,

$$\begin{Bmatrix} \alpha_1 \\ \alpha_2 \\ \alpha_3 \end{Bmatrix} = \frac{1}{2a} \begin{bmatrix} Y_2 - Y_3 & X_3 - X_2 & X_2Y_3 - X_3Y_2 \\ Y_3 - Y_1 & X_1 - X_3 & X_3Y_1 - X_1Y_3 \\ Y_1 - Y_2 & X_2 - X_1 & X_1Y_2 - X_2Y_1 \end{bmatrix} \begin{Bmatrix} X \\ Y \\ 1 \end{Bmatrix} \tag{2.39}$$

where

$$a = \frac{1}{2} \begin{vmatrix} X_1 & X_2 & X_3 \\ Y_1 & Y_2 & Y_3 \\ 1 & 1 & 1 \end{vmatrix} \tag{2.40}$$

is the *area of the leading triangle which is constructed with leading points 1, 2, and 3*, that are located at $\boldsymbol{R_1}, \boldsymbol{R_2}$, and $\boldsymbol{R_3}$, respectively.

Elements of F and D: Replacing α_k ($k = 1,2,3$) in eqn. (2.36) by eqn. (2.39) and then equating right hand side of eqns. (2.16) and (2.36), leads elements of $F(t)$ and $D(t)$ to be as follows:

$$F_{11}(t) = \frac{1}{4a} \varepsilon_{ijk} x_i(t) \big(Y_j - Y_k\big) \tag{2.41}$$

$$F_{12}(t) = \frac{1}{4a} \varepsilon_{ijk} x_i(t) \big(X_k - X_j\big) \tag{2.42}$$

$$F_{21}(t) = \frac{1}{4a} \varepsilon_{ijk} y_i(t) \big(Y_j - Y_k\big) \tag{2.43}$$

$$F_{22}(t) = \frac{1}{4a} \varepsilon_{ijk} y_i(t) \big(X_k - X_j\big) \tag{2.44}$$

$$D_1(t) = \frac{1}{4a}\varepsilon_{ijk}x_i(t)\left(X_jY_k - Y_jX_k\right) \tag{2.45}$$

$$D_2(t) = \frac{1}{4a}\varepsilon_{ijk}y_i(t)\left(X_jY_k - Y_jX_k\right) \tag{2.46}$$

In eqns. (2.41-2.46), elements of $F(t)$ and $D(t)$ are expressed by using Einstein's summation convention, where *i* is the free index, *j* and *k* are dummy indices, ε_{ijk} is the permutation symbol [113],(X_i, Y_i) and (x_i, y_i) denote initial and current positions of the leading point *i*, respectively.

2.3.3.1 Material Description of Velocity and Acceleration Fields

One can replace elements of F and D in eqn. (2.18) by eqns. (2.41-2.46) and then rewrite material description of the velocity field, $(X, Y, t) = v_x(X, Y, t)\boldsymbol{e}_x + v_y(X, Y, t)\boldsymbol{e}_y$, as follows:

$$v_x(X, Y, t) = \frac{\varepsilon_{ijk}\dot{x}_i(t)}{4a}\left\{\left(Y_j - Y_k\right)X + \left(X_k - X_j\right)Y + \left(X_jY_k - Y_jX_k\right)\right\} \tag{2.47}$$

$$v_y(X, Y, t) = \frac{\varepsilon_{ijk}\dot{y}_i(t)}{4a}\left\{\left(Y_j - Y_k\right)X + \left(X_k - X_j\right)Y + \left(X_jY_k - Y_jX_k\right)\right\} \tag{2.48}$$

Similarly, components of material description of the acceleration field ($\boldsymbol{a} = a_x\boldsymbol{e}_x + a_y\boldsymbol{e}_y$) are formulated as

$$a_x(X, Y, t) = \frac{\varepsilon_{ijk}\ddot{x}_i(t)}{4a}\left\{\left(Y_j - Y_k\right)X + \left(X_k - X_j\right)Y + \left(X_jY_k - Y_jX_k\right)\right\} \tag{2.49}$$

$$a_y(X, Y, t) = \frac{\varepsilon_{ijk}\ddot{y}_i(t)}{4a}\left\{\left(Y_j - Y_k\right)X + \left(X_k - X_j\right)Y + \left(X_jY_k - Y_jX_k\right)\right\} \tag{2.50}$$

where *i* and *j* are dummy indices denoting index numbers of the leading points.

2.3.3.2 Spatial Description of Velocity and Acceleration Fields

Let $\boldsymbol{v} = v_x(x,y,t)\boldsymbol{e}_x + v_y(x,y,t)\boldsymbol{e}_y$ denote the spatial description of the velocity field, then, components of the velocity field can be obtained from eqn. (2.21) and be rewritten in the following form:

$$v_x(x,y,t) = c(t)x + d(t)y + e(t) \tag{2.51}$$

$$v_y(x,y,t) = f(t)x + g(t)y + h(t) \tag{2.52}$$

where

$$c(t) = \frac{1}{|F(t)|}\left(\dot{F}_{11}F_{22} - \dot{F}_{12}F_{21}\right) \tag{2.53}$$

$$d(t) = \frac{1}{|F(t)|}\left(\dot{F}_{12}F_{11} - \dot{F}_{11}F_{12}\right) \tag{2.54}$$

$$f(t) = \frac{1}{|F(t)|}\left(\dot{F}_{21}F_{22} - \dot{F}_{22}F_{21}\right) \tag{2.55}$$

$$g(t) = \frac{1}{|F(t)|}\left(\dot{F}_{22}F_{11} - \dot{F}_{21}F_{12}\right) \tag{2.56}$$

$$e(t) = \dot{D}_1 - \frac{1}{|F(t)|}\left(\left(\dot{F}_{11}F_{22} - \dot{F}_{12}F_{21}\right)D_1 + \left(\dot{F}_{12}F_{11} - \dot{F}_{11}F_{12}\right)D_2\right) \tag{2.57}$$

$$h(t) = \dot{D}_2 - \frac{1}{|F(t)|}\left(\left(\dot{F}_{21}F_{22} - \dot{F}_{22}F_{21}\right)D_1 + \left(\dot{F}_{22}F_{11} - \dot{F}_{21}F_{12}\right)D_2\right) \tag{2.58}$$

Similarly, spatial description of acceleration field, $\boldsymbol{a} = a_x(x,y,t)\boldsymbol{e}_x + a_y(x,y,t)\boldsymbol{e}_y$, can be formulated as follows:

$$a_x(x,y,t) = l(t)x + m(t)y + n(t) \tag{2.59}$$

$$a_y(x,y,t) = p(t)x + q(t)y + s(t) \tag{2.60}$$

where

$$l(t) = \frac{1}{|F(t)|}\left(\ddot{F}_{11}F_{22} - \ddot{F}_{12}F_{21}\right) \tag{2.61}$$

$$m(t) = \frac{1}{|F(t)|}\left(\ddot{F}_{12}F_{11} - \ddot{F}_{11}F_{12}\right) \tag{2.62}$$

$$p(t) = \frac{1}{|F(t)|}\left(\ddot{F}_{21}F_{22} - \ddot{F}_{22}F_{21}\right) \tag{2.63}$$

$$q(t) = \frac{1}{|F(t)|}\left(\ddot{F}_{22}F_{11} - \ddot{F}_{21}F_{12}\right) \tag{2.64}$$

$$n(t) = \ddot{D}_1 - \frac{1}{|F(t)|}\left(\left(\ddot{F}_{11}F_{22} - \ddot{F}_{12}F_{21}\right)D_1 + \left(\ddot{F}_{12}F_{11} - \ddot{F}_{11}F_{12}\right)D_2\right) \tag{2.66}$$

$$s(t) = \ddot{D}_2 - \frac{1}{|F(t)|}\left(\left(\ddot{F}_{21}F_{22} - \ddot{F}_{22}F_{21}\right)D_1 + \left(\ddot{F}_{22}F_{11} - \ddot{F}_{21}F_{12}\right)D_2\right) \tag{2.67}$$

2.4 Example

Let leaders *1*, *2*, and *3* be initially distributed at the vertices of the leading triangle as shown in Fig. 2.5. In Fig. 2.5, paths of leader agents from initial configuration to the final destination are also illustrated.

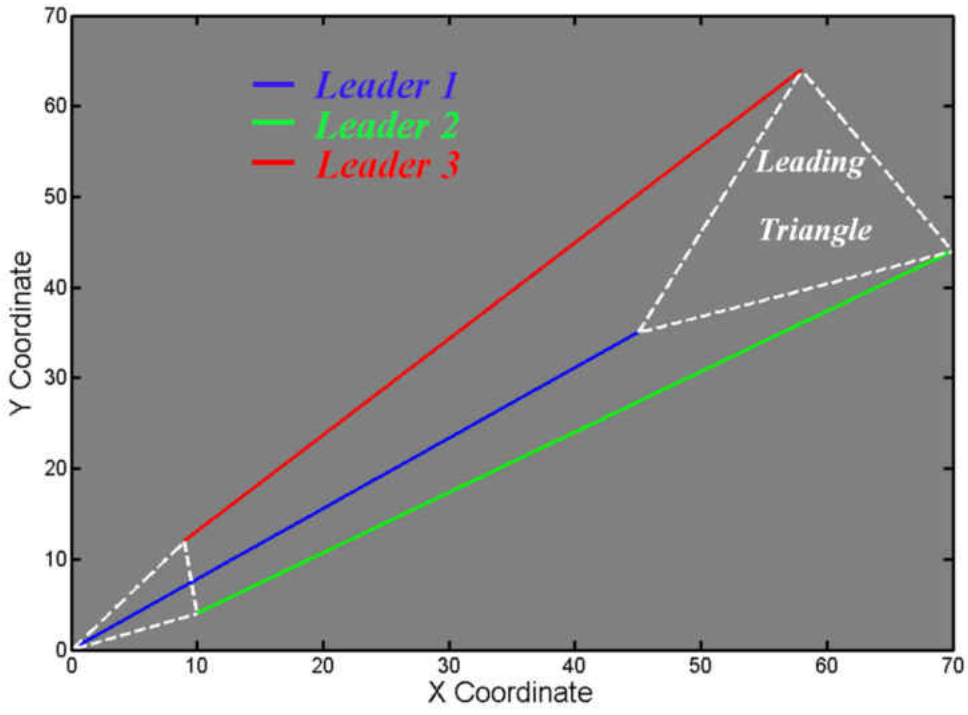

Figure 2.5 Paths of leader agents 1, 2, and 3

Moreover, in Figs. 2.6 and 2.7, *x* and *y* coordinates of leader agents versus time are shown.

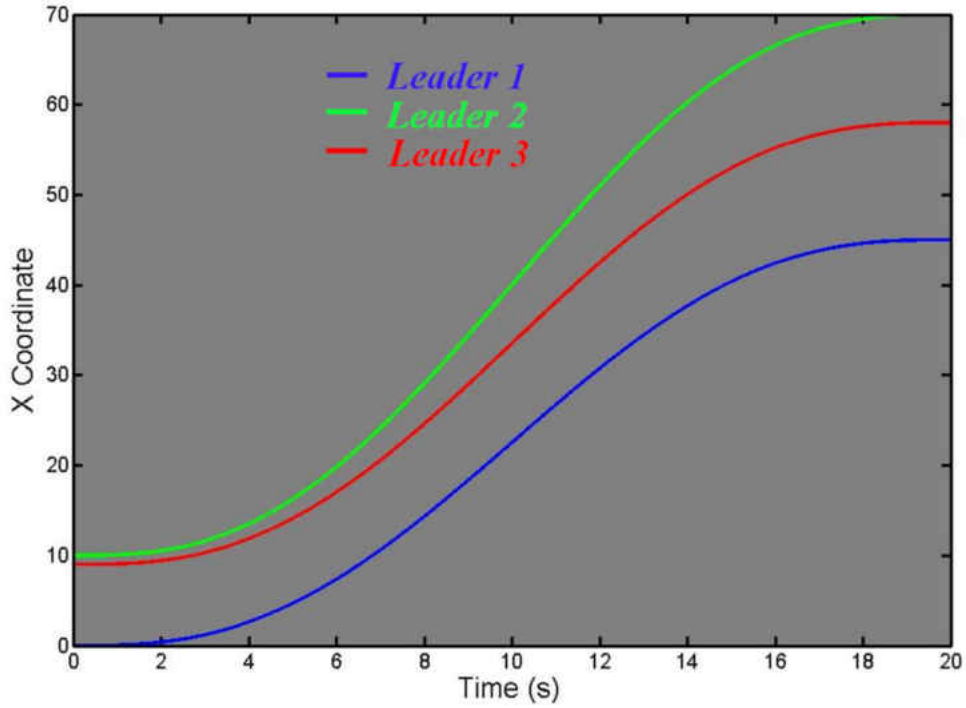

Figure 2.6 *x* coordinate of leading points versus time

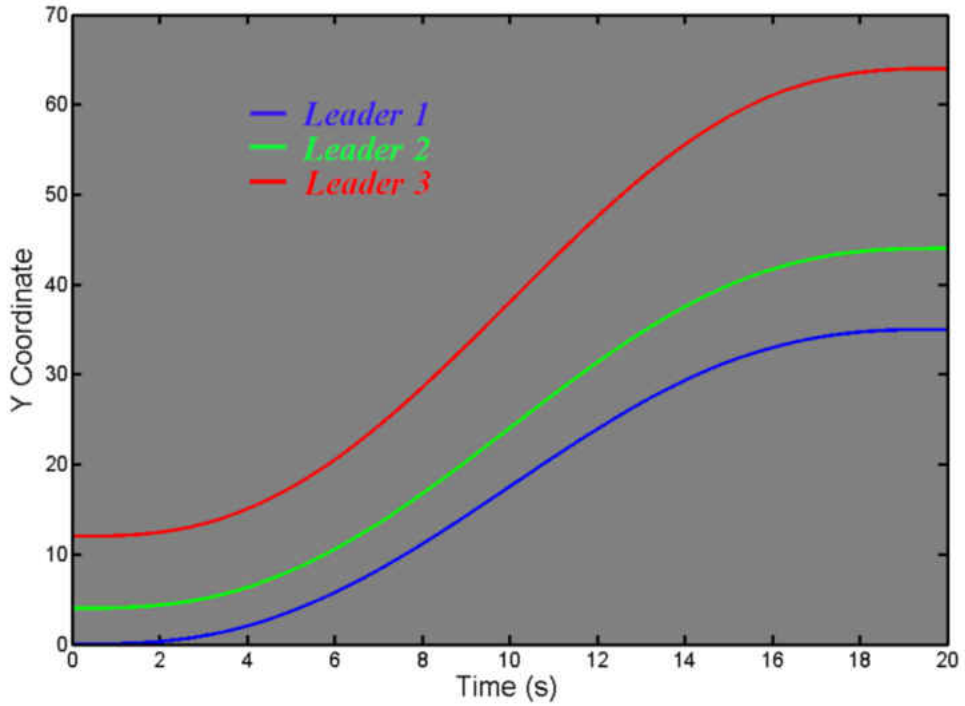

Figure 2.7 *y* coordinate of leading points versus time

As seen leaders settle in $20s$. Using eqn. (2.35), initial positions of the leader agents yield a $6x6$ matrix that relates current positions of the leaders to the elements of F and D. Shown in Fig. 2.8 and 2.9 are entries of F and D versus time.

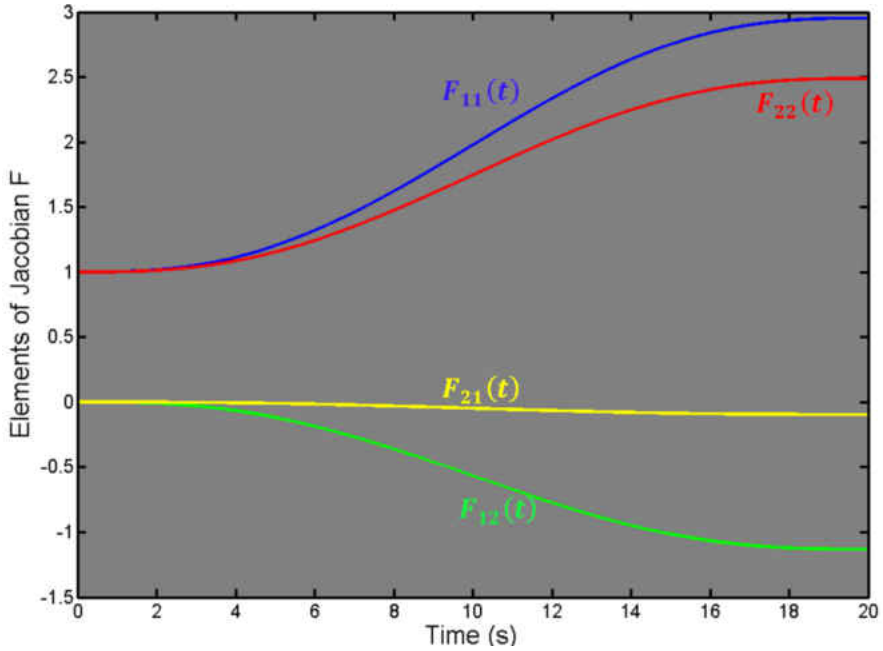

Figure 2.8 Elements of $F(t)$

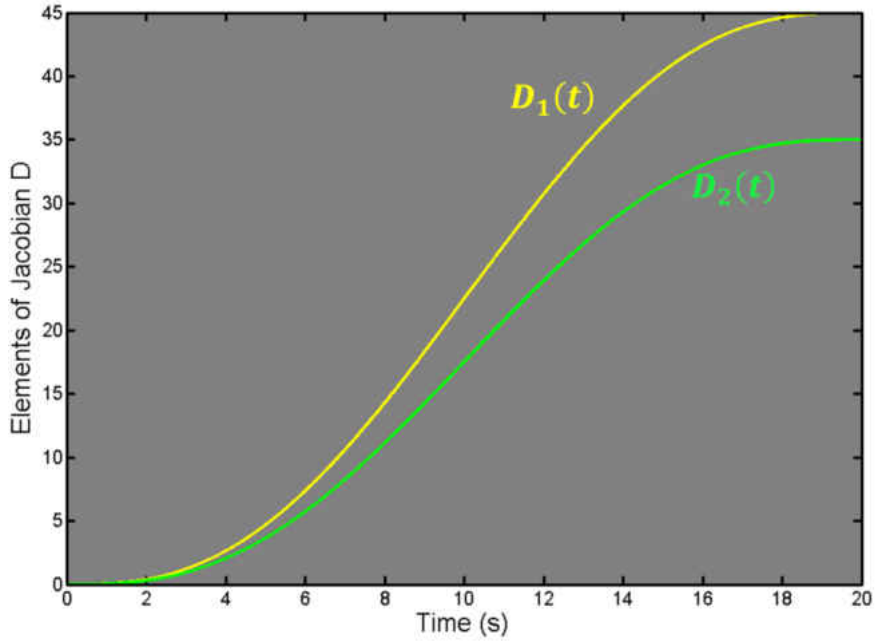

Figure 2.9 Elements of $D(t)$

As observed, $F(0) = I$ and $D(0) = \mathbf{0}$. These validate the first requirement for a homeomorphism to be a continuum based mapping. Eigenvalues of the Jacobian matrix F are also shown in Fig. 2.10.

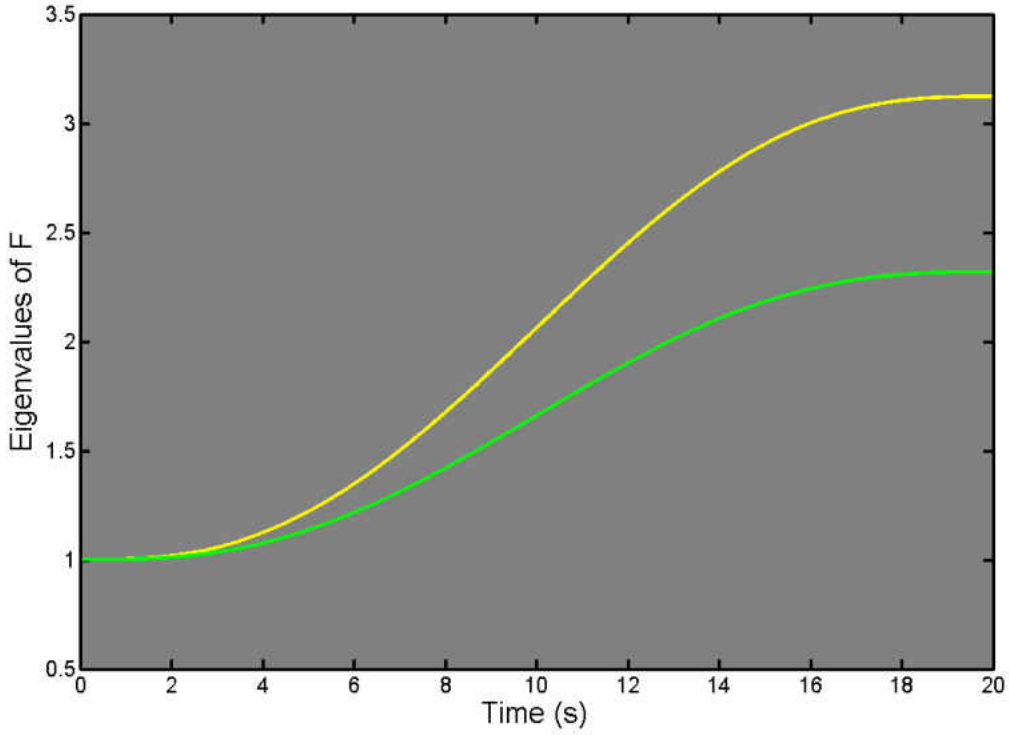

Figure 2.10 Eigenvalues of $F(t)$

As the eigenvalues are always positive F remains non-singular.

CHAPTER 3: MULTI AGENT SYSTEM AS PARTICLES OF A CONTINUUM

In this chapter, we consider agents of a MAS as material particles of a continuum whose evolution is modeled as kinematics of a deformable body. Without loss of generality, we assume that MAS is transformed under a homogenous mapping. A MAS under consideration consists of *N* agents numbered by *1*, *2*, ..., *N* and evolve in an *n-D* space where leader agents are numbered by *1*, *2*,…, *n+1*. Rest of the agents of the MAS (numbered by *n+2, n+3*, …, *N*) are called follower agents.

As stated in the previous chapter, leader agents evolve independently such that the rank condition (2.27) is satisfied. In addition, since homogenous transformation is a linear mapping, position of a follower agent *i* (*i=n+2*, *n+3*, *..., N*) can be expressed as a linear combination of positions of the leader agents as follows:

$$\boldsymbol{r}_i(t) = \sum_{k=1}^{n+1} \alpha_{i,k}\, \boldsymbol{r}_k(t) \tag{3.1}$$

where constant parameters $\alpha_{i,k}$ satisfy

$$\sum_{k=1}^{n+1} \alpha_{i,k} = 1. \tag{3.2}$$

In the following homogenous transformation of a MAS evolving in one, two, or three dimensional space is formulated.

3.1 Homogenous Transformation of MAS Evolving in a *1-D* Space

Suppose that agents of the a MAS are constrained to move on a straight line where agents are initially distributed on a segment called *leading segment*. As shown in

Fig. 3.1, green end points of the leading segment are located by the leader agents and followers are initially distributed at the red interior points.

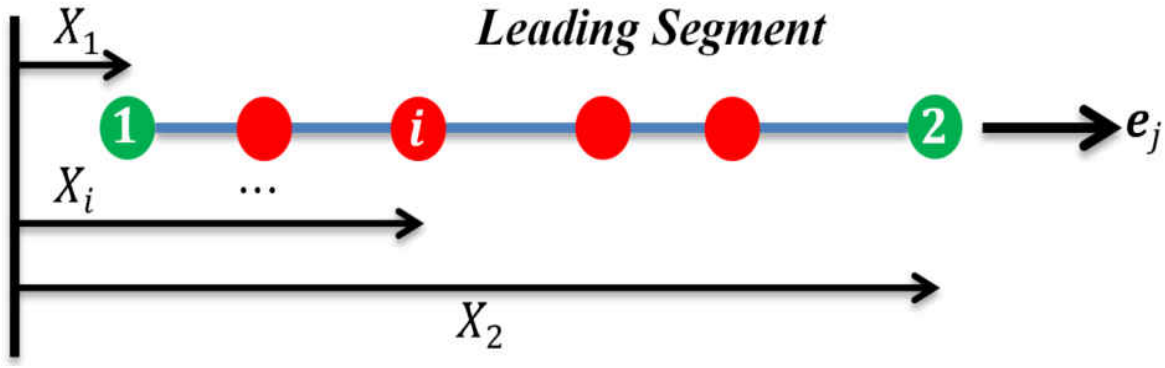

Figure 3.1 Leading segment

For 1-D MAS evolution, position of follower agent *i* can be expressed as a linear combination of position vectors of two leader agents. Let $X_1 = x_1(0)$, $X_2 = x_2(0)$, and $X_i = x_i(0)$ denote initial positions of leader agent *1*, leader agent *2*, and follower agent *i*, respectively, then, one can simplify eqn. (3.1) and (3.2) to the following form to express position of agent *i* as a linear combination of positions of the leader agents:

$$X_i = \alpha_{i,1}X_1 + \alpha_{i,2}X_2 \tag{3.3}$$

subject to

$$\alpha_{i,1} + \alpha_{i,2} = 1 \tag{3.4}$$

One can write eqns. (3.3) and (3.4) in the following matrix form:

$$\begin{bmatrix} X_1 & X_2 \\ 1 & 1 \end{bmatrix} \begin{Bmatrix} \alpha_{i,1} \\ \alpha_{i,2} \end{Bmatrix} = \begin{Bmatrix} X_i \\ 1 \end{Bmatrix} \tag{3.5}$$

Hence, weights ratios $\alpha_{i,1}$ and $\alpha_{i,2}$ are obtained to be

$$\alpha_{i,1} = \frac{X_2 - X_i}{X_2 - X_1} \tag{3.6}$$

$$\alpha_{i,2} = \frac{X_i - X_1}{X_2 - X_1} \tag{3.7}$$

and position of agent *i* under homogenous mapping can be written as follows:

$$x_i(t) = \alpha_{i,1}x_1(t) + \alpha_{i,2}x_2(t) = \frac{X_2 - X_i}{X_2 - X_1}x_1(t) + \frac{X_i - X_1}{X_2 - X_1}x_2(t) \tag{3.8}$$

As seen constant weight ratios $\alpha_{i,1}$ and $\alpha_{i,2}$ are only dependent on initial position of follower agent *i*, and leader agents *1* and *2*.

One can rewrite eqn. (3.8) as

$$x_i(t) = F(t)X_i + D(t) \tag{3.9}$$

where

$$F(t) = \frac{x_2(t) - x_1(t)}{X_2 - X_1} \tag{3.10}$$

$$D(t) = \frac{X_2x_1(t) - X_1x_2(t)}{X_2 - X_1} \tag{3.11}$$

are the Jacobian and the rigid body displacement of homogenous transformation, respectively.

3.2 Homogenous Transformation of a MAS Evolving in a *2-D* Space

Let leader agents *1*, *2*, and *3* are located at the vertices of the leading triangle and followers are distributed inside the leading triangle. In Fig. 3.2 an schematic of agents' distribution is shown. As seen green spots represent leader agents and they are located at the vertices of the leading triangle. Furthermore, red spots representing followers where they are distributed inside the leading triangle.

Under homogenous transformation of the MAS in the *x-y* plane, eqn. (3.1) is simplified to

$$\boldsymbol{r}_i(t) = \alpha_{i,1}\boldsymbol{r}_1(t) + \alpha_{i,2}\boldsymbol{r}_2(t) + \alpha_{i,3}\boldsymbol{r}_3(t) \tag{3.12}$$

subject to

$$\alpha_{i,1} + \alpha_{i,2} + \alpha_{i,3} = 1 \tag{3.13}$$

where $\alpha_{i,1}$, $\alpha_{i,2}$, and $\alpha_{i,3}$ are constant weight ratios, $\boldsymbol{r}_1(t) = x_1(t)\boldsymbol{e}_x + y_1(t)\boldsymbol{e}_y$, $\boldsymbol{r}_2(t) = x_2(t)\boldsymbol{e}_x + y_2(t)\boldsymbol{e}_y$, $\boldsymbol{r}_3(t) = x_3(t)\boldsymbol{e}_x + y_3(t)\boldsymbol{e}_y$, and $\boldsymbol{r}_i(t) = x_i(t)\boldsymbol{e}_x + y_i(t)\boldsymbol{e}_y$ denote position vectors of leader agents *1*, *2*, *3*, and follower agents *i* (*i=4, 5, ..., N*), respectively.

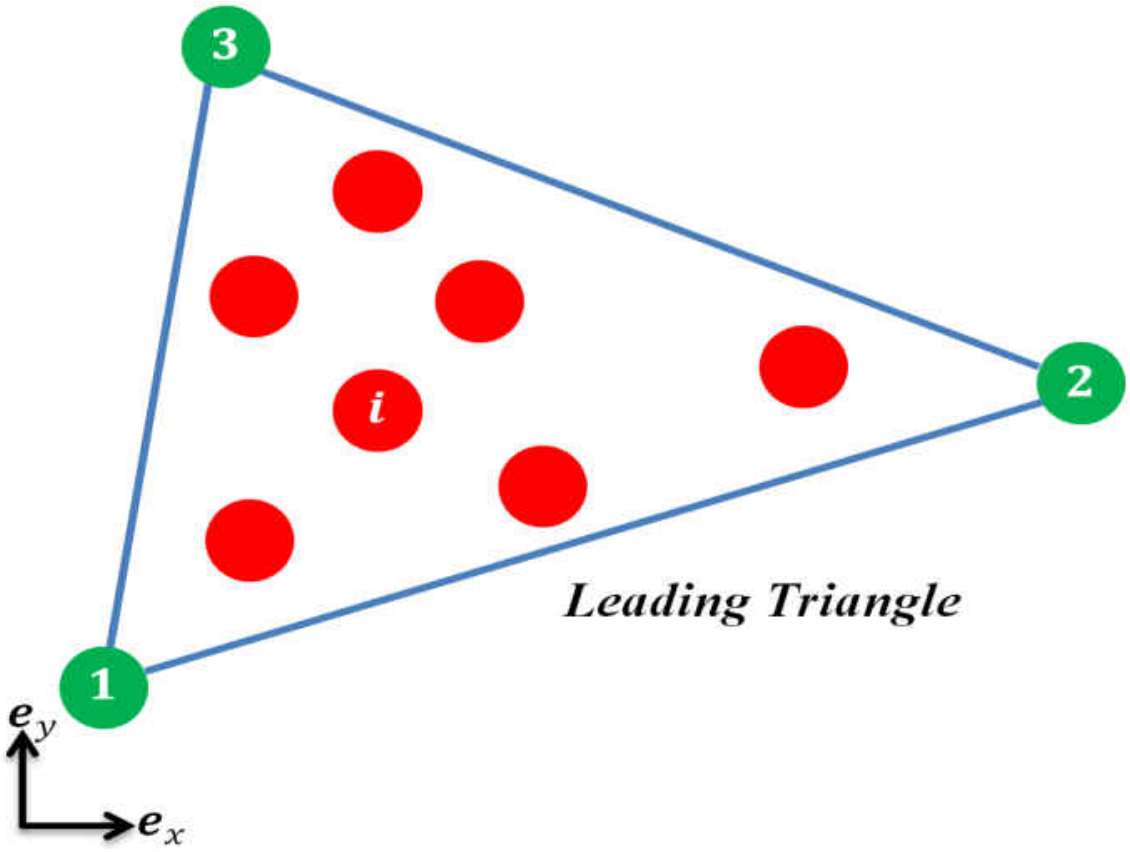

Figure 3.2 Leading triangle

Let $\boldsymbol{R}_1 = \boldsymbol{r}_1(0) = X_1\boldsymbol{e}_x + Y_1\boldsymbol{e}_y$, $\boldsymbol{R}_2 = \boldsymbol{r}_2(0) = X_2\boldsymbol{e}_x + Y_2\boldsymbol{e}_y$, and $\boldsymbol{R}_3 = \boldsymbol{r}_3(0) = X_3\boldsymbol{e}_x + Y_3\boldsymbol{e}_y$ denote initial positions of leader agents and $\boldsymbol{R}_i = \boldsymbol{r}_i(0) = X_i\boldsymbol{e}_x + Y_i\boldsymbol{e}_y$ denote initial position of flower agent i (*i* spans *3, 2, ..., N*), then, weights ratios $\alpha_{i,1}$, $\alpha_{i,2}$, and $\alpha_{i,3}$can be obtained by replacing $\boldsymbol{R}_i$, $\boldsymbol{R}_1$, $\boldsymbol{R}_2$, and $\boldsymbol{R}_3$ into eqn. (3.12). As the result,

following three set of linear algebraic equations needs to be solved in order to assign $\alpha_{i,1}$, $\alpha_{i,2}$, and $\alpha_{i,3}$:

$$\begin{bmatrix} X_1 & X_2 & X_3 \\ Y_1 & Y_2 & Y_3 \\ 1 & 1 & 1 \end{bmatrix} \begin{Bmatrix} \alpha_{i,1} \\ \alpha_{i,2} \\ \alpha_{i,3} \end{Bmatrix} = \begin{Bmatrix} X_i \\ Y_i \\ 1 \end{Bmatrix} \tag{3.14}$$

Thus,

$$\alpha_{i,1} = \frac{X_i(Y_2 - Y_3) + Y_i(X_3 - X_2) + X_2Y_3 - X_3Y_2}{X_1(Y_2 - Y_3) + X_2(Y_3 - Y_1) + X_3(Y_1 - Y_2)} \tag{3.15}$$

$$\alpha_{i,2} = \frac{X_i(Y_3 - Y_1) + Y_i(X_1 - X_3) + X_3Y_1 - X_1Y_3}{X_1(Y_2 - Y_3) + X_2(Y_3 - Y_1) + X_3(Y_1 - Y_2)} \tag{3.16}$$

$$\alpha_{i,3} = \frac{X_i(Y_1 - Y_2) + Y_i(X_2 - X_1) + X_1Y_2 - X_2Y_1}{X_1(Y_2 - Y_3) + X_2(Y_3 - Y_1) + X_3(Y_1 - Y_2)} \tag{3.17}$$

One can rewrite weight ratios $\alpha_{i,1}$, $\alpha_{i,2}$, and $\alpha_{i,3}$ in the following form:

$$\alpha_{i,1} = \frac{(X_3 - X_2)(Y_i - Y_2) - (Y_3 - Y_2)(X_i - X_2)}{(X_3 - X_2)(Y_1 - Y_2) - (Y_3 - Y_2)(X_1 - X_2)} \tag{3.18}$$

$$\alpha_{i,2} = \frac{(X_1 - X_3)(Y_i - Y_3) - (Y_1 - Y_3)(X_i - X_3)}{(X_1 - X_3)(Y_2 - Y_3) - (Y_1 - Y_3)(X_2 - X_3)} \tag{3.19}$$

$$\alpha_{i,3} = \frac{(X_2 - X_1)(Y_i - Y_1) - (Y_2 - Y_1)(X_i - X_1)}{(X_2 - X_1)(Y_3 - Y_1) - (Y_2 - Y_1)(X_3 - X_1)} \tag{3.20}$$

Interpretation of weight ratios: As seen $\alpha_{i,j} = constant$ represent a line that is parallel to one of the sides of the leading triangle. For instance, $\alpha_{i,3} = constant$ is a line parallel to the s_{12} i.e. s_{12} is the side of the leading triangle ended by positions of agents 1 and 2. As observed, $\alpha_{i,3} = 1$ represent a line passing $\boldsymbol{R}_3$ (initial position of leader agent 3) and parallel to s_{12}. Shown in Fig. 3.3 are the lines representing $\alpha_{i,j} = constnt$. It is also noted that weight ratios of the material points located inside the leading triangle are all positive.

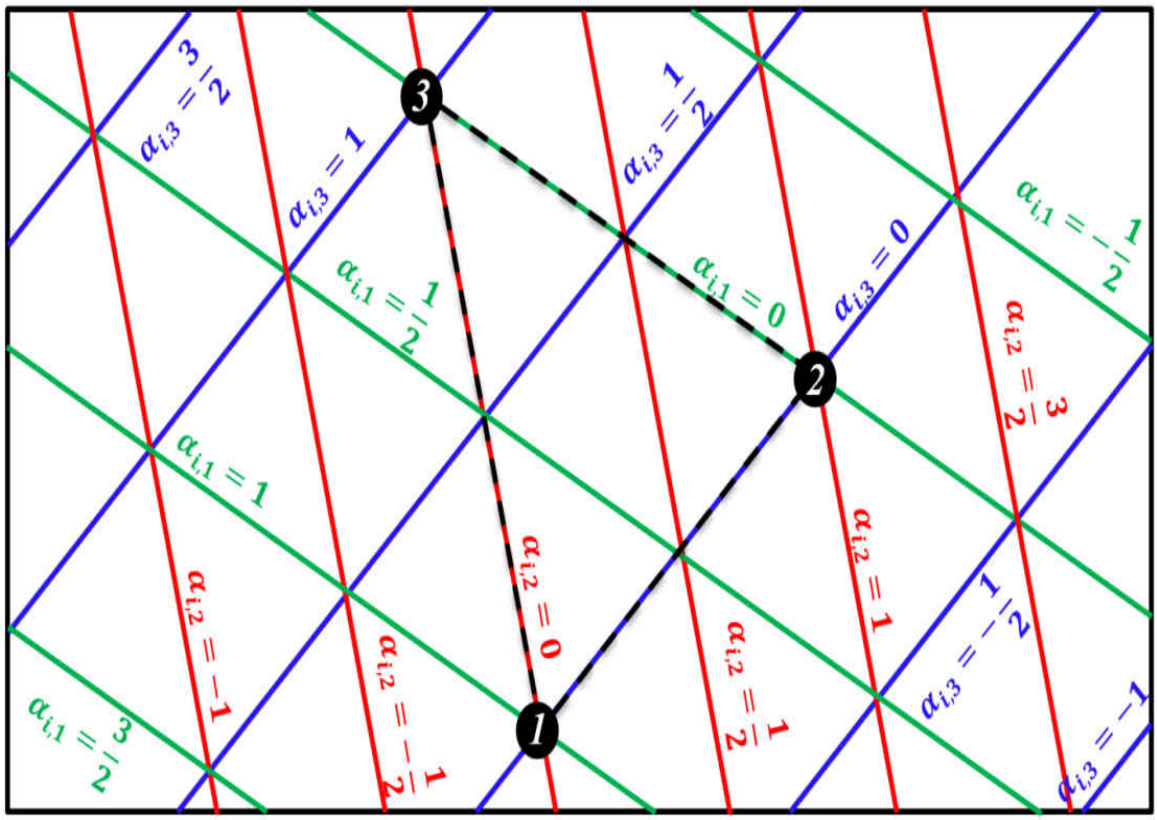

Figure 3.3 Parallel lines representing $\alpha_{i,j} = constant$

3.3 Homogenous Transformation of MAS Evolving in a *3-D* Space

Suppose that leader agents *1*, *2*, *3*, and *4* are located at the vertices of a leading tetrahedron that surround rest of the agents, the followers indexed by *5*, *6*, …, *N*. Under homogenous transformation of the leading tetrahedron, position of a follower agent *i* can be expressed as a linear combination of position of the leaders as follows:

$$\boldsymbol{r}_i(t) = \alpha_{i,1}\boldsymbol{r}_1(t) + \alpha_{i,2}\boldsymbol{r}_2(t) + \alpha_{i,3}\boldsymbol{r}_3(t) + \alpha_{i,4}\boldsymbol{r}_4(t) \tag{3.21}$$

where $\alpha_{i,1}$, $\alpha_{i,2}$, $\alpha_{i,3}$, and $\alpha_{i,4}$ are constant weight ratios,

$$\alpha_{i,1} + \alpha_{i,2} + \alpha_{i,3} + \alpha_{i,4} = 1 \tag{3.22}$$

and $\boldsymbol{r}_i(t) = x_i(t)\boldsymbol{e}_x + y_i(t)\boldsymbol{e}_y + z_i(t)\boldsymbol{e}_z$, $\boldsymbol{r}_1(t) = x_1(t)\boldsymbol{e}_x + y_1(t)\boldsymbol{e}_y + z_1(t)\boldsymbol{e}_z$, $\boldsymbol{r}_2(t) = x_2(t)\boldsymbol{e}_x + y_2(t)\boldsymbol{e}_y + z_2(t)\boldsymbol{e}_z$, $\boldsymbol{r}_3(t) = x_3(t)\boldsymbol{e}_x + y_3(t)\boldsymbol{e}_y + z_3(t)\boldsymbol{e}_z$and $\boldsymbol{r}_4(t) = x_4(t)\boldsymbol{e}_x + y_4(t)\boldsymbol{e}_y + z_4(t)\boldsymbol{e}_z$ denote position of follower *i*, leader agents *1*, *2*, 3 and *4*, respectively. Let us denote initial positions of follower agent *i* and leaders *1*, *2*, 3 and *4* by $\boldsymbol{R}_i = \boldsymbol{r}_i(0) = X_i\boldsymbol{e}_x + Y_i\boldsymbol{e}_y + Z_i\boldsymbol{e}_z$, $\boldsymbol{R}_1 = \boldsymbol{r}_1(0) = X_1\boldsymbol{e}_x + Y_1\boldsymbol{e}_y + Z_1\boldsymbol{e}_z$, $\boldsymbol{R}_2 = \boldsymbol{r}_2(0) = X_2\boldsymbol{e}_x + Y_2\boldsymbol{e}_y + Z_2\boldsymbol{e}_z$, $\boldsymbol{R}_3 = \boldsymbol{r}_3(0) = X_3\boldsymbol{e}_x + Y_3\boldsymbol{e}_y + Z_3\boldsymbol{e}_z$ and $\boldsymbol{R}_4 = \boldsymbol{r}_4(0) = X_4\boldsymbol{e}_x + Y_4\boldsymbol{e}_y + Z_4\boldsymbol{e}_z$, respectively, then, weight ratios can be assigned by solving following set of four linear algebraic equations:

$$\begin{bmatrix} X_1 & X_2 & X_3 & X_4 \\ Y_1 & Y_2 & Y_3 & Y_4 \\ Z_1 & Z_2 & Z_3 & Z_4 \\ 1 & 1 & 1 & 1 \end{bmatrix} \begin{Bmatrix} \alpha_{i,1} \\ \alpha_{i,2} \\ \alpha_{i,3} \\ \alpha_{i,4} \end{Bmatrix} = \begin{Bmatrix} X_i \\ Y_i \\ Z_i \\ 1 \end{Bmatrix} \tag{3.23}$$

Solving eqn. (3.23) leads $\alpha_{i,j}$ to be as follows:

$$\alpha_{i,1} = \frac{(X_i - X_2)[(Y_3 - Y_2)(Z_4 - Z_2) - (Y_4 - Y_2)(Z_3 - Z_2)] + (Y_i - Y_2)[(Z_3 - Z_2)(X_4 - X_2) - (Z_4 - Z_2)(X_3 - X_2)] + (Z_i - Z_2)[(X_3 - X_2)(Y_4 - Y_2) - (X_4 - X_2)(Y_3 - Y_2)]}{(X_1 - X_2)[(Y_3 - Y_2)(Z_4 - Z_2) - (Y_4 - Y_2)(Z_3 - Z_2)] + (Y_1 - Y_2)[(Z_3 - Z_2)(X_4 - X_2) - (Z_4 - Z_2)(X_3 - X_2)] + (Z_1 - Z_2)[(X_3 - X_2)(Y_4 - Y_2) - (X_4 - X_2)(Y_3 - Y_2)]} \tag{3.24}$$

$$\alpha_{i,2} = \frac{(X_i - X_3)[(Y_4 - Y_3)(Z_1 - Z_3) - (Y_1 - Y_3)(Z_4 - Z_3)] + (Y_i - Y_3)[(Z_4 - Z_3)(X_1 - X_3) - (Z_1 - Z_3)(X_4 - X_3)] + (Z_i - Z_3)[(X_4 - X_3)(Y_1 - Y_3) - (X_1 - X_3)(Y_4 - Y_3)]}{(X_2 - X_3)[(Y_4 - Y_3)(Z_1 - Z_3) - (Y_1 - Y_3)(Z_4 - Z_3)] + (Y_2 - Y_3)[(Z_4 - Z_3)(X_1 - X_3) - (Z_1 - Z_3)(X_4 - X_3)] + (Z_2 - Z_3)[(X_4 - X_3)(Y_1 - Y_3) - (X_1 - X_3)(Y_4 - Y_3)]} \tag{3.25}$$

$$\alpha_{i,3} = \frac{(X_i - X_4)[(Y_1 - Y_4)(Z_2 - Z_4) - (Y_2 - Y_4)(Z_1 - Z_4)] + (Y_i - Y_4)[(Z_1 - Z_4)(X_2 - X_4) - (Z_2 - Z_4)(X_1 - X_4)] + (Z_i - Z_4)[(X_1 - X_4)(Y_2 - Y_4) - (X_2 - X_4)(Y_1 - Y_4)]}{(X_3 - X_4)[(Y_1 - Y_4)(Z_2 - Z_4) - (Y_2 - Y_4)(Z_1 - Z_4)] + (Y_3 - Y_4)[(Z_1 - Z_4)(X_2 - X_4) - (Z_2 - Z_4)(X_1 - X_4)] + (Z_3 - Z_4)[(X_1 - X_4)(Y_2 - Y_4) - (X_2 - X_4)(Y_1 - Y_4)]} \tag{3.26}$$

$$\alpha_{i,4} = \frac{(X_i - X_1)[(Y_2 - Y_1)(Z_3 - Z_1) - (Y_3 - Y_1)(Z_2 - Z_1)] + (Y_i - Y_1)[(Z_2 - Z_1)(X_3 - X_1) - (Z_3 - Z_1)(X_2 - X_1)] + (Z_i - Z_1)[(X_2 - X_1)(Y_3 - Y_1) - (X_3 - X_1)(Y_2 - Y_1)]}{(X_4 - X_1)[(Y_2 - Y_1)(Z_3 - Z_1) - (Y_3 - Y_1)(Z_2 - Z_1)] + (Y_4 - Y_1)[(Z_2 - Z_1)(X_3 - X_1) - (Z_3 - Z_1)(X_2 - X_1)] + (Z_4 - Z_1)[(X_2 - X_1)(Y_3 - Y_1) - (X_3 - X_1)(Y_2 - Y_1)]} \tag{3.27}$$

One can see $\alpha_{i,j} = c$ (c is a constant parameter.) as equation of a plane that is parallel to one of the triangular surfaces of the leading tetrahedron. For instance, $\alpha_{i,1} = c$ represents equation of a plane that is parallel to the triangular surface p_{234}, i.e. the triangular surface of the leading tetrahedron that is constructed on the vertices *i, j,* and *k*

is denoted by p_{ijk}. In addition, planes denoted by $\alpha_{i,1} = 1$, $\alpha_{i,2} = 1$, $\alpha_{i,3} = 1$, $\alpha_{i,4} = 1$ pass through vertices *1*, *2*, *3*, and *4* of the leading tetrahedron, respectively. Also, triangular surfaces of the leading tetrahedron p_{234}, p_{341}, p_{412}, and p_{123} are part of the planes $\alpha_{i,1} = 0$, $\alpha_{i,2} = 0$, $\alpha_{i,3} = 0$, $\alpha_{i,4} = 0$, respectively. Furthermore, all weight ratios $\alpha_{i,j}$ are positive if a material point i is located inside the leading tetrahedron.

3.4 Force Analysis

Under homogenous transformation, acceleration of each follower agent i ($i = n + 1, n + 2, \dots, N$) can be expressed as a linear combination of acceleration of the leaders, that is

$$\ddot{\boldsymbol{r}}_i(t) = \sum_{k=1}^{n+1} \alpha_{i,k}\, \ddot{\boldsymbol{r}}_k(t) \tag{3.28}$$

Thus, *j-th* ($j = 1,2, \dots, n$) coordinate of acceleration of follower *i*, $\ddot{x}_{j_i}(t)$, can be written as

$$\ddot{x}_{j_i}(t) = \sum_{k=1}^{n+1} \alpha_{i,k}\, \ddot{x}_{j_k}(t) \tag{3.29}$$

Let $a_j(t)$ be the maximum of magnitude of component *j* of acceleration of all leader agents, $a_j(t) = max\left\{\ddot{x}_{j_1}, \ddot{x}_{j_2}, \dots, \ddot{x}_{j_{n+1}}\right\}$, then,

$$\left\|\ddot{x}_{j_i}(t)\right\| \le \sum_{k=1}^{n+1} \alpha_{i,k} \left\|\ddot{x}_{j_k}(t)\right\| \le a_j(t) \sum_{k=1}^{n+1} \alpha_{i,k} = a_j(t) \tag{3.30}$$

As the result, the magnitude of the force required for motion of agent *i*, $f_i(t)$, satisfies the following inequality

$$f_i(t) = m\sqrt{\sum_{j=1}^{n} \ddot{x}_{j_i}{}^2(t)} \leq m\sqrt{\sum_{j=1}^{n} a_j{}^2(t)} \tag{3.31}$$

where *m* denote the mass of every follower agent *i*.

3.5 Optimal Paths for Leader Agents

In this section we derive optimal paths connecting given initial and final positions of the leaders. We assume that initial and final velocities of the leaders are zero and reach the final positions in finite time *T*. Also, leader agents satisfy the following simple second order dynamics:

$$\ddot{x}_i = u_i \qquad for\ i = 1,2,3 \qquad (3.32 - 3.34)$$

$$\ddot{y}_i = v_i \qquad for\ i = 1,2,3 \qquad (3.35 - 3.37)$$

where their trajectories are constrained to preserve the area of the leading triangle given by

$$a(t) = \frac{1}{2}\begin{vmatrix} x_1(t) & x_2(t) & x_3(t) \\ y_1(t) & y_2(t) & y_3(t) \\ 1 & 1 & 1 \end{vmatrix} \tag{3.38}$$

Problem of optimal paths: Let a_0 denote the area of the leading triangle at the initial time $t = 0$, and suppose the leader agents move from known initial positions and velocities to a final positions and velocities in such a way that

- the area preserving holonomic constraint

$$C = a(t) - a_0 = \frac{1}{2}\{x_1(y_2 - y_3) + x_2(y_3 - y_1) + x_3(y_1 - y_2)\} - a_0 = 0 \tag{3.39}$$

is met, and

- the cost function

$$J = \int_0^T \left\{ \sum_{i=1}^{3} ({u_i}^2 + {v_i}^2) \right\} dt \tag{3.40}$$

is minimized.

3.5.1 State Space Representation

The dynamics of the leader agents (eqns. (3.32-3.37)) can be cast in state space form as follows:

$$\begin{cases} \dot{p}_1 = p_7 & \dot{p}_2 = p_8 & \dot{p}_3 = p_9 & \dot{p}_4 = p_{10} & \dot{p}_5 = p_{11} & \dot{p}_6 = p_{12} \\ \dot{p}_7 = q_1 & \dot{p}_8 = q_2 & \dot{p}_9 = q_3 & \dot{p}_{10} = q_4 & \dot{p}_{11} = q_5 & \dot{p}_{12} = q_6 \end{cases} \tag{3.41}$$

where $p_1 = x_1,\ p_2 = x_2,\ p_3 = x_3,\ p_4 = y_1, p_5 = y_2,\ p_6 = y_3,\ q_1 = u_1,\ q_2 = u_2,\ q_3 = u_3, q_4 = u_4, q_5 = u_5$, and $q_6 = u_6$ and

$$P(0) = \begin{bmatrix} {P_0}_{6\times1} \\ \mathbf{0}_{6\times1} \end{bmatrix} \tag{3.42}$$

$$P(T) = \begin{bmatrix} {P_T}_{6\times1} \\ \mathbf{0}_{6\times1} \end{bmatrix} \tag{3.43}$$

denote imposed conditions at initial time $t = 0$ and terminal time $t = T$. Let

$$P_0 = \begin{bmatrix} x_{1_0} & x_{2_0} & x_{3_0} & y_{1_0} & y_{2_0} & y_{3_0} \end{bmatrix}^T \tag{3.44}$$

$$P_T = \begin{bmatrix} x_{1_T} & x_{2_T} & x_{3_T} & y_{1_T} & y_{2_T} & y_{3_T} \end{bmatrix}^T \tag{3.45}$$

represent given initial and final positions of the leader agents where initial and final velocities are zero. In order for control inputs q_i to appear in the constraint equation for the motion of the leaders, one can obtain the second time derivative of constraint eqn. (3.39) and state it as

$$C' = q_1(p_5 - p_6) + q_2(p_6 - p_4) + q_3(p_4 - p_5) + q_4(p_3 - p_2) + q_5(p_1 - p_3) +$$
$$q_6(p_2 - p_1) + p_7(p_{11} - p_{12}) + p_8(p_{12} - p_{10}) + p_9(p_{10} - p_{11}) + p_{10}(p_9 - p_8) +$$
$$p_{11}(p_7 - p_9) + p_{12}(p_8 - p_7) = 0 \tag{3.46}$$

To obtain the optimal trajectories for the leader agents the augmented cost function is

$$J' = \int_0^T \left\{ \sum_{i=1}^{6} \left({q_i}^2 + \lambda_i(p_{i+6} - \dot{p}_i) + \lambda_{i+6}(q_i - \dot{p}_{i+6}) \right) + \gamma C' \right\} dt \tag{3.47}$$

where $\lambda = [\lambda_1 \quad ... \quad \lambda_6]^T$ is the co-state vector and $\gamma(t)$ is a scalar. To minimize J', the first variation $\delta J'$ must be zero, thus

$$\delta J' = \int_0^T \left\{ \sum_{i=1}^{6} \left(2q_i \delta q_i + \delta\lambda_i(p_{i+6} - \dot{p}_i) + \lambda_i(\delta p_{i+6} - \delta\dot{p}_i) + \delta\lambda_{i+6}(q_i - \dot{p}_{i+6}) \right.\right.$$
$$\left.\left. + \lambda_{i+6}(\delta q_i - \delta\dot{p}_{i+6}) \right) + \delta\gamma C' + \gamma\delta C' \right\} dt = 0 \tag{3.48}$$

Satisfying $\delta J' = 0$ leads to the 24-th order state space dynamics

$$\dot{S} = A_s S \tag{3.49}$$

that if solved, optimal trajectories minimizing augmented cost function J' are obtained for the leaders agents. It is noted that

$$A_S = \begin{bmatrix} 0_{6\times6} & I_{6\times6} & 0_{6\times6} & 0_{6\times6} \\ -\frac{\gamma(t)}{2} K1_{6\times6} & 0_{6\times6} & 0_{6\times6} & -\frac{1}{2} I_{6\times6} \\ \frac{\gamma^2(t)}{2} K2_{6\times6} & 0_{6\times6} & 0_{6\times6} & \frac{\gamma(t)}{2} K1_{6\times6} \\ 0_{6\times6} & -2\gamma(t)K1_{6\times6} & -I_{6\times6} & 0_{6\times6} \end{bmatrix}, \tag{3.50}$$

$0_{6\times6}$ denote a zero matrix, $I_{6\times6}$ is the identity matrix, $S = \begin{bmatrix} P_{12\times1} \\ \lambda_{12\times1} \end{bmatrix} = [p_1 \quad \cdots \quad p_{12} \quad \lambda_1 \quad \cdots \quad \lambda_{12}]^T$, and

$$K1 = \begin{bmatrix} 0 & 0 & 0 & 0 & 1 & -1 \\ 0 & 0 & 0 & -1 & 0 & 1 \\ 0 & 0 & 0 & 1 & -1 & 0 \\ 0 & -1 & 1 & 0 & 0 & 0 \\ 1 & 0 & -1 & 0 & 0 & 0 \\ -1 & 1 & 0 & 0 & 0 & 0 \end{bmatrix} \tag{3.51}$$

$$K2 = \begin{bmatrix} 2 & -1 & -1 & 0 & 0 & 0 \\ -1 & 2 & -1 & 0 & 0 & 0 \\ -1 & -1 & 2 & 0 & 0 & 0 \\ 0 & 0 & 0 & 2 & -1 & -1 \\ 0 & 0 & 0 & -1 & 2 & -1 \\ 0 & 0 & 0 & -1 & -1 & 2 \end{bmatrix} \tag{3.52}$$

Furthermore, the constraint eqn. (3.46) can be written as

$$C' = -\frac{1}{2}(\gamma\rho + \sigma) + \tau = 0 \tag{3.53}$$

where

$$\rho = (p_5 - p_6)^2 + (p_6 - p_4)^2 + (p_4 - p_5)^2 + (p_3 - p_2)^2 + (p_1 - p_3)^2 + (p_2 - p_1)^2 \tag{3.54}$$

$$\sigma = \lambda_7(p_5 - p_6) + \lambda_8(p_6 - p_4) + \lambda_9(p_4 - p_5) + \lambda_{10}(p_3 - p_2) + \lambda_{11}(p_1 - p_3) + \lambda_{12}(p_2 - p_1) \tag{3.55}$$

$$\tau = p_7(p_{11} - p_{12}) + p_8(p_{12} - p_{10}) + p_9(p_{10} - p_{11}) + p_{10}(p_9 - p_8) + p_{11}(p_7 - p_9) + p_{12}(p_8 - p_7) \tag{3.56}$$

Hence, $\gamma(t)$ can be obtained from eqn. (3.53) which is

$$\gamma = \frac{2\tau - \sigma}{\rho} \tag{3.57}$$

and then is replaced in the matrix dynamics (3.49). In other words, optimal trajectories of the leader agents is obtained by solving the state space dynamic (3.49) where γ is assigned by relations (3.54-3.57).

3.5.2 Example

In this example, we consider a MAS that consists of 20 agents, three leaders and seventeen followers, and move in a plane. Leader agents *1, 2,* and *3* are initially at rest and placed at the vertices of the leading triangle at $(-5,0)$, $(5,0)$, and $(0,10)$, respectively. It is desired that leader agents *1, 2,* and *3* finally settle at $(30,20)$, $(35,60)$, and $(30,40)$ in $10s$, where they are the vertices of the leading triangle. It is noted that the area of both initial and final triangles are 50 m^2. As shown in Fig. 3.4 follower agents are initially placed inside the leading triangle.

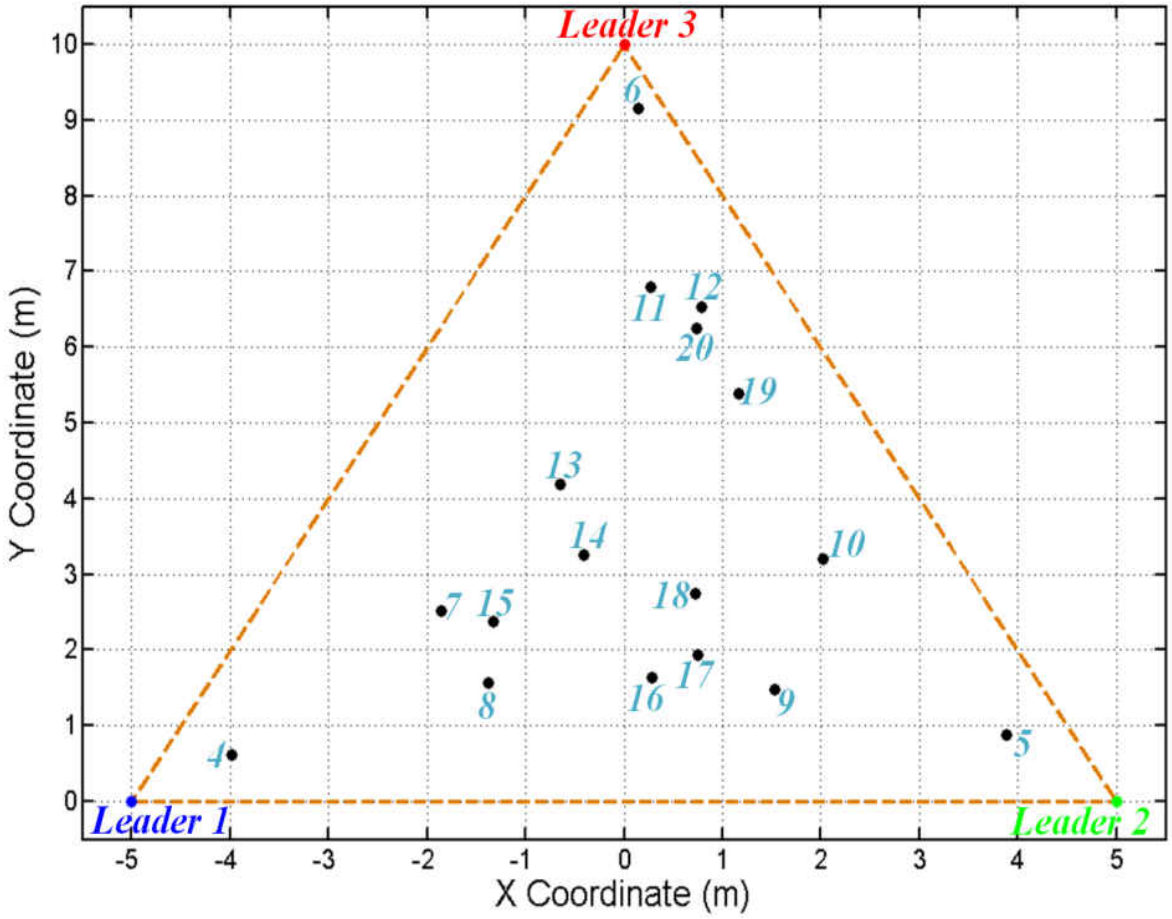

Figure 3.4 Initial formation of the MAS

We are first interested in obtaining the optimal trajectories of the leader agents that are subjected to satisfying the constraint eqn. (3.46) and minimize the cost function in eqn. (3.47). Then, position of every follower agents i is updated according to eqn. (3.12) where we assign the weight ratios $\alpha_{i,1}$, $\alpha_{i,2}$, and $\alpha_{i,3}$ based on initial positions of the agents (See relations (3.18-3.20)) and list them in Table 3.1.

Table 3.1 Weight Ratios $\boldsymbol{\alpha_{i,j}}$

	$\alpha_{i,1}$	$\alpha_{i,2}$	$\alpha_{i,3}$
$i = 4$	0.8679	0.0708	0.0613
$i = 5$	0.0672	0.8447	0.0882
$i = 6$	0.0276	0.0564	0.9160
$i = 7$	0.5596	0.1886	0.2517
$i = 8$	0.5594	0.2837	0.1569
$i = 9$	0.2728	0.5786	0.1487
$i = 10$	0.1379	0.5414	0.3207
$i = 11$	0.1339	0.1868	0.6793
$i = 12$	0.0949	0.2515	0.6536

	$\alpha_{i,1}$	$\alpha_{i,2}$	$\alpha_{i,3}$
$i = 13$	0.3556	0.2258	0.4186
$i = 14$	0.3780	0.2966	0.3254
$i = 15$	0.5142	0.2479	0.2379
$i = 16$	0.3891	0.4464	0.1645
$i = 17$	0.3279	0.4786	0.1935
$i = 18$	0.2898	0.4349	0.2752
$i = 19$	0.1137	0.3469	0.5394
$i = 20$	0.1142	0.2617	0.6241

3.5.2.1 Leaders' Paths

As seen, the optimal trajectories for the leader agents is the solution of the non-linear 24-th order dynamics (See eqn. (3.49) and (3.57)) where initial and final position and velocities of the leader agents are all given but the initial value of the co-state vector λ is not known. On the other hand, $\gamma(t)$, used in A_s, is a nonlinear feedback of p_i and λ_i, thus, the dynamics (3.49) and (3.57) are difficult to solve analytically. Therfore we deal

with the problem by first estimating $\gamma(t)$ with $\gamma_1(t)$ and replacing $\gamma_1(t)$ in eqn. (3.49). Then, we obtain state transition matrix $\Phi_{\gamma_1}(t,0)$ numerically with the solution of eqn. (3.49) written as

$$\forall t \geq 0, \begin{bmatrix} P_{\gamma_1} \\ \lambda_{\gamma_1} \end{bmatrix} = \Phi_{\gamma_1}(t,0) \begin{bmatrix} P_0 \\ \lambda_{0_{\gamma_1}} \end{bmatrix} = \begin{bmatrix} \Phi_{11_{\gamma_1}}(t,0) & \Phi_{12_{\gamma_1}}(t,0) \\ \Phi_{21_{\gamma_1}}(t,0) & \Phi_{22_{\gamma_1}}(t,0) \end{bmatrix} \begin{bmatrix} P_0 \\ \lambda_{0_{\gamma_1}} \end{bmatrix} \tag{3.58}$$

where

$$P_0 = [x_1(0) \;\; x_2(0) \;\; x_3(0) \;\; y_1(0) \;\; y_2(0) \;\; y_3(0) \;\; \dot{x}_1(0) \;\; \dot{x}_2(0) \;\; \dot{x}_3(0) \;\; \dot{y}_1(0) \;\; \dot{y}_2(0) \;\; \dot{y}_3(0)]^T = [-5 \;\; 5 \;\; 0 \;\; 0 \;\; 0 \;\; 10 \;\; 0 \;\; 0 \;\; 0 \;\; 0 \;\; 0 \;\; 0]^T \tag{3.59}$$

denote known initial positions and velocities of the leader agents. Since,

$$P_F = [x_1(T) \;\; x_2(T) \;\; x_3(T) \;\; y_1(T) \;\; y_2(T) \;\; y_3(T) \;\; \dot{x}_1(T) \;\; \dot{x}_2(T) \;\; \dot{x}_3(T) \;\; \dot{y}_1(T) \;\; \dot{y}_2(T) \;\; \dot{y}_3(T)]^T = [30 \;\; 35 \;\; 30 \;\; 20 \;\; 60 \;\; 40 \;\; 0 \;\; 0 \;\; 0 \;\; 0 \;\; 0 \;\; 0]^T \tag{3.60}$$

is also known, one can write

$$P_F = \Phi_{11_{\gamma_1}}(T,0)P_0 + \Phi_{12_{\gamma_1}}(T,0)\lambda_{0_{\gamma_1}} \tag{3.61}$$

Hence, initial values of the co-state vector λ is as

$$\lambda_{0_{\gamma_1}} = \left(\Phi_{12_{\gamma_1}}(T,0)\right)^{-1} \left(P_F - \Phi_{11_{\gamma_1}}(T,0)P_0\right) \tag{3.62}$$

where γ is estimated by γ_1. Thus, both P_{γ_1} and λ_{γ_1} can be assigned at any time $t\epsilon[0,T]$by using eqn. (3.58). Now, we obtain the second estimation for $\gamma(t)$, $\gamma_2(t)$, by using eqn. (3.57). New, estimation $\gamma_2(t)$ is used in eqns. (3.58-3.62) and similarly P_{γ_2} and $\lambda_{\gamma_2}$are assigned and the third estimation for $\gamma(t)$, $\gamma_3(t)$, is obtained by using eqn. (3.57). We keep updating $\gamma_k(t)$ until

$$\forall t\epsilon[0,T], \|\gamma_k(t) - \gamma_{k-1}(t)\| \to 0 \tag{3.62}$$

is met. Then, $\gamma_k(t)$, P_{γ_k} and λ_{γ_k} can be considered the solution of $\gamma(t)$, $P(t)$, and $\lambda(t)$, respectively, for all $t\epsilon[0,T]$. In Fig. 3.5, variation of the parameter γ_1,…, $\gamma_6$versus time t

is illustrated. As seen, at the first attempt $\gamma_1(t)$ is estimated by 1 for all $t\epsilon[0,10]$ and $\gamma(t)$ can be approximated by $\gamma_6(t)$ with a very good accuracy.

Optimal trajectories of the leader agents 1, 2, and 3 are shown by blue, green and red curves in Fig. 3.6. In addition, Fig. 3.6 depicts the leading triangle at initial time $t = 0s$, final time $t = 10s$, and three sample times $t = 3.5s$, $t = 5.5s$ and $t = 7.5s$. Also, control inputs u_i and v_i $(q_1, \dots, q_6)$ are illustrated versus time in Fig. 3.7. Moreover, the magnitude of the control force per mass ($f_i = \sqrt{{u_i}^2 + {v_i}^2}$) exerted on each leader agent is shown in Fig. 3-8 for all $t\epsilon[0,10]$. As gotten, around $t = 5s$, the direction of the control inputs q_i changes. This implies that q_i leads the leader i to accelerate in the first half of the motion and then decelerate in the rest of the motion period.

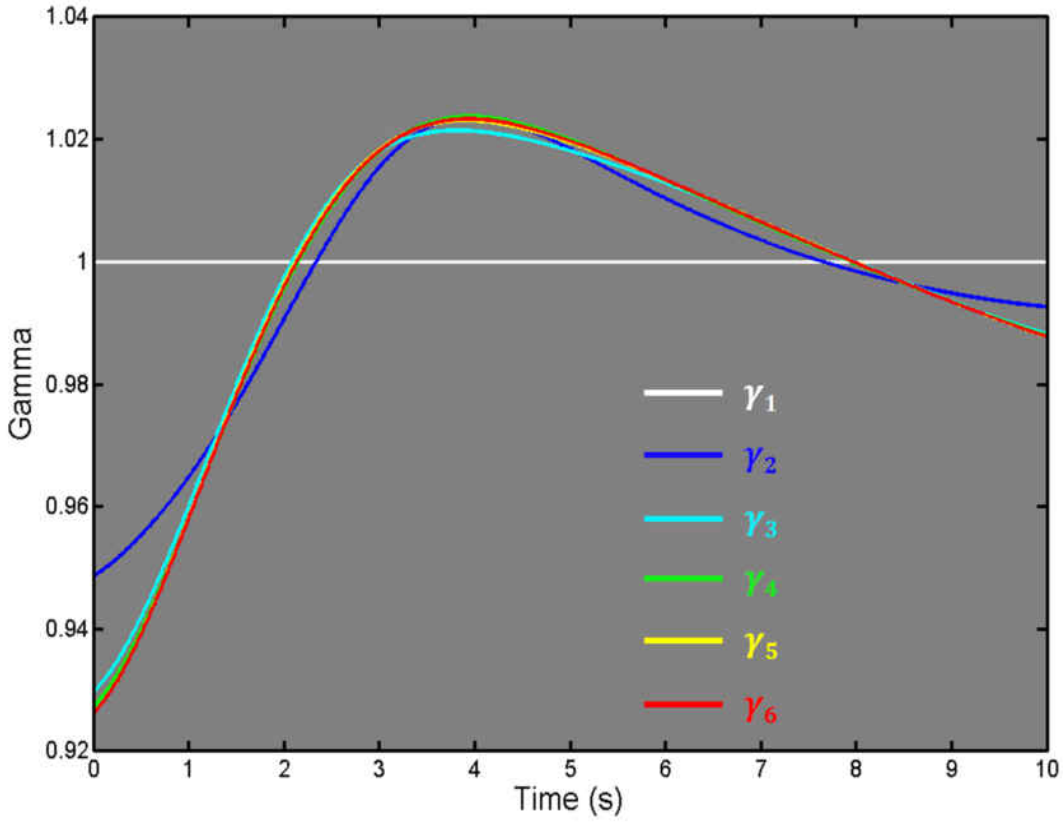

Figure 3.5 Parameter γ

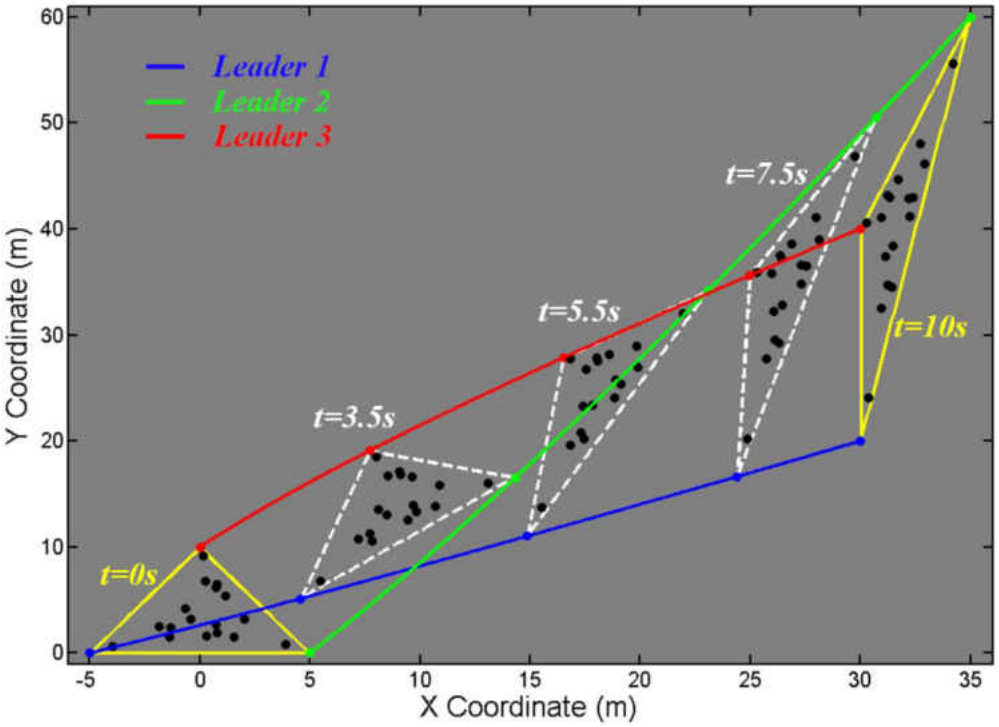

Figure 3.6 Evolution of the MAS under a homogeneous mapping

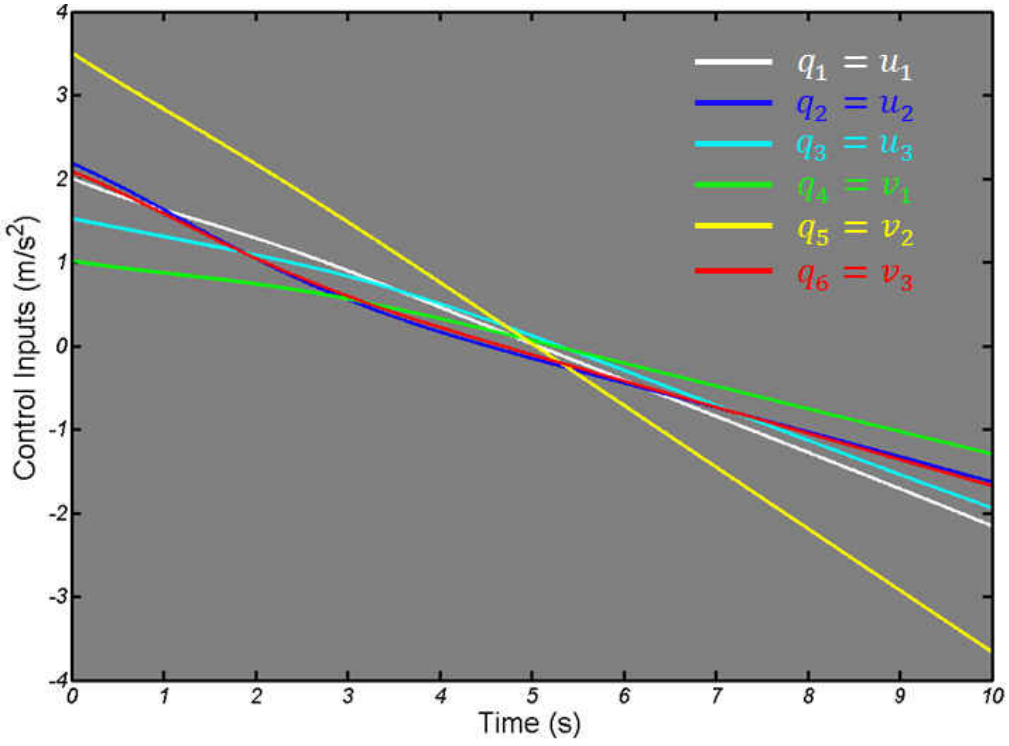

Figure 3.7 Control inputs q_i

In Fig. 3.9, we depict $\sqrt{{a_1}^2 + {a_2}^2}$ versus time that can be considered as the cap of the required force per mass for motion of all follower agents (See eqn. (3.31).).

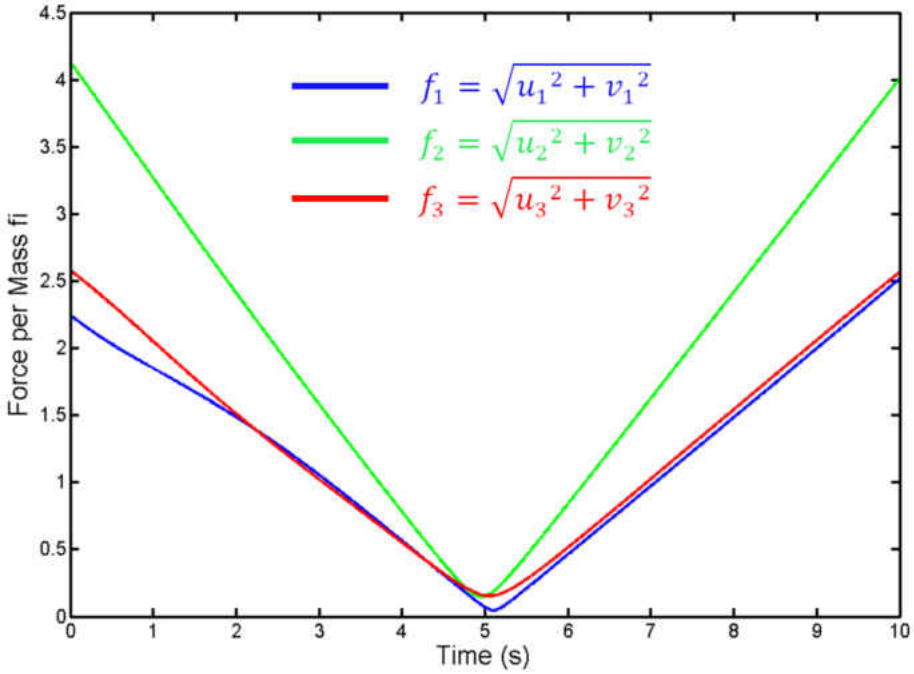

Figure 3.8 Control force per mass (f_i) exerted on leader agent i

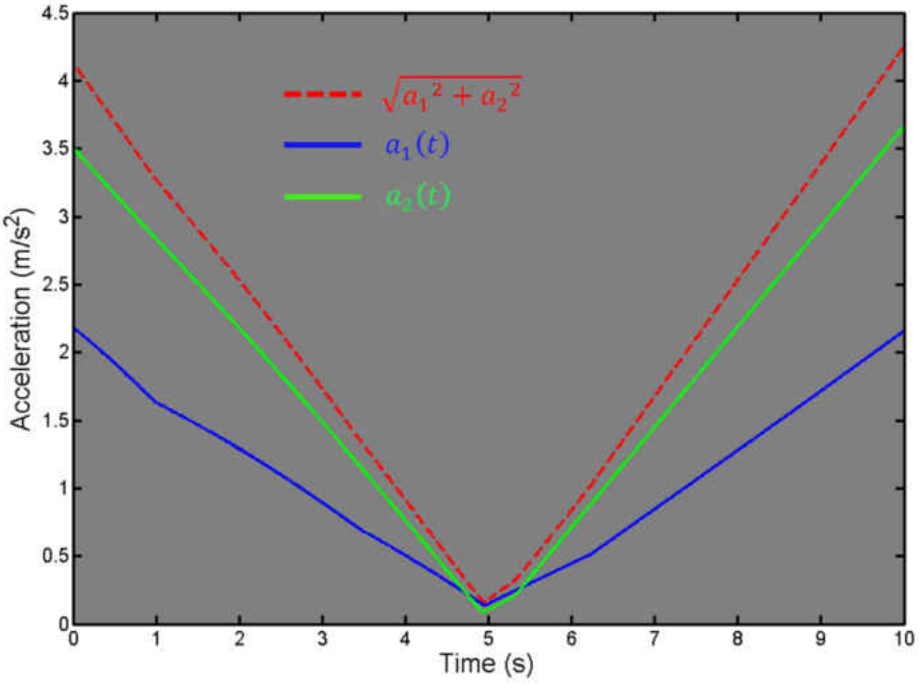

Figure 3.9 Control force per mass (f_i) exerted on leader agent i

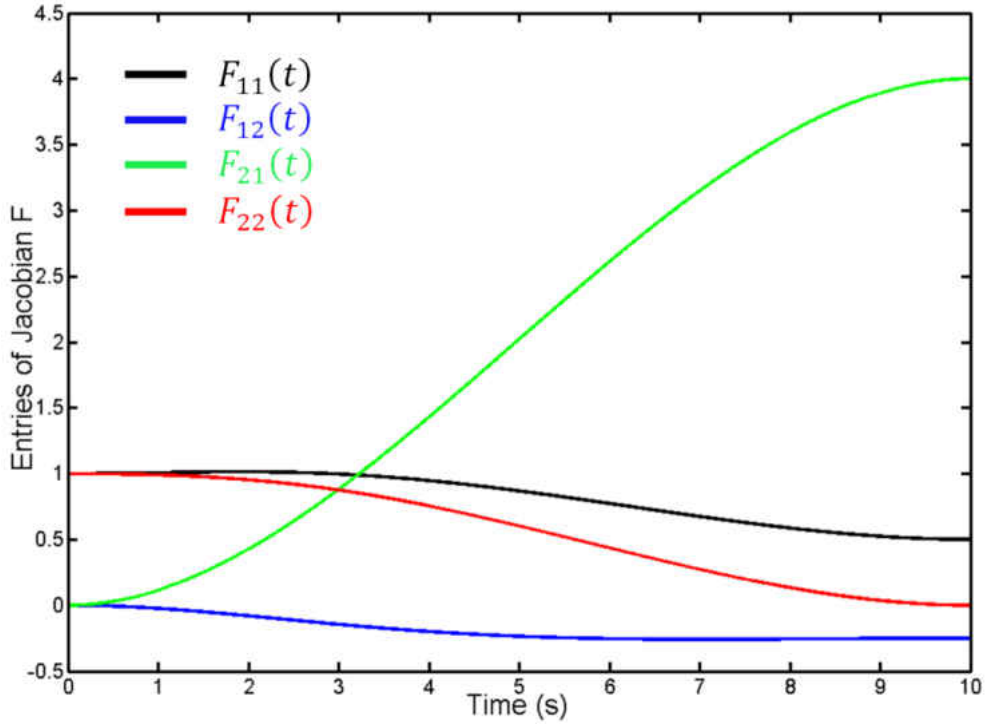

Figure 3.10 Elements of the Jacobian matrix *F*

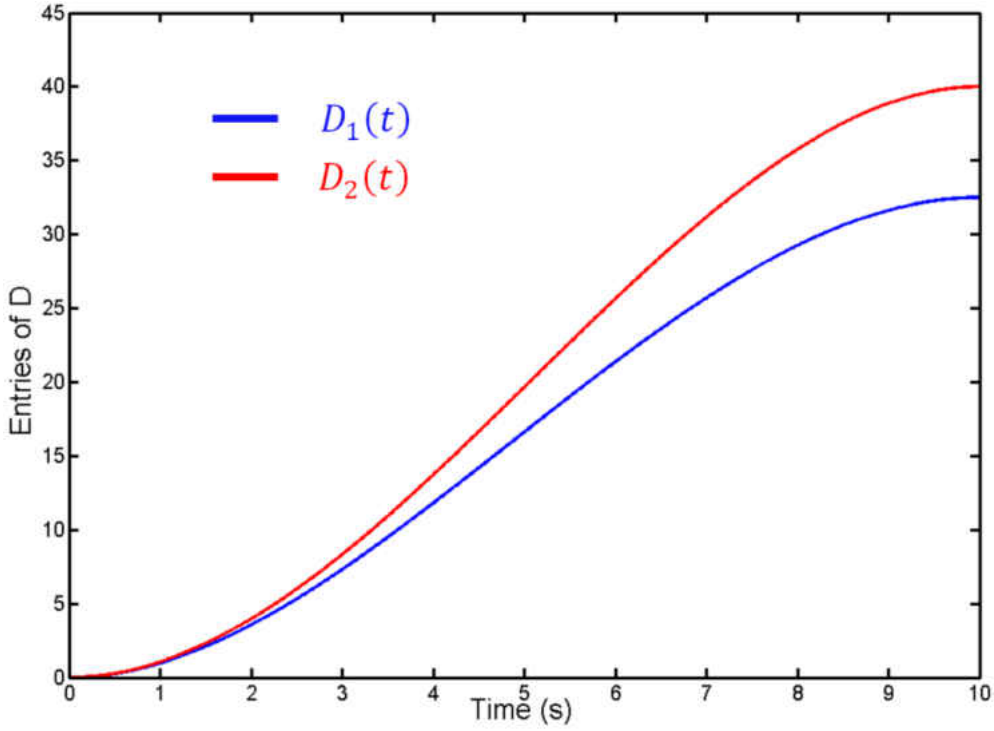

Figure 3.11 Elements of the rigid body displacement vector *D*

Shown in Figs. 3.10 and 3.11 are the elements of the matrix $F_{2\times2}(t)$ and rigid body displacement vector $D_{2\times1}(t)$ of the homogenous transformation of the MAS. As seen at $t = 0$ $F(0) = I$ and $D(0) = \mathbf{0}$.

3.5.2.2 Followers' Paths and Forces

As seen in Fig. 3.6, formation of followers are shown as black nodes inside the leading triangle at initial and final time and three sample times. Here each follower agent i updates its position according to eqn. (3.12) where $\alpha_{i,j}$ are listed in Table 1. In Fig. 3.12, x and y coordinates of position of the sample follower 18 is depicted as a function of time.

The optimal control inputs (forces per unit mass or accelerations) q_i, resulting from eqn. (3.48), $\delta J' = 0$, are expressed as follows:

$$q_1 = -\frac{1}{2}(\gamma(p_5 - p_6) + \lambda_7) \tag{3.63}$$

$$q_2 = -\frac{1}{2}(\gamma(p_6 - p_4) + \lambda_8) \tag{3.64}$$

$$q_3 = -\frac{1}{2}(\gamma(p_4 - p_5) + \lambda_9) \tag{3.65}$$

$$q_4 = -\frac{1}{2}(\gamma(p_3 - p_2) + \lambda_{10}) \tag{3.66}$$

$$q_5 = -\frac{1}{2}(\gamma(p_1 - p_3) + \lambda_{11}) \tag{3.67}$$

$$q_6 = -\frac{1}{2}(\gamma(p_3 - p_2) + \lambda_{12}) \tag{3.68}$$

This leads to accelerations of follower agents given below:

$$\ddot{x}_i = \sum_{k=1}^{3} \alpha_{i,k} q_k \tag{3.69}$$

$$\ddot{y}_i = \sum_{k=1}^{3} \alpha_{i,k} q_{k+3} \tag{3.70}$$

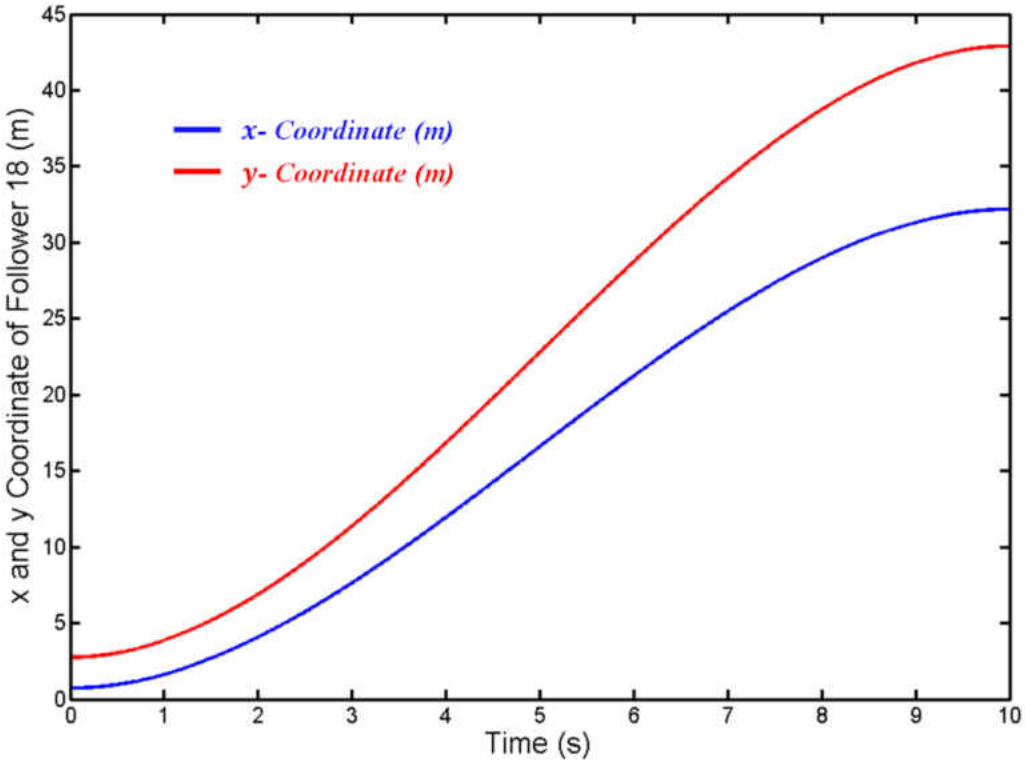

Figure 3.12 x and y coordinates of position of follower agent 18

Therefore, replacing q_i by eqns. (3.63-3.68) and using Einstein's convention, results in the following expression for $\ddot{x}_i$ and $\ddot{y}_i$:

$$\ddot{x}_i = \ddot{p}_i = -\frac{\alpha_{i,k}}{4}(\varepsilon_{kmn}\gamma(p_{m+3} - p_{n+3}) + 2\lambda_{k+6}) \tag{3.71}$$

$$\ddot{y}_i = \ddot{p}_{i+6} = -\frac{\alpha_{i,k}}{4}(\varepsilon_{kmn}\gamma(p_n - p_m) + 2\lambda_{k+9}) \tag{3.72}$$

where i is a free index; k, m and n are dummy indices. In Fig. 3-13, the magnitude of acceleration of six sample follower agents 6, 10, 11, 16, and 18 are shown versus time by white, blue, cyan, yellow, and green continuous curves, respectively. As seen the

magnitude of acceleration of followers are all less that the cap $\sqrt{{a_1}^2 + {a_2}^2}$ that is assigned by relation (3.31) and is shown by red hashed curve.

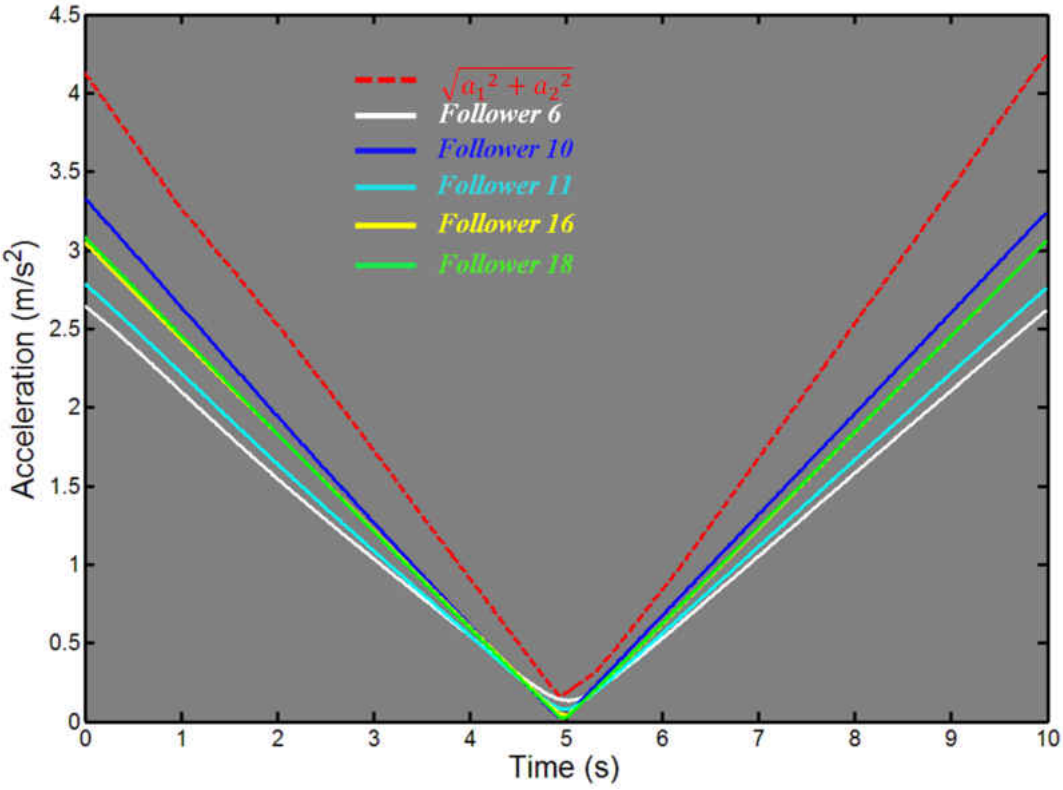

Figure 3.13 Magnitude of accelerations of six different follower agents

CHAPTER 4: EVOLUTION OF A MULTI AGENT SYSTEM UNDER LOCAL COMMUNICATION

In the previous chapter, homogenous deformation of a MAS under a predefined mapping, prescribed by the leaders' positions, was discussed. As described, followers know leaders' positions and therefore homogenous mapping is achieved with zero inter agent communication. Although proposed approach has many advantageous features and can address many limitations of common methods, it restricts followers to communicate directly with leaders and leads to a pre-known path planning problem. In this chapter, a framework for communication based homogenous deformation of a MAS is developed where followers grasp the mapping, prescribed by the leaders, through local communication with some neighboring agents. Therefore, transformation of a MAS to a final homogenous formation can be guaranteed even in the presence of unpredictable change in the leaders' motion plan [114 and 115]. In the following, evolution of a MAS in 1-D and 2-D space under local communication is formulated.

4.1 One Dimensional MAS Evolution Problem

Let a MAS consist of N agents, numbered by $1, 2, .., N$ and all distributed on a segment, called *leading segment*, where agents 1 and 2 are initially placed at the right most and the left most points, respectively (end points of the leading segment), and rest of the agents are distributed in-between. Agents 1 and 2 are considered the leaders that move independently, and agents $3, 4, ..., N$ are the followers, where every follower agent i communicates with two adjacent agents to update its position accordingly. Shown in

Fig. 4.1 is a sample MAS that consists of six agents where agents 1 and 2 are the leaders and the rest are the followers [115].

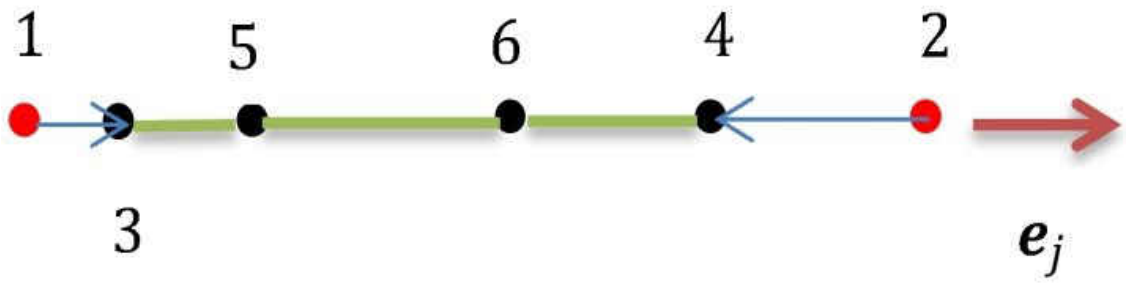

Figure 4.1 Schematic of agents of a 1-D MAS distributed on the leading segment

4.1.1 Communication Topology

For a 1-D MAS evolution problem, every follower agent *i* communicates with two neighboring agents as shown in Fig. 4.2 [115].

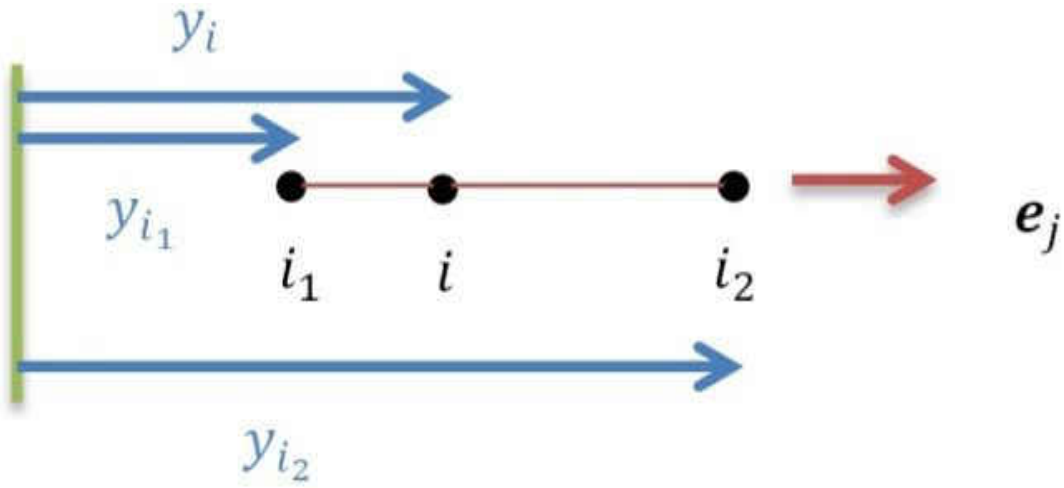

Figure 4.2 Communication topology of 1-D MAS evolution

Here, *weights of communication,* w_{i,i_1} and w_{i,i_2}, are calculated based on initial positions of agents *i,* i_1, and i_2, y_i, y_{i_1}, and y_{i_2}, respectively, by [115]

$$w_{i,i_1} = \frac{Y_{i_{12}} - Y_i}{Y_{i_2} - Y_{i_1}} \tag{4.1}$$

$$w_{i,i_2} = \frac{Y_i - Y_{i_1}}{Y_{i_2} - Y_{i_1}} \tag{4.2}$$

It is noted that

- $w_{i,i_1} + w_{i,i_2} = 1$, and
- weights of communication will be positive if follower agent i is initially placed in between i_1 and i_2.

4.1.2 Weight Matrix

Let us define an $(N-2)$ by N matrix W, as the weight matrix, where

$$W_{ij} = \begin{cases} w_{(i+2),j} & If\ follower\ i+2\ is\ adjacent\ to\ agent\ j \\ -1 & If\ i+2 = j \\ 0 & Otherwise \end{cases},$$

then, W can be partitioned as follows:

$$W = [B_{(N-2)\times 2} \quad \vdots \quad A_{(N-2)\times(N-2)}]. \tag{4.3}$$

The weight matrix W has following properties:

- W is zero-sum row-stochastic.
- There are three non-zero elements at every row of W.
- All diagonal elements of A are -1. The first two columns of W, partition B, each has one nonzero element.
- Partition A is not necessarily symmetric, however, if $A_{ij} = 0$, then $A_{ji} = 0$ and if $A_{ij} \neq 0$, then $A_{ji} \neq 0$.

Remark: As every follower agent of the MAS is initially located between two adjacent agents, all weight ratios are positive, and consequently, all non-zero element of B and nonzero off diagonal element of A will be positive.

4.1.3 MAS Evolution Dynamics

Let

$$y_{i_d} = \sum_{i\sim j} w_{i,j}\, y_i \tag{4.4}$$

be the desired position of the follower agent *i,* which is a linear combination of position vectors of adjacent agents. It is noted that the symbol "~" denotes adjacency between two follower agents *i* and *j.* Equation (4.4) can be rewritten as follows:

$$y_{i_d} = \sum_{j=1}^{N} w_{i,j} y_j\,, \tag{4.5}$$

where

$$\begin{cases} w_{i,j} > 0 & If\ i\sim j\ (i \text{ is adjacent to } j) \\ w_{i,j} = 0 & \text{Otherwise} \end{cases} \tag{4.6}$$

Let position of follower agent *i* is updated by

$$\dot{y}_i = g\left(y_{i_d} - y_i\right) = g\left(\sum_{j=3}^{N} w_{i,j} y_j - y_i\right) + g\sum_{j=1}^{2} w_{i,j} y_j \tag{4.7}$$

where g is a positive control parameter, then, eqn. (4.7) is the row *(i-2)* of the following state space dynamic:

$$\dot{\boldsymbol{Z}} = g(A\boldsymbol{Z} + B\boldsymbol{U}) \tag{4.8}$$

where $\boldsymbol{Z} = [y_3 \quad \cdots \quad y_N]^{\boldsymbol{T}}$, $\boldsymbol{U} = [y_1 \quad y_2]^{\boldsymbol{T}}$.

Theorem 1 [115]: Consider a MAS M are distributed on a straight line, where

- Leader agents of the MAS are located at the most left and the most right of a leading segment,

- Follower agents are initially distributed at the interior points of the leading segment,
- Every follower agent of the MAS updates its position according to eqn. (4.7), where weights of communication are assigned based on initial formation by eqns. (4.1) and (4.2),

then, agents of the MAS asymptotically converge to a final formation, that is a homogenous transformation of the initial configuration.

Proof:

The matrix A can be written as $A = -(I - Q)$ *where I is the identity matrix and* Q *is a non-negative matrix as all weights of communication are positive. As mentioned W is zero-sum row stochastic, and A is obtained by elimination of the first two columns of the matrix W, thus, sum of two rows of A is negative, while sum of rest of the rows of A is zero. This leads matrix -A to be a non-singular M-matrix. Then, by using Perron-Frobenius theorem, we can conclude that the spectrum of Q,* $\rho(Q) < 1$*, and therefore, matrix A is negative definite. Both initial and final formations of the MAS are the solution of equilibrium state* $Z_s = -A^{-1}BU_s$ *(where* U_s *can be either initial or final formations of the leader agents.). By applying some appropriate algebraic row operations on matrix W, W is converted to* $S = [-A^{-1}B \quad \vdots \quad -I]$*. Since W is zero-sum row stochastic, and S is obtained by applying algebraic row operations on W, thus,* S *is zero-sum row stochastic as well, and sum of every row of* $-A^{-1}B$ *is 1. An entry* $(-A^{-1}B)_{ij}$ *represents weights of communications follower agent (i+2) with respect to leader agents j. Since, for both initial and final formations, weights of communication with respect to the leader agents*

are the same, hence, final formation of the MAS is a homogenous transformation of the initial configuration.■

Remark: Homogenous transformation of a MAS in an n-D space can be decomposed to n 1-D MAS evolution problems, when the Jacobian of the desired homogenous transformation is diagonal. For this case, evolution of every coordinate of the motion of all agents of the MAS is viewed as a 1-D MAS evolution problem, that can be achieved under local inter-agent communication, as described above.

4.2 Two Dimensional MAS Evolution Problem Based

Let a MAS M consist of N agents moving in a plane where agents *1, 2,* and *3* are the leader agents and initially located at the vertices of a leading triangle, and the rest of the agents of the MAS, numbered by 4, 5, …., N, are follower agents that are initially distributed inside the leading triangle. As stated, leader agents move independently such that they remain non-aligned during motion, and every follower agent communicates with three local agents to grasp the homogenous transformation, prescribed by the leader agents.

4.2.1 Communication Topology

A graph $G = \varphi \cup \partial\varphi$ assigns communication topology of a MAS under a homogenous deformation, where

- The nodes that belong to the boundary of G, $\partial\varphi$, represent leader agents, and the nodes belonging to the sub-graph φ represent follower agents.

- Communication between a follower and a leader is shown by an arrow ended to the follower. This implies that the leader agent moves independently, while its position is tracked by a follower.
- Communication between two follower agents is shown by a non-directed edge that illustrates bi-communication between two follower agents, where weights of communication are not necessarily the same.

Shown in Fig. 4.3 is a sample communication topology for a MAS that consists of 14 agents (three leaders and eleven followers) [114].

4.2.2 Weights of Communication

In Fig. 4.4, communication of a follower agent *i* with three adjacent agents i_1, i_2, and i_3 is depicted, where agents i, i_1, i_2, and i_3 are initially distributed at (X_i, Y_i), (X_{i_1}, Y_{i_1}), (X_{i_2}, Y_{i_2}), and (X_{i_3}, Y_{i_3}), respectively.

Weights of communication of follower agent *i* with agents i_1, i_2, and i_3 are formulated as

$$w_{i,i_1} = \frac{(X_{i_3}-X_{i_2})(Y_i-Y_{i_2})-(Y_{i_3}-Y_{i_2})(X_i-X_{i_2})}{(X_{i_3}-X_{i_2})(Y_{i_1}-Y_{i_2})-(Y_{i_3}-Y_{i_2})(X_{i_1}-X_{i_2})} \tag{4.9}$$

$$w_{i,i_2} = \frac{(X_{i_1}-X_{i_3})(Y_i-Y_{i_3})-(Y_{i_1}-Y_{i_3})(X_i-X_{i_3})}{(X_{i_1}-X_{i_3})(Y_{i_2}-Y_{i_3})-(Y_{i_1}-Y_{i_3})(X_{i_2}-X_{i_3})} \tag{4.10}$$

$$w_{i,i_3} = \frac{(X_{i_2}-X_{i_1})(Y_i-Y_{i_1})-(Y_{i_2}-Y_{i_1})(X_i-X_{i_1})}{(X_{i_2}-X_{i_1})(Y_{i_3}-Y_{i_1})-(Y_{i_2}-Y_{i_1})(X_{i_3}-X_{i_1})} \tag{4.11}$$

where

$$w_{i,i_1} + w_{i,i_2} + w_{i,i_3} = 1 \tag{4.12}$$

In Fig. 4.5, plane of motion is divided into seven sub-regions, where at every sub-region weights of communication have different signs.

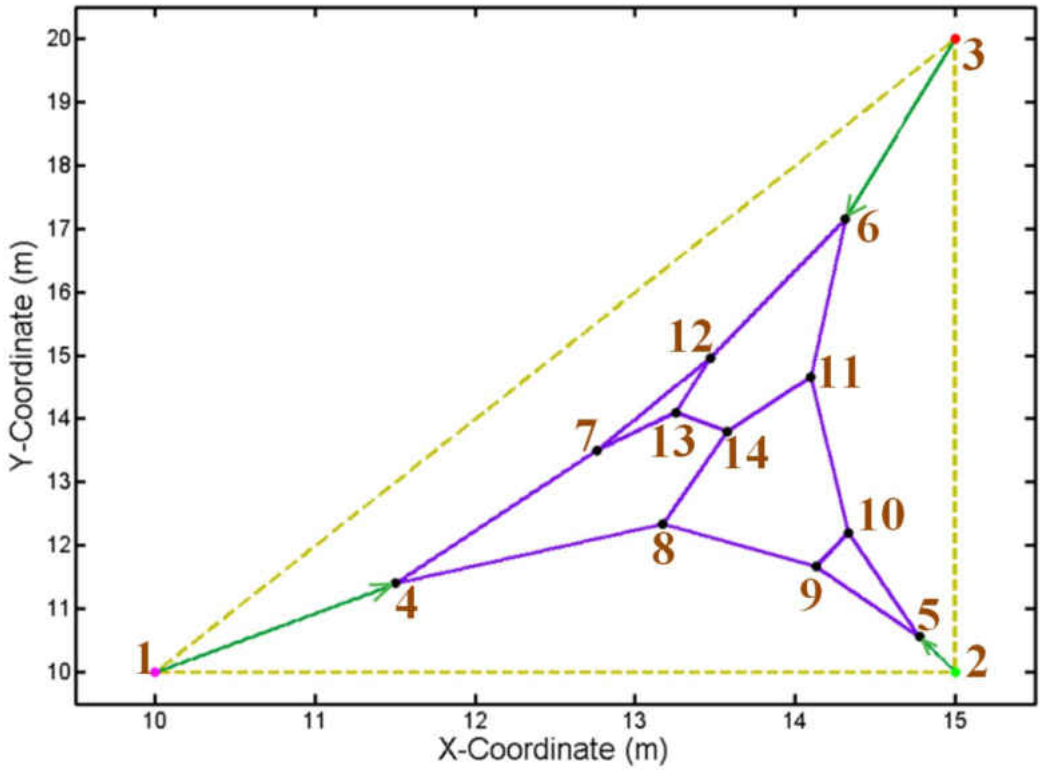

Figure 4.3 A sample communication topology for a MAS moving in a plane

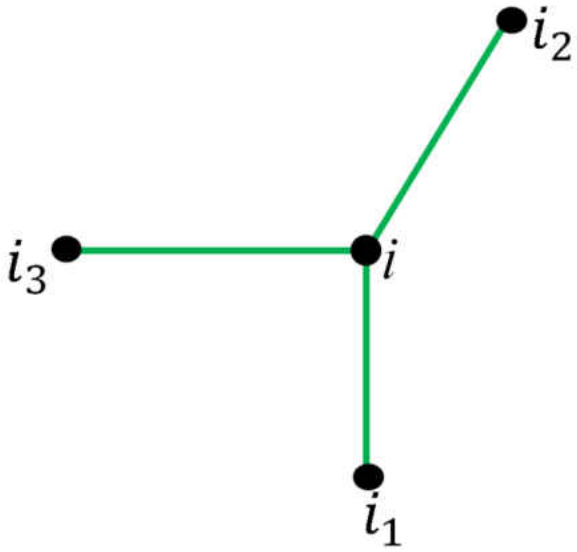

Figure 4.4 Schematic of communication of follower agent *i*

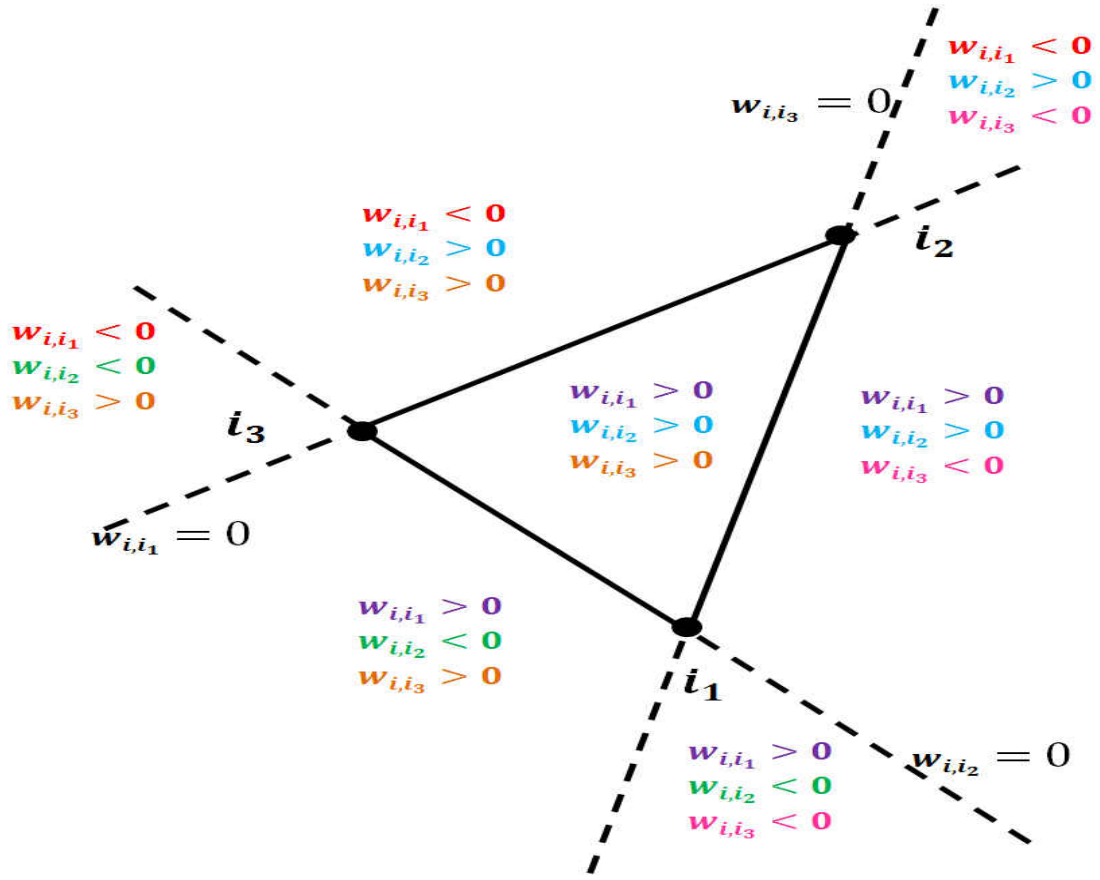

Figure 4.5 Seven sub-regions that with different signs for weights of communication

As it is obvious, if follower agent i is initially located inside the *communication triangle* whose vertices are placed by agents i_1, i_2, and i_3, then, w_{i,i_1}, w_{i,i_2}, and w_{i,i_3} are all positive.

4.2.3 Weight Matrix

Let an $(N-3)$ by N matrix W be the weight matrix, where

$$W_{ij} = \begin{cases} w_{(i+3),j} & If\ follower\ \boldsymbol{i+3}\ is\ adjacent\ to\ agent\ \boldsymbol{j} \\ -1 & If\ i+3=j \\ 0 & Otherwise \end{cases}. \tag{4.13}$$

The weight matrix W can be partitioned as follows:

$$W = [B_{(N-3)\times 3} \ \vdots \ A_{(N-3)\times(N-3)}]. \tag{4.14}$$

The weight matrix *W* has following properties:

- It is zero-sum row stochastic.
- All diagonal elements of *A* are *-1*.
- There are four non-zero elements at every row of the weight matrix *W*.
- Every column of partition *B* has one non-zero element.
- Although, *A* is not necessarily symmetric, however, if $A_{ij} = 0$, then $A_{ji} = 0$ and if $A_{ij} \neq 0$, then $A_{ji} \neq 0$.

4.2.4 MAS Evolution Dynamics

4.2.4.1 Single Integrator Kinematic Model

Let

$$\boldsymbol{r}_{i_d} = \sum_{\substack{j=1 \\ i \sim j}}^{N} w_{i,j} \boldsymbol{r}_j, \tag{4.15}$$

be the desired position of every follower agent *i,* then, position of follower *i* is continuously updated toward $\boldsymbol{r}_{i_d}$ at any time *t* during MAS evolution [114], as shown in Fig. 4.6.

In other words [114],

$$\dot{\boldsymbol{r}}_i = g\left(\boldsymbol{r}_{i_d} - \boldsymbol{r}_i\right), \tag{4.16}$$

where g is a positive control parameter.

Substituting $\boldsymbol{r}_{i_d}$ in eqn. (4.16) by eqn. (4.15) leads to following state space form for MAS evolution dynamic:

$$\dot{\boldsymbol{Z}} = g(A\boldsymbol{Z} + B\boldsymbol{U}), \tag{4.17}$$

where $\boldsymbol{Z} = [\boldsymbol{r}_4 \quad \dots \quad \boldsymbol{r}_N]^T$, $\boldsymbol{U} = [\boldsymbol{r}_1 \quad \boldsymbol{r}_2 \quad \boldsymbol{r}_3]^T$, A is $(N-3)$ by $(N-3)$ matrix, and B is $(N-3)$ by 3 matrix. It is noted that eqn. (4.16) is the row (*i-3*) of the matrix dynamic eqn. (4.17).

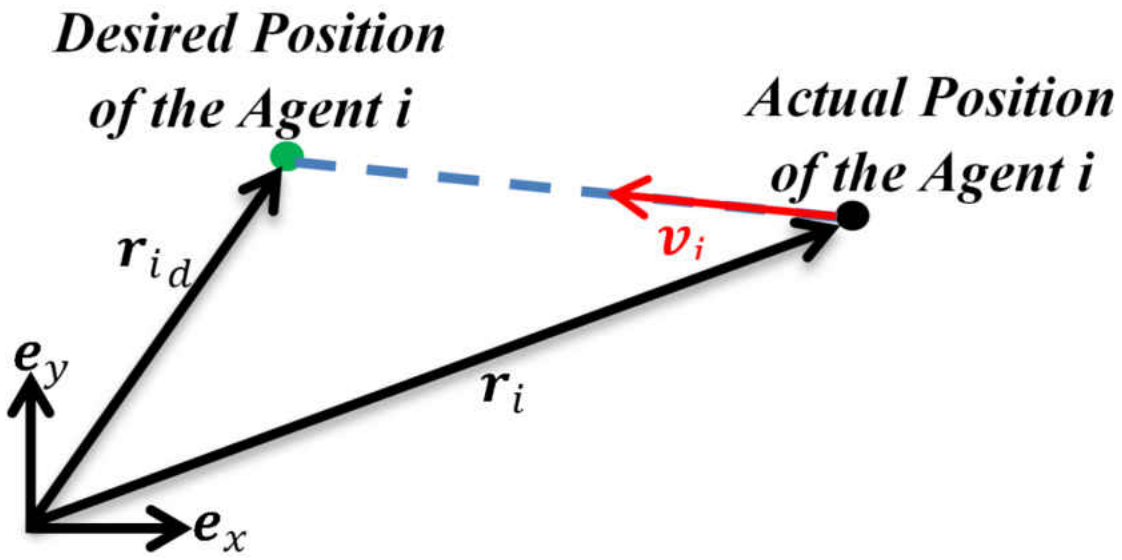

Figure 4.6 Schematic of updating position of every follower agent *i*

Theorem 2 [114]:

Let MAS *M* consist of *N* agents and move in a plane, where

- agents *1, 2* and *3,* are the leaders initially distributed at the vertices of the leading triangle,
- every follower agent communicates with three adjacent agents and updates its position according to eqn. (4.16),
- and every follower agent of the MAS is initially located inside a communication triangle whose vertices are placed by adjacent agents

then, initial formation of the MAS asymptotically converges to a final formation that is a homogenous transformation of the initial configuration.

Proof:

Since position of every follower agent is updated according to eqn. (4.16), the dynamic of all followers of the MAS is updated by eqn. (4.17). Since every follower agent i is initially located inside the triangle constructed on the adjacent agents, all weights of communication will be positive (See Fig. 4.5). Consequently, the matrix A can be written as

$$A = -(I - Q),$$

where Q is a non-negative matrix. Since, A is obtained by elimination of the first three columns of the weight matrix W and W is zero-sum row-stochastic, thus, sum of three rows of A is negative while sum of the rest of the rows of A is zero and – A is non-singular M-matrix. Using Perron-Ferobenius theorem, it is concluded that spectrum of Q is less than one, $\rho(Q) < 1$, and A is negative definite. Thus asymptotic convergence of the initial formation to a final configuration, where the leaders are settled, is guaranteed. Similar to the proof of theorem 1, it can also be concluded that both initial and final formations of the MAS have the same weights with respect to the leaders, thus, final formation of the MAS is a homogenous transformation of the initial configuration.

Remark: Assumption 3 of theorem 2 is a sufficient condition but it is not necessary. As an example, for initial distribution of a MAS that is shown in Fig. 4.7, the corresponding matrix *A* will be negative definite, although, weights of communication of follower agents are not all positive. For instance, by considering Fig. 4.7, we can figure out $w_{11,13} < 0$ while $w_{11,14} > 0$ and $w_{11,13} > 0$. Since *A* is negative definite, if position of every follower agent is updated by eqn. (4.16), then final formation of the MAS is a homogenous transformation of initial configuration that is achieved asymptotically.

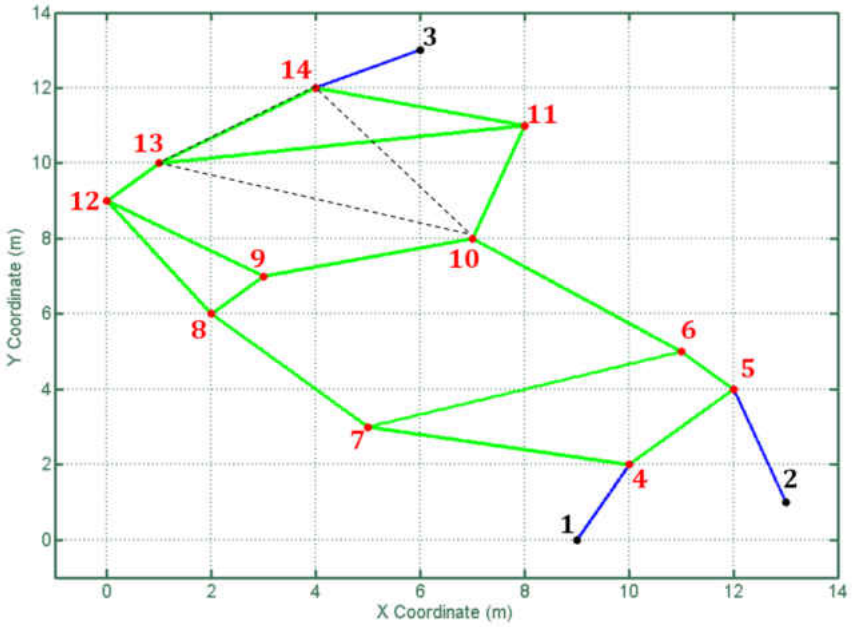

Figure 4.7 Sample of a initial distribution of agents of a MAS leads to some negative weight ratios while corresponding matrix A is negative definite

4.2.4.2 Double Integrator Kinematic Model

For double integrator kinematic model, position and velocity of every follower agent is updated by

$$\begin{cases} \dot{\boldsymbol{r}}_i = \boldsymbol{v}_i \\ \dot{\boldsymbol{v}}_i = -c\boldsymbol{v}_i + g(\boldsymbol{r}_{i_d} - \boldsymbol{r}_i) \end{cases}, \tag{4.18}$$

where control parameter g and $\boldsymbol{r}_{i_d}$ are already defined for the case of single integrator kinematic model. Equation (4.18) is the row (*i-3*) of the following matrix dynamic equation:

$$\ddot{\boldsymbol{Z}} + cI\dot{\boldsymbol{Z}} - gA\boldsymbol{Z} = gB\boldsymbol{U}. \tag{4.19}$$

It is noted that $\boldsymbol{Z}$ and $\boldsymbol{U}$ representing position of followers and leaders, respectively, are same as single integrator model. Also, if weights of communication are

all positive, then, A will be negative definite and therefore by using theorem 2, we can conclude that initial formation of the MAS asymptotically converges to a final configuration, that is a homogenous mapping of initial distribution of agents.

4.3 Examples

4.3.1 Deployment of a MAS on a Specific Curve

Let a MAS M have 6 agents and be initially distributed as shown in Fig. 4.8 [115].

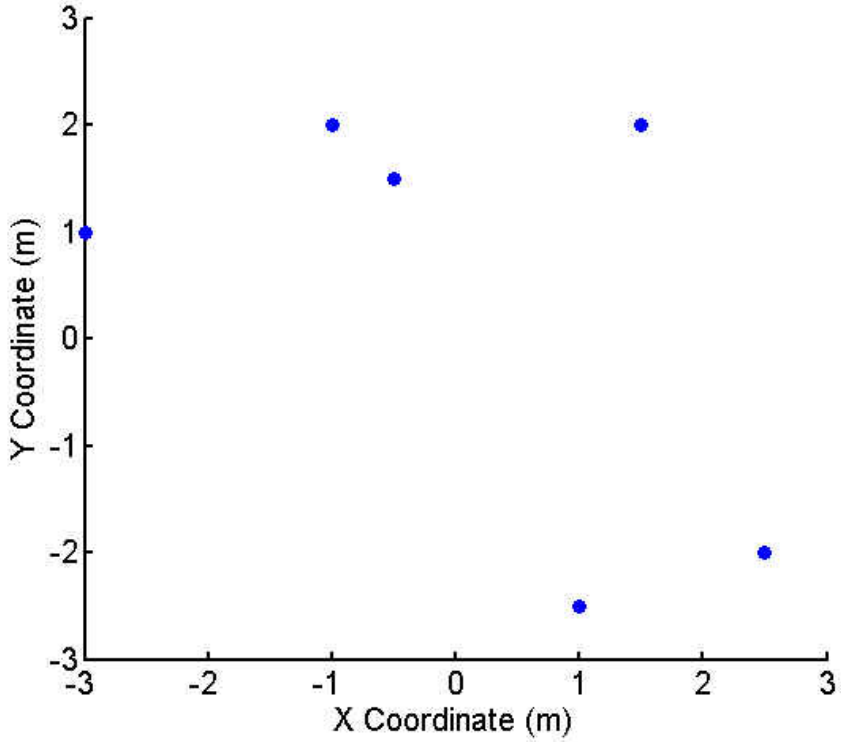

Figure 4.8 Initial distribution of the MAS M

Initial positions of the agents are listed in Table 4.1. It is desired that agents of the MAS be finally placed on the circle with radius 2, that is centered at the origin, as shown in Fig. 4.9. Final positions of the agents are also listed in Table 4.1.

Table 4.1 Initial and final position of the agents

Agent Number	Initial		Final	
	x	y	x	y
1	-3	1	-1.8794	-0.6840
2	2.5	-2	1.8794	0.6840
6	1	-2.5	0.3473	1.9696
3	-1	2	-1.5321	1.2856
5	-0.5	1.5	-0.3473	-1.9696
4	1.5	2	1.5321	-1.2856

In order to achieve the desired formation shown in Fig. 4.9, x and y coordinates of the motion of the followers must be guided separately by two leader agents. It is noted that for MAS deployment on a desired curve, weights of communications are assigned according to eqns. (4.1) and (4.2), based on desired final formations of the MAS.

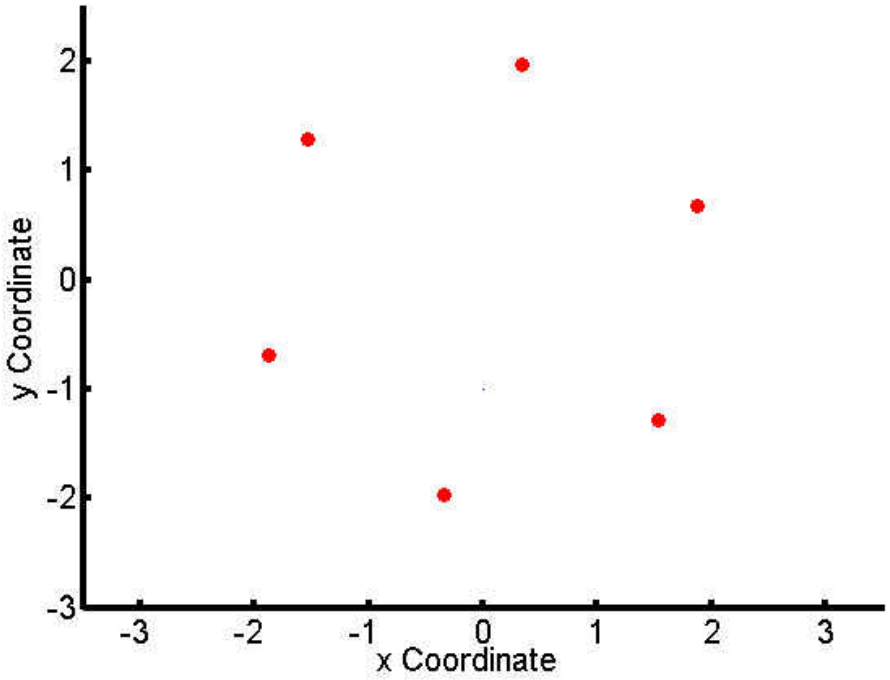

Figure 4.9 Desired final formation of the MAS

4.3.1.1 x Coordinate of MAS Evolution

The communication topology shown in Fig. 4.1 is considered for evolution of *x* coordinate of MAS. *x* coordinate of trajectories of the leader agents 1 and 2, guiding x coordinate of MAS evolution, are given as follows:

$$\text{Leader1}\begin{cases}-3+\frac{-1.8749+3}{20}t & t\le 20\\ -1.8749 & t>20\end{cases}$$

$$\text{Leader2}\begin{cases}2.5+\frac{1.8749-2.5}{20}t & t\le 20\\ 1.8749 & t>20\end{cases}$$

Weights of communications are assigned by eqns. (4.1) and (4.2) based on *x* coordinates of final formation of the MAS. Weights of communications are listed in Table 4.2.

Table 4.2 Weight ratios of the followers for $\boldsymbol{x}$ coordinate of the motion

Follower Agent	Weight Ratios	
3	$w_{3,1}=0.7733$	$w_{3,5}=0.2267$
5	$w_{5,3}=0.3969$	$w_{5,6}=0.6304$
6	$w_{6,5}=0.6304$	$w_{6,4}=0.3696$
4	$w_{4,2}=0.7733$	$w_{4,6}=0.2267$

4.3.1.2 Minimum Value for Control Parameter g

The minimum value for control parameter g that guarantees none of the follower agents leave the leading segment during evolution is 4.792. This minimum value is obtained by checking transient weights of communication with respect to leaders, which they are defined as follows:

$$\alpha_{i,1}(t)=\frac{x_2(t)-x_i(t)}{x_2(t)-x_1(t)} \tag{4.20}$$

$$\alpha_{i,i_2}(t) = \frac{x_i(t) - x_1(t)}{x_2(t) - x_1(t)} \tag{4.21}$$

In order to guarantee that none of the followers leave the leading segment, $\alpha_{i,1}(t)$ and $\alpha_{i,i_2}(t)$ must be positive for every follower agent i ($i = 3,4,5$ and 6).

For the simulation, we choose $g = 6$. In Fig. 4.10 x coordinate of evolution of MAS versus time is shown.

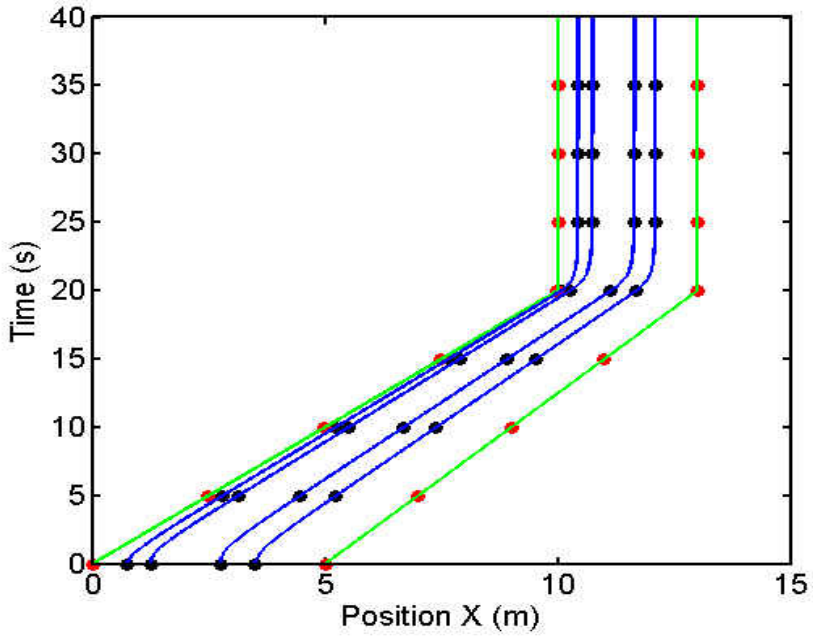

Figure 4.10 x coordinate of MAS evolution

4.3.1.3 y Coordinate of MAS Evolution

Communication topology of y coordinate of MAS evolution is shown in Fig. 4.11.

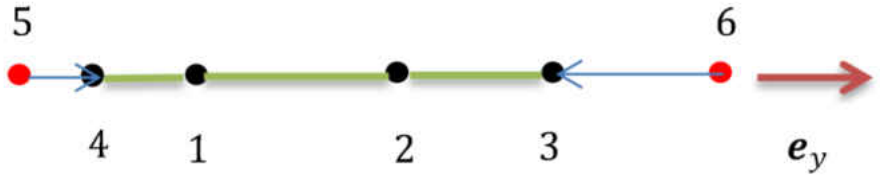

Figure 4.11 Communication topology of y coordinates of MAS evolution

Weights of communication of evolution of y coordinates of follower agents are listed in Table 4. 3, where they are calculated based on y coordinates of agents in the final formation.

Table 4.3 Weight ratios of the followers for $\boldsymbol{y}$ coordinate of the motion

Follower Agent	Weight Ratios	
4	$w_{4,5} = 0.4680$	$w_{4,1} = 0.5320$
1	$w_{1,4} = 0.6946$	$w_{1,2} = 0.3054$
2	$w_{2,1} = 0.3054$	$w_{2,3} = 0.6946$
3	$w_{3,2} = 0.5320$	$w_{3,6} = 0.4680$

Evolution of *y* coordinate of MAS is shown in Fig. 4.12. Also, trajectories of the agents of the MAS in x-y coordinates are shown in Fig. 4.13.

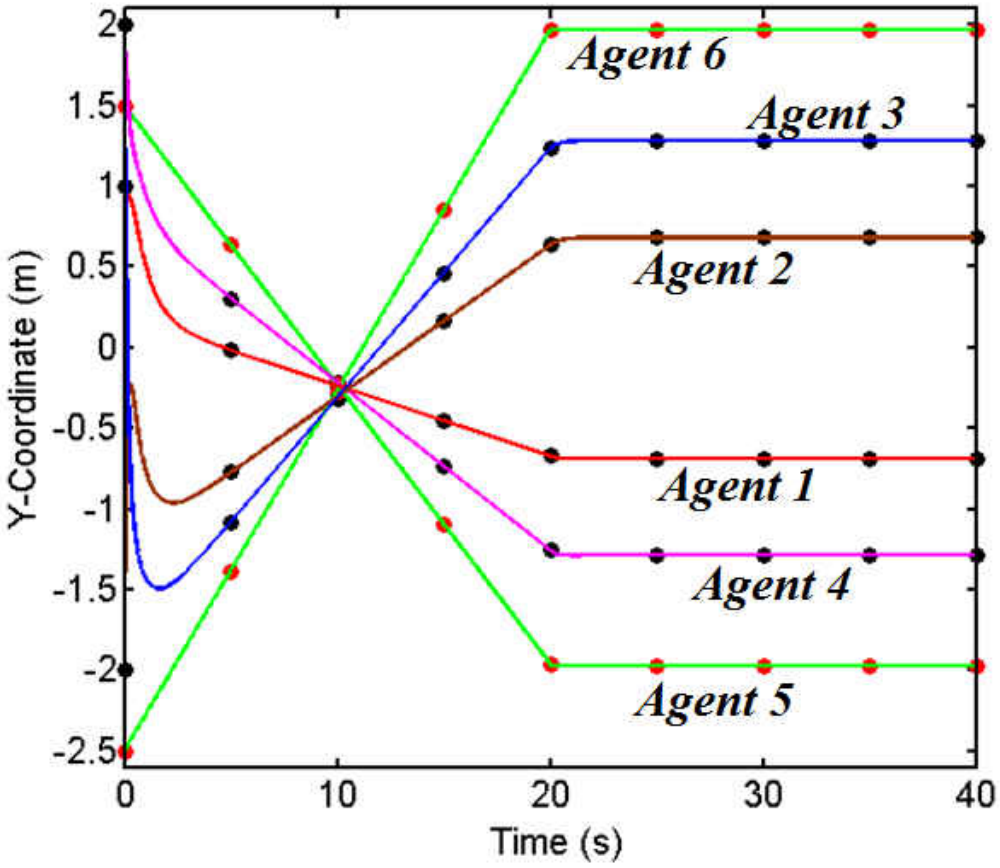

Figure 4.12 y coordinate of MAS evolution

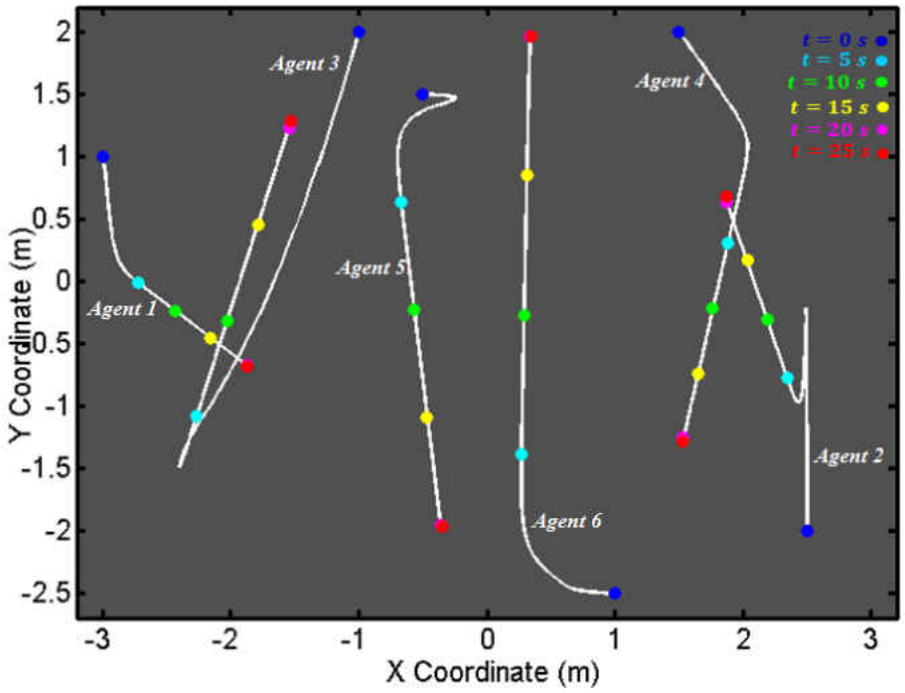

Figure 4.13 Trajectories of MAS evolution moving the x-y plane

4.3.2 MAS Evolution in a 2-D Space under Local Communication

Let a MAS *M* consist of 14 agents (three leaders and eleven followers) moving in a plane. Leader agents 1, 2, and 3 are initially located at $(10,10)$, $(15,10)$, and $(15,20)$, respectively. It is desired that they are finally settled at $(30,20)$, $(40,15)$, and $(35,25)$, respectively. Initial positions of follower agents are sorted in Table 4.4.

Table 4.4 Position of the followers in the initial formation

Agent	*x*	*y*
4	**11.50**	**11.40**
5	**14.78**	**10.56**
6	**14.32**	**17.16**
7	**12.76**	**13.50**
8	**13.17**	**12.34**
9	**14.13**	**11.67**

Agent	*x*	*y*
10	**14.33**	**12.20**
11	**14.10**	**14.66**
12	**13.47**	**14.96**
13	**13.25**	**14.10**
14	**13.58**	**13.80**

Also, Initial and final leading triangles are shown in Fig. 4.14.

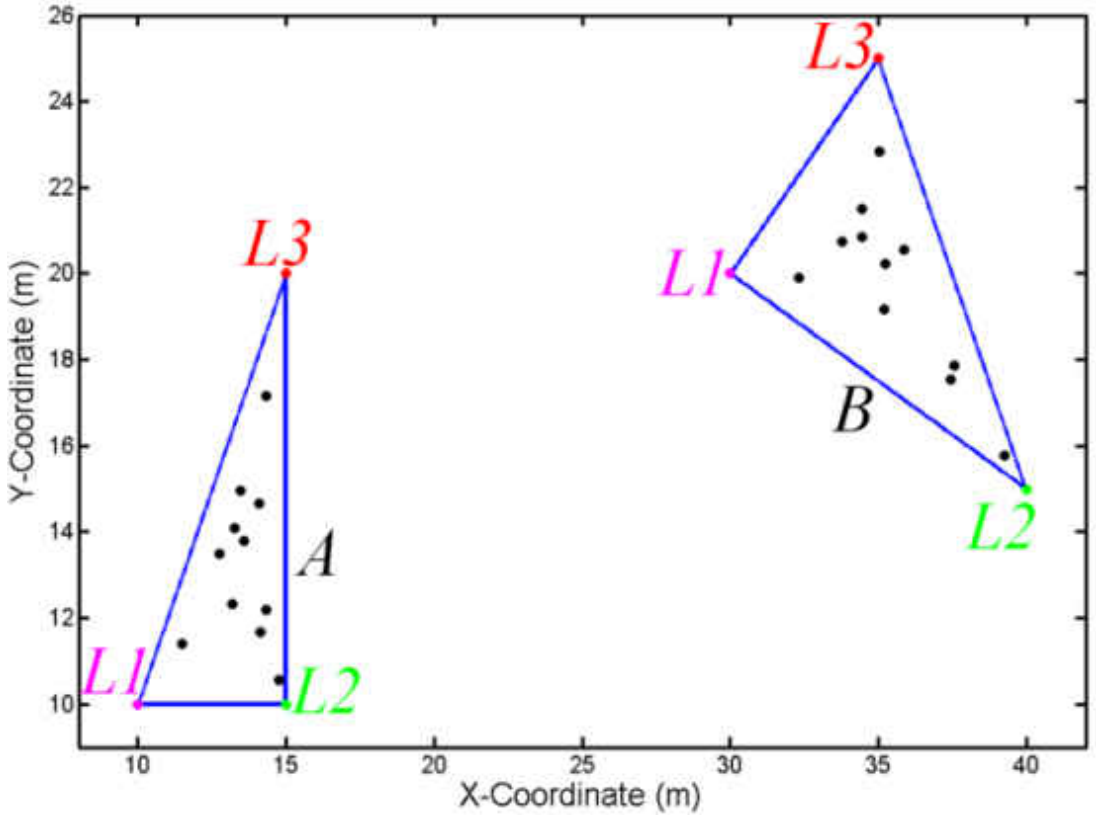

Figure 4.14 Initial and desired final formations of the MAS

Here, every follower agent communicates with three local agents to update its position according eqn. (4.16), where weights of communication, assigned based on initial formation, are listed in Table 5.

Table 4.5 Weights of Communications of follower agents

	Weights of Communication
F4	$w_{4,1} = 0.5, w_{4,7} = 0.2, w_{4,8} = 0.3$
F5	$w_{5,2} = 0.71, w_{5,9} = 0.15, w_{5,10} = 0.14$
F6	$w_{6,3} = 0.45, w_{6,11} = 0.25, w_{6,12} = 0.3$
F7	$w_{7,4} = 0.32, w_{7,12} = 0.30, w_{7,13} = 0.38$
F8	$w_{8,4} = 0.29, w_{8,9} = 0.36, w_{8,14} = 0.35$
F9	$w_{9,5} = 0.35, w_{9,8} = 0.31, w_{9,10} = 0.34$

	Weights of Communication
F10	$w_{10,5} = 0.33, w_{10,9} = 0.37, w_{10,11} = 0.40$
F11	$w_{11,6} = 0.4, w_{11,10} = 0.3, w_{11,14} = 0.3$
F12	$w_{12,6} = 0.34, w_{12,7} = 0.29, w_{12,13} = 0.37$
F13	$w_{13,7} = 0.35, w_{13,12} = 0.35, w_{13,14} = 0.30$
F14	$w_{14,8} = 0.30, w_{14,11} = 0.41, w_{14,13} = 0.29$

Also, control parameter g must be chosen such that transient weights of communication of every follower agent i with respect to leader agents, $\alpha_{i,j}(t)$, remain positive at any time t. This assures that none of the followers leave leading triangle during evolution. The minimum control parameter $g_{min}$is obtained to be 9.488. Simulation is performed for $g = 15$.

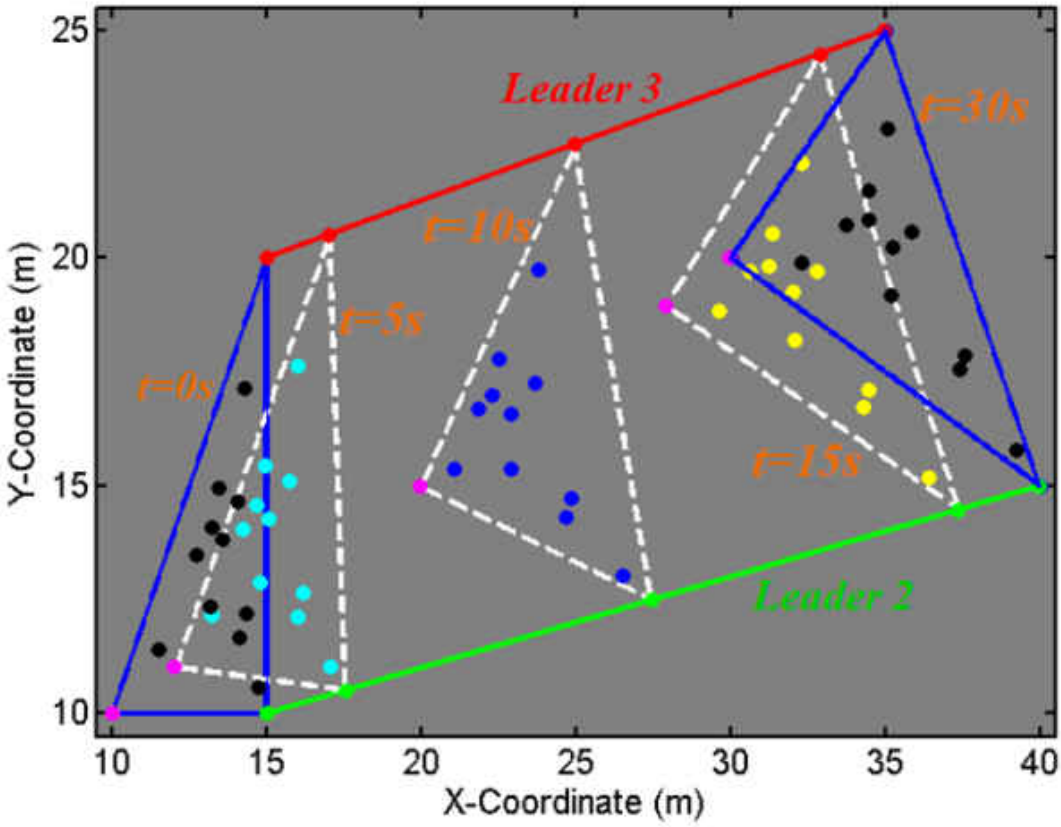

Figure 4.15 Formation of the MAS at times $t = 0s$, $t = 5s$, $t = 10s$, $t = 15s$, $t = 20s$, and $t = 30s$

Formation of the MAS at five sample times $t = 0s$, $t = 5s$, $t = 10s$, $t = 20s$ and $t = 30s$, are shown in Fig. 4.15. Also, x and y coordinates of actual position of follower agent 13, $\boldsymbol{r}_{13}(t)$ versus time are shown in Fig. 4.16, by blue and red, respectively. In

addition, x and y coordinates of desired position of follower agent 13, $\boldsymbol{r}_{13_d}(t)$ are depicted by hashed green and black curves, respectively.

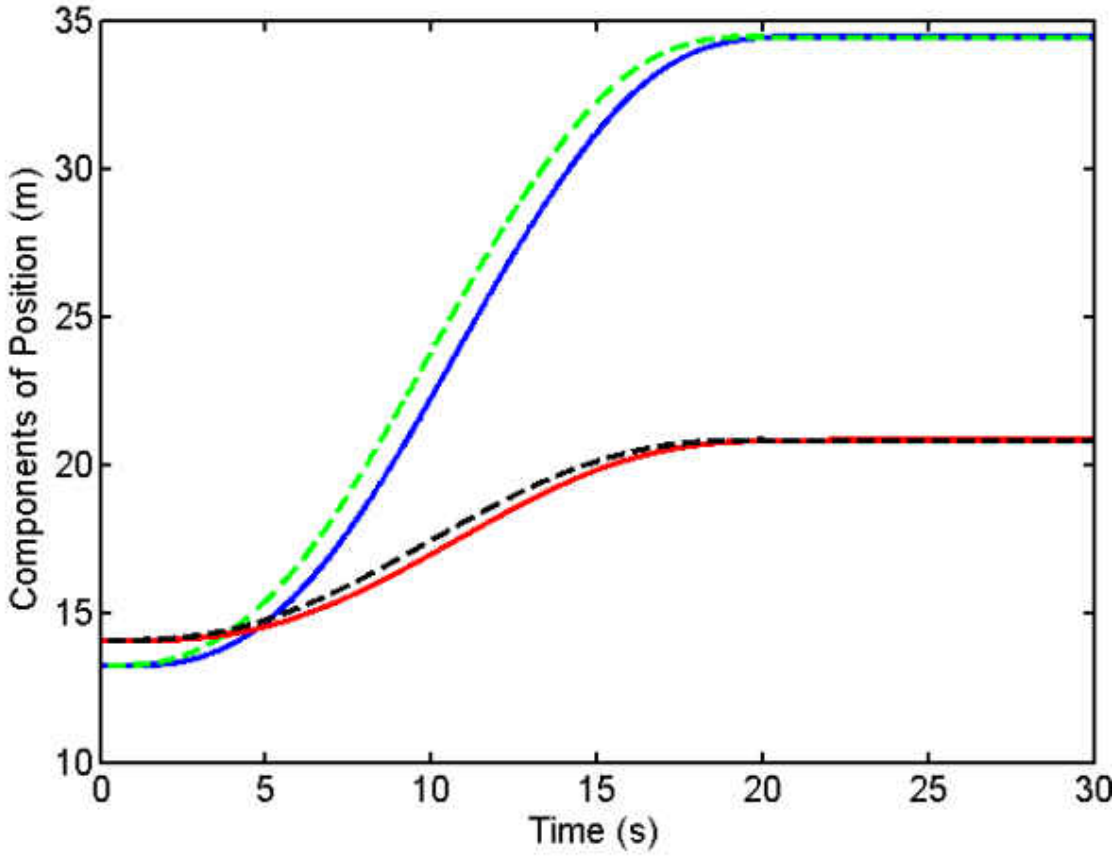

Figure 4.16 x and y coordinates of $\boldsymbol{r}_{13}(t)$ shown by blue and red, respectively;x and y coordinates of $\boldsymbol{r}_{13_d}(t)$ shown by hashed green and black, respectively

CONCLUSION

Our proposed continuum based method for evolution of MAS offers some novel insights and a unique perspective in comparison with common approaches for formation control of swarms.

Homogenous transformation technique can address mentioned issues corresponding to PDE based approaches. First, exact desired position of follower agents can be simply obtained through local communication with some nearby agents. This desired position can be defined as a linear combination of position vectors of some agents that are adjacent to a follower agent, where constant parameters of the combination are assigned based on initial positions of the agents. Furthermore, we define a mechanism to assure that none of the followers leave the leading region, that are surrounded by leader agents, during MAS evolution. Thus, collision avoidance can be guaranteed if trajectories of leader agents, placed at the boundary of the MAS are designed properly. Under homogenous transformation protocol, evolution of the MAS in an *n-D* space can be achieved with less inter-agent communications, where fewer leaders are required to prescribe the motion mapping. For this case, communication based MAS evolution can be prescribed by the independent motion of $n+1$ leader agents of the MAS and grasped by every follower agent through local communication with $n+1$ nearby agents.

Under rigidity assumptions, a swarm may not be able to pass through a narrow channel. This limitation can be addressed by homogenous transformations where the size of a swarm can be enlarged or shrunk by designing appropriate trajectories for the leader agents. In this regard, if leader agents are located at the boundary of the MAS, then it is guaranteed that followers don't leave the region bounded by the leaders if the MAS is

transformed under homogenous mapping. In addition, an *n-D* homogenous mapping can be assigned based on trajectories *n+1* leaders. Hence, if leaders' paths are designed properly swarm can be shrunk appropriately as well, to pass through a narrow channel.

REFERENCES

[1] Bahceci E., Soysal O. and Sahin E.,2003,"A Review: Pattern Formation and Adaptation in Multi-Robot Systems" *Report under copyright of Robotics Institute Carnegie Mellon University Pittsburgh, Pennsylvania 15213.*

[2] Jia Q., Li G., 2007, "Formation Control and Obstacle Avoidance Algorithm of Multiple Autonomous Underwater Vehicles(AUVs) Based on Potential Function and Behavior Rules," *Proceedings of the IEEE International Conference on Automation and Logistics, Jinan, China.*

[3] Chen Y. Q. and Wang Zh., 2005, "Formation control: a review and a new consideration," *Intelligent Robots and Systems, Edmonton, Alberta, Canada.*

[4] Rastgoftar H. and Jayasuriya S., 2012, "Planning and Control of Swarm Motion as Deformable Body," *ASME Dynamic Systems and Control Conference, Fort Lauderdale, Florida, USA.*

[5] Murray R. M., 2007, "Recent Research in Cooperative Control of Multi-Vehicle Systems," *Journal of Dynamic Systems, Measurement and Control, 129, 571-583.*

[6] Martin S. K. M., Klupar P., and Winter J., 2001, "TechSat 21 and Revolutionizing Space Missions Using Microsatellites," *in In Proc. of USU/AIAA Conf., Logan, UT.*

[7] Bender J. G., 1991, "An Overview of Systems Studies of Automated Highway Systems," *IEEE Transactions on Vehicular Technology, vol. 40, no. 1, pp. 82 – 99.*

[8] Barnes L. E., Fields M. A., and Valavanis K. P., 2009, "Swarm Formation Control Utilizing Elliptical Surfaces and Limiting Functions," *IEEE Transactions on Systems, Man, and Cybernetics—Part B: Cybernetics, Vol. 39, No. 6.*

[9] Almonfrey D., Vassallo R. F. and Dalfior J. S., 2010, "Visual-Servo Controller Applied to the Leader of a Robot Team with a Centralized Formation Control," *IEEE International Conference on Industrial Technology (ICIT).*

[10] Cruz C. D. L. and Carelli R., 2006, "Dynamic Modeling and Centralized Formation Control of Mobile Robots", *32 Annual Conference on IEEE Industrial Electronics, IECON.*

[11] Yang E., Gu D., and Hu H., 2005, "Nonsingular Formation Control of Cooperative

Mobile Robots via Feedback Linearization," *IEEE conference on Intelligent Robots and Systems.*

[12] Kopfstedt T., Mukai M., Fujita M. and Sawodny O., 2006, "A Networked Formation Control for Groups of Mobile Robots using Mixed Integer Programming" *Proceedings of the 2006 IEEE International Conference on Control Applications Munich, Germany.*

[13] Shao J., Xie G. and Wang L., 2007, "Leader-Following Formation Control of Multiple Mobile Vehicles" IET Control Theory Appl., 1, (2), pp. 545–552.

[14] Vassilaras S., Vogiatzis D. and Yovanof G. S., 2006, "Security and Cooperation in Clustered Mobile Ad Hoc Networks with Centralized Supervision," *IEEE Journal on Selected Areas in Communications, Vol. 24, No. 2.*

[15] Bazoula A., Djouadi M.S. and Maaref H., 2008, "Formation Control of Multi-Robots via Fuzzy Logic Technique," *Int. J. of Computers, Communications & Control, ISSN 1841-9836, E-ISSN 1841-9844.*

[16] Desai J. P., Ostrowski J., and Kumar V., 1998, "Controlling Formations of Multiple Mobile Robots," *International Conference on Robotic and Automation, Leuven, Belgium.*

[17] Consolinia L., Morbidib F., Prattichizzob D. and Tosques M., 2008, "Leader–Follower Formation Control of Nonholonomic Mobile Robots with Input Constraints," *Automatica 44 1343–1349.*

[18] Vidal R., Shakernia O., and Sastry S., 2004, "Distributed Formation Control with Omnidirectional Vision-Based Motion Segmentation and Visual Servoing," *Robotics & Automation Magazine, IEEE Volume 11.*

[19] Gian Luca Mariottini, Fabio Morbidi, Domenico Prattichizzo, Nicholas Vander Valk, Nathan Michael, George Pappas, and Kostas Daniilidis, 2009, "Vision-Based Localization for Leader–Follower Formation Control," *IEEE Transactions on Robotics, Vol. 25, No. 6.*

[20] Shi-Cai L., Da-Long T. and Guang-Jun L., 2007, "Robust Leader-follower Formation Control of Mobile Robots Based on a Second Order Kinematics Model," *Acta Automatica Sinica, Volume 33, Issue 9, , Pages 947-955.*

[21] Soorki, M.N., Talebi, H.A. and Nikravesh, S.K.Y., 2011, "A Leader-Following Formation Control of Multiple Mobile Robots with Active Obstacle Avoidance,"*19th Iranian Conference Electrical Engineering (ICEE).*

[22] Soorki, M.N.; Talebi, H.A. and Nikravesh, S.K.Y., 2011, "A Robust Leader-Obstacle Formation Control," *IEEE International Conference on Control Applications (CCA).*

[23] Soorki, M.N., Talebi, H.A. and Nikravesh, S.K.Y., 2011, "A Robust Dynamic Leader-Follower Formation Control with Active Obstacle Avoidance," *IEEE International Conference on Systems, Man, and Cybernetics (SMC).*

[24] Ahmed S., Karsiti M. N., and Cruz J. B., 2007, "Observer Based Feedback Control Strategies for Collaborative Robots," *International Conference on Intelligent and Advanced Systems (ICIAS).*

[25] Gamage G. W., Mann G. K. I. and Gosine R. G., 2010, "Leader Follower Based Formation Control Strategies for Nonholonomic Mobile Robots: Design, Implementation and Experimental Validation" *American Control Conference Marriott Waterfront, Baltimore, MD, USA.*

[26] Zhao D. Zou T. Li S. and Zhu Q., 2011, "Adaptive Backstepping Sliding Mode Control for Leader–Follower Multi-Agent Systems," *IET Control Theory and Applications.*

[27] Bouteraa Y. and Ghommam J., 2011, "Coordinated backstepping control of multiple robot system of the leader-follower structure," *8th International Multi-Conference on Systems, Signals & Devices.*

[28] Dierks T. and Jagannathan S., 2007, "Control of Nonholonomic Mobile Robot Formations: Backstepping Kinematics into Dynamics," *16th IEEE International Conference on Control Applications Part of IEEE Multi-conference on Systems and Control Singapore.*

[29] Li X., Xiao J and Cai Z., 2005, "Backstepping Based Multiple Mobile Robots Formation Control," *International Conference on Intelligent Robots and Systems.*

[30] Cui R., Ge S. S., How B. V. E. and Choo Y. S., 2010, "Leader–Follower Formation Control of Underactuated Autonomous Underwater Vehicles," *Ocean Engineering 37(2010)1491–1502.*

[31] Chen X. and Serrani A., 2007, "Smith Predictors in Nonlinear Systems - Application to ISS-based Leader/follower Trailing Control," *American Control Conference Marriott Waterfront, Baltimore, MD, USA.*

[32] Castro R., Alvarez J. and Martinez J., 2009, "Robot Formation Control Using Backstepping and Sliding mode techniques," *6th International Conference on Electrical Engineering, Computing Science and Automatic Control.*

[33] Breivik M., Subbotin M. V. and Fossen T. I., 2006, "Guided Formation Control for Wheeled Mobile Robots," *9th International Conference on Control, Automation, Robotics and Vision.*

[34] Yang E., and Gu D., Member, IEEE, 2007, "Nonlinear Formation-Keeping and Mooring Control of Multiple Autonomous Underwater Vehicles," *American Control Conference Marriott Waterfront, Baltimore, MD, USA.*

[35] Khoo S., Xie L., Yu Zh. and Man Zh., 2008, "Finite-time Consensus Algorithm of Multi-agent Networks," *10th International Conference on Control, Automation, Robotics and Vision, Hanoi, Vietnam.*

[36] Yang E., Gu D., 2007, "Nonlinear Formation-Keeping and Mooring Control of Multiple Autonomous Underwater Vehicles," *IEEE/ASME Transactions on Mechatronics, Vol. 12, N0. 2.*

[37] Yang E., Gu D., and Hu H., 2005, "Improving the Formation-Keeping Performance of Multiple Autonomous Underwater Robotic Vehicles," *IEEE International Conference on Mechatronics & Automation Niagara Canada.*

[38] Ghommam J., Mehrjerdi H. and Saad M., 2011, "Leader-Follower Formation Control of Nonholonomic Robots with Fuzzy Logic Based Approach for Obstacle Avoidance," *IEEE/RSJ International Conference on Intelligent Robots and Systems September 25-30, San Francisco, CA, USA.*

[39] Gu D. and Yang E., 2005, "Fuzzy Policy Gradient Reinforcement Learning for Leader-Follower Systems," *IEEE International Conference on Mechatronics & Automation Niagara Falls, Canada.*

[40] Kang X., Xu H. and Feng X., 2009, "Fuzzy Logic Based Behavior Fusion for Multi-AUV Formation Keeping in Uncertain Ocean Environment," MTS/IEEE Biloxi - Marine Technology for Our Oceans.

[41] Sisto M. and Gu D., 2006, "A Fuzzy Leader-Follower Approach to Formation Control of Multiple Mobile Robots," *IEEE/RSJ International Conference on Intelligent Robots and Systems.*

[42] Yang E. and Gu D., 2007, "An Integrated Fuzzy and Learning Approach to Performance Improvement of Model-Based Multi-Agent Robotic Control Systems," *IEEE International Conference on Mechatronics and Automation Harbin, China.*

[43] Gu D. and Wang Z., 2007, "Distributed Cohesion Control for Leader-follower Flocking," *IEEE International Fuzzy Systems Conference.*

[44] Cheok K. C., Smid G.E., Kobayashi K. Overholt, J.L. and Lescoe P., 1997, "A Fuzzy Logic Intelligent Control System Architecture for an Autonomous Leader-Following Vehicle," *American Control Conference Albuquerque, USA.*

[45] Dierks T., and Jagannathan S., 2010, "Neural Network Output Feedback Control of Robot Formations," *IEEE Transactions on Systems, Man, and Cybernetics—Part B: Cybernetics, Vol. 40, No. 2.*

[46] Dierks T., and Jagannathan S., 2009, "Neural Network Control of Mobile Robot Formations Using RISE Feedback," *IEEE Transactions on Systems, Man, and Cybernetics—Part B: Cybernetics, Vol. 39, No. 2.*

[47] Khoo S., Yin J., Wang B., Zhao Sh. and Man Zh., 2011, "Adaptive Data Based Neural Network Leader follower Control of Multi-agent Networks," *37th Annual Conference on IEEE Industrial Electronics Society (IECON)* .

[48] Dierks T., Brenner B. and Jagannathan S., 2013, "Neural Network-Based Optimal Control of Mobile Robot Formations With Reduced Information Exchange," *IEEE Transactions on Control Systems Technology.*

[49] Dierks T., and Jagannathan S., 2009, "Neural Network Control of Quadrotor UAV Formations," *American Control Conference Hyatt Regency Riverfront, St. Louis, MO, USA.*

[50] Dierks T., and Jagannathan S., 2007, "Control of Nonholonomic Mobile Robot Formations Using Neural Networks" *IEEE International Symposium on Intelligent Control Part of IEEE Multi-conference on Systems and Control.*

[51] Yao Z., Song Y. D. and Cai W., 2010, "Neuro-Adaptive Virtual Leader Based Formation Control of Multi-Unmanned Ground Vehicles," *11th Int. Conf. Control, Automation, Robotics and Vision Singapore.*

[52] Summers T. H., Yu Ch., Dasgupta S Anderson B. D. O., 2011, "Control of Minimally Persistent Leader-Remote-Follower and Coleader Formations in the Plane" *IEEE Transactions on Automatic Control, Vol. 56, N0. 12.*

[53] Gazi V. and Passino K. M., 2011, "Swarm Stability and Optimization," *Springer New York.*

[54] Jia Q. and Li G., 2007, "Formation Control and Obstacle Avoidance Algorithm of Multiple Autonomous Underwater Vehicles (AUVs) Based on Potential Function and Behavior Rules" *IEEE International Conference on Automation and Logistics.*

[55] Ren J. and McIsaac K. A., 2003, "A Hybrid-Systems Approach to Potential Field Navigation for a Multi-Robot Team," *IEEE lnteroslional Conference on Robotics &Automation Taipei, Taiwan.*

[56] Roussos G. and Kyriakopoulos K. J., 2010, "Completely Decentralised Navigation of Multiple Unicycle Agents with Prioritisation and Fault Tolerance," *49th IEEE Conference on Decision and Control Hilton Atlanta Hotel, Atlanta, GA, USA.*

[57] Wolf M. T. and Burdick J. W., 2008, "Artificial Potential Functions for Highway Driving with Collision Avoidance," *IEEE International Conference on Robotics and Automation Pasadena, CA, USA.*

[58] Gerdes J. C. and Rossetter E. J., 2001,"A Unified Approach to Driver Assistance Systems based on Artificial Potential Felds," *Journal of Dynamic Systems Measurement and Control – Transations of the ASME, vol. 123, no. 3, pp. 431–438.*

[59] Rossetter E. J., Switkes J. P. and Gerdes J. C. , 2004 ,"Experimental Validation of the Potential Field Lanekeeping System," *International Journal of Automotive Technology, vol. 5, no. 2, pp. 95–108.*

[60] Motee1 N., Jadbabaie A. and Pappas G., 2009, "Path Planning for Multiple Robots: An Alternative Duality Approach," *American Control Conference Marriott Waterfront, Baltimore, MD, USA.*

[61] Zhao J., Su X. and Yan J., 2009, "A Novel Strategy for Distributed Multi-Robot Coordination in Area Exploration," *International Conference on Measuring Technology and Mechatronics Automation.*

[62] Sabattini L., Secchi C., Fantuzzi C. and de Macedo Possamai D., 2010, "Tracking of Closed–Curve Trajectories for Multi–Robot Systems" *IEEE/RSJ International Conference on Intelligent Robots and Systems, Taipei, Taiwan.*

[63] Yamashita A., Fukuchi M., Ota J., Arai T. and Asama H., 2000, "Motion Planning for Cooperative Transportation of a Large Object by Multiple Mobile Robots in a 3D Environment," *IEEE International Conference on Robotics & Automation San Francisco, CA.*

[64] Kang Y. H., Lee M. Ch., Kim Ch. Y., Yoon S. M. and Noh Ch. B., 2011, "A Study of Cluster Robots Line Formatted Navigation Using Potential Field Method," *IEEE International Conference on Mechatronics and Automation.*

[65] Xu X., Xie J., Xie K., 2006, "Path Planning and Obstacle-Avoidance for Soccer Robot Based on Artificial Potential Field and Genetic Algorithm" *6th World Congress on Intelligent Control and Automation.*

[66] Weijun S., Rui M., Chongchong Y., 2010, "A Study on Soccer Robot Path Planning with Fuzzy Artificial Potential Field," *International Conference on Computing, Control and Industrial Engineering.*

[67] Dimarogonas1 D.V. and Johansson K.H., 2009, " Xue D., Yao J. Chen G. and Yu Y. L., 2009, "Formation Control of Networked Multi-Agent Systems*," IET Control Theory and Applications.*

[68] Ajorlou A., Momeni A. and G. Aghdam A., 2010, "A Class of Bounded Distributed Control Strategies for Connectivity Preservation in Multi-Agent Systems," *IEEE Transactions on Automatic Control, Vol. 55, No. 12.*

[69] Ajorlou A., Momeni A. and G. Aghdam A., 2009, "Connectivity Preservation in a Network of Single Integrator Agents*," 48th IEEE Conference on Decision and Control and 28th Chinese Control ConferenceShanghai, P.R. China.*

[70] Ranjbar-Sahraei B., Shabaninia F., Nemati A. and Stan S. D., 2012, "A Novel Robust Decentralized Adaptive Fuzzy Control for Swarm Formation of Multiagent Systems," *IEEE Transactions on Industrial Electronics, Vol. 59, No. 8.*

[71] Ghommam J., Saad M. and Mnif F., 2010, "Robust Adaptive Formation Control of Fully Actuated Marine Vessels Using Local Potential Functions," *International Conference on Robotics and Automation Anchorage Convention District Alaska, USA.*

[72] Yu W. and Chen G., 2010, "Robust Adaptive Flocking Control of Nonlinear Multi-agent Systems," *IEEE International Symposium on Computer-Aided Control System Design Yokohama, Japan.*

[73] Miyasato Y., 2010, "Adaptive H∞ Formation Control for Euler-Lagrange Systems," *49th IEEE Conference on Decision and Control, Hilton Atlanta Hotel, Atlanta, GA, USA.*

[74] Miyasato Y., 2011, "Adaptive H∞ Formation Control for Euler-Lagrange Systems by Utilizing Neural Network Approximators," *American Control Conference on O'Farrell Street, San Francisco, CA, USA.*

[75] Ranjbar Sahraei B. and Shabaninia F., 2010, "A Robust *H*∞ Control Design for Swarm Formation Control of Multi-Agent Systems: A Decentralized Adaptive Fuzzy Approach,"*3rd International Symposium on Resilient Control Systems (ISRCS).*

[76] Pereira A. R., Hsu L. and Ortega R., 2009, "Globally Stable Adaptive Formation Control of Euler-Lagrange Agents via Potential Functions," *American Control Conference Hyatt Regency Riverfront, St. Louis, MO, USA.*

[77] Ren W. and Beard R.W., 2004, "Formation Feedback Control for Multiple Spacecraft via Virtual Structures," *IEE Proceedings - Control Theory and Applications, Volume: 151 , Issue: 3.*

[78] Low C. B. and Ng Q. S., 2011, "A Flexible Virtual Structure Formation Keeping Control for Fixed-Wing UAVs," *9th IEEE International Conference on Control and Automation (ICCA) Santiago, Chile.*

[79] Kloetzer M. and Belta C., 2007, "Temporal LogicPlanning and Control of Robotic Swarms by Hierarchical Abstractions", *IEEE Transactions on Robotics, vol. 23, No. 2.Inbook, A., ed., 1991. Book title, 1st ed., Vol. 2 of Series Title. Publisher Name, Publisher address, Chap. 1, pp. 1–3.*

[80] Mehrjerdi H., Ghommamb J. and Saad M, 2011, "Nonlinear Coordination Control for a Group of Mobile Robots Using a Virtual Structure," *Mechatronics 21 1147–1155.*

[81] Low Ch. B., 2011, "A dynamic Virtual Structure Formation Control for Fixed-Wing UAVs" 9th IEEE *International Conference on Control and Automation (ICCA).*

[82] Yuan J. and Tang G. U., 2010, "Formation Control for Mobile Multiple Robots Based on Hierarchical Virtual Structures*," 8th IEEE International Conference on Control and Automation Xiamen, China.*

[83] Yang X. X., Tang G. U., Li Y. and Wang P.D., 2012, "Formation Control for Multiple Autonomous Agents Based on Virtual Leader Structure," 24th Chinese Control and Decision Conference (CCDC).

[84] Wang Sh. and Schuab H., 2011, "Nonlinear Feedback Control of a Spinning Two-Spacecraft Coulomb Virtual Structure," *IEEE Transactions on Aerospace and Electronic Systems, Volume: 47 , Issue: 3.*

[85] Binglong C., Xiangdong L. and Zhen Ch., 2010, "Attitude Coordination of Deep Space Formation Flying via Virtual Structure," *29th Chinese Control Conference (CCC).*

[86] Zhong-Hai Zh., Yuan J.; Zhang W. X. and Zhao J. P., 2012, "Virtual-Leader-Follower Structure and Tinite-Time Controller Based Cooperative Control of Multiple Autonomous Underwater Vehicles," *24th Chinese Control and Decision Conference (CCDC).*

[87] Xin M., Balakrishnan S.N. and Pernicka H.J., 2007, "Multiple Spacecraft Formation Control with O-D Method," *Control Theory & Applications, IET Volume: 1 , Issue: 2.*

[88] Li Q. and Jiang Zh. P., 2008, "Formation Tracking Control of Unicycle Teams with Collision Avoidance," *47th IEEE Conference on Decision and Control Cancun, Mexico.*

[89] Huang1 T. and Chen X., 2008, "A Geometric Method of Swarm Robot Formation Controls," *7th World Congress on Intelligent Control and Automation, Chongqing, China.*

[90] Urcola P., Riazuelo, L., Lazaro M.T. and Montano L., 2008, "Cooperative Navigation Using Environment Compliant Robot Formations," *International Conference on Intelligent Robots and Systems.*

[91] Yoo S.J., Park J.B. and Y.H. Choi, 2009, "Adaptive Formation Tracking Control of Electrically Driven Multiple Mobile Robots," *IET Control Theory and Applications.*

[92] Balch T. and Arkin R. C., 1998, "Behavior-Based Formation Control for Multirobot Teams," *IEEE Transactions on Robotics and Automation, Vol. 14, No. 6.*

[93] Liu B., Zhang R. and Shi C., 2006, "Formation Control of Multiple Behavior-Based Robots," *International Conference on Computational Intelligence and Security.*

[94] Antonelli G., Arrichiello F. and Chiaverini S., 2006, "Experiments of Formation Control with Collisions Avoidance using the Null-Space-Based Behavioral Control" *International Conference on Intelligent Robots and Systems.*

[95] Antonelli G., Arrichiello F. and Chiaverini S., 2009, "Experiments of Formation Control With Multirobot Systems Using the Null-Space-Based Behavioral Control" *IEEE Transactions on Control Systems Technology, Vol. 17, No. 5.*

[96] Rezaee H. and and Abdollahi F., 2011, "Mobile Robots Cooperative Control and Obstacle Avoidance Using Potential Field," *IEEE-ASME International Conference on Advanced Intelligent Mechatronics Budapest, Hungary.*

[97] Olfati-Saber R., Fax J. A. and Murray R. M., 2007, "Consensus and Cooperation in Networked Multi-Agent Systems," *Proceedings of the IEEE, Vol. 95, Issue 1.*

[98] Olfati-Saber R., Fax J. A. and Murray R. M., 2004, "Consensus Problems in Networks of Agents With Switching Topology and Time-Delays*," IEEE Transactions on Automatic Control, Vol. 49, No. 9.*

[99] Zhinhua Qu, 2009, "Cooperative Control of Dynamical Systems [electronic resource] : Applications to Autonomous Vehicles," *Springer, c2009*.

[100] Guisheng Zhai, Shohei Okuno, Joe Imae and Tomoaki Kobayashi, 2009, "A New Consensus Algorithm for Multi-Agent Systems via Dynamic Output Feedback Control*," IEEE International Symposium on Intelligent Control, Saint Petersburg, Russia.*

[101] Türker Bıyıkoğlu, 2007, "Laplacian Eigenvectors of Graphs [electronic resource] : Perron-Frobenius and Faber-Krahn type theorems," *Springer e-books.*

[102] J.A. Bondy, U.S.R. Murty, 2008, "Graph theory," *New York: Springer.*

[103] Ghods N. and Krstic M., 2012, "Multi Agent Deployment Over a Source," IEEE Transactions on Control Systems Technology, Vol. 20, No. 1.

[104] Frihauf P. and Krstic M., 2011, "Leader-Enabled Deployment onto Planar Curves: A PDE-Based Approach*," IEEE Transactions on Automatic Control, Vol. 56, No. 8.*

[105] Frihauf P. and Krstic M., 2010, "Multi-Agent Deployment to a Family of Planar Arcs," *American Control Conference Marriott Waterfront, Baltimore, MD, USA.*

[106] Kima J., Kima K. D., Natarajan V., Kelly S. D. and Bentsman J., 2008, "PdE-Based Model Reference Adaptive Control of Uncertain Heterogeneous Multi Agent Networks," *Nonlinear Analysis: Hybrid Systems 2 1152-1167.*

[107] Liu W., 2003, "Boundary Feedback Stabilization of an Unstable Heat Equation," *SIAM J. Control Optim. Vol. 42, No. 3, pp. 1033–104.*

[108] Boskovic D. M., Krstic M. and Liu W., 2001, "Boundary Control of an Unstable Heat Equation Via Measurement of Domain-Averaged Temperature," *IEEE Transactions On Automatic Control, Vol. 46, No. 12.*

[109] Liu W. J. and Krstic M., 2000, "Backstepping Boundary Control of Burgers' Equation with Actuator Dynamics," *Systems & Control Letters 41 291–303.*

[110] Smyshlyaev A. and Krstic M., 2007, "Adaptive Boundary Control for Unstable Parabolic PDEs—Part II: Estimation-based designs," *Automatica 43 1543 – 1556.*

[111] Rastgoftar H., Eghtesad M. and Khayatian A. , 2011, "Boundary Control of Temperature Distribution in a Rectangular Functionally Graded Material Plate*," J HEAT TRANS-T ASME.*

[112] Rastgoftar H., Eghtesad M. and Khayatian A. , 2012, "Boundary Control of Temperature Distribution in a Spherical Shell With Spatially Varying Parameters", *J HEAT TRANS-T ASME.*

[113] Lai W. M., Rubin M., and Krempl E., 1993, "Introduction to Continuum Mechanics" *Pergamon Press Ltd.*

[114] Rastgoftar H. and Jayasuriya S., 2013, "Distributed Control of Swarm Motions as ontinua using Homogeneous Maps and Agent Triangulation" *to appear at the European Control Conference, Zurich, Switzerland.*

[115] Rastgoftar H. and Jayasuriya S., 2013, “Multi-agent Deployment based on Homogenous Maps and a Special Inter-Agent Communication Protocol,” *6th IFAC Symposium on Mechatronic Systems, Mechatronics '13), Hangzhou, China.*